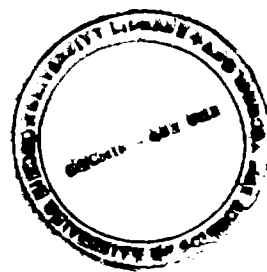# STUDIES ON PULSE PROPAGATION IN SINGLE MODE OPTICAL FIBERS

Thesis submitted

in partial fulfilment of the requirements

for the award of the DEGREE of

DOCTOR OF PHILOSOPHY

R. GANAPATHY

DEPARTMENT OF PHYSICS

COCHIN UNIVERSITY OF SCIENCE AND TECHNOLOGY
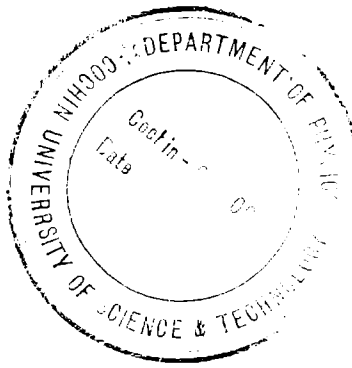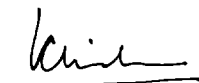
KOCHI-682 022

NOVEMBER 2002

CERTIFICATE

Certified that the work presented in this thesis is the bonafide work done by Mr. R. Ganapathy, under my guidance in the Department of Physics, Cochin University of Science and Technology and that this work has not been included in any other thesis submitted previously for the award of any degree.

Kochi-682 022

November 2002

Dr. V. C. Kuriakose

Supervising Teacher

DECLARATION

I here by declare that the work presented in this thesis is based on the original work done by me under the guidance of Dr. V. C. Kuriakose, Professor, in the Department of Physics, Cochin University of Science and Technology and has not been included in any other thesis submitted previously for the award of any degree.

Kochi-682 022

November 2002

R. Ganapathy

Dedicated To

Appa and Amma

PREFACE

The work presented in this thesis has been carried out by the author as a full-time research scholar in the Department of Physics, Cochin University of Science and Technology during the period 1996-2002.

Studies on pulse propagation in single mode optical fibers have attracted interest from a wide area of science and technology as they have laid down the foundation for an in-depth understanding of the underlying physical principles, especially in the field of optical telecommunications. The foremost among them is discovery of the optical soliton which is considered to be one of the most significant events of the twentieth century owing to its fantastic ability to propagate undistorted over long distances and to remain unaffected after collision with each other. To exploit the important properties of optical solitons, innovative mathematical models which take into account proper physical properties of the single mode optical fibers demand special attention. This thesis contains a theoretical analysis of the studies on soliton pulse propagation in single mode optical fibers. The thesis is arranged as follows:

In chapter one, a general introduction underlying the fundamental linear and nonlinear electrical properties of single mode optical fibers is presented. A derivation of the model equation for the slowly varying electric field envelope of the light wave in single mode optical fibers, basic theoretical and engineering concepts of optical solitons in single mode optical fibers are also presented in this chapter.

For the higher order scalar nonlinear Schrödinger equation which describes pulse propagation in a single mode optical fiber in the femto second regime,

exact solutions in the form of solitary waves and periodic solutions are presented in chapter two by using travelling wave method.

When breakup of continuous wave and quasi-continuous wave radiates into a train of pico second and femto second pulses in the normal dispersion regime for an elliptically birefringent single mode optical fiber, higher-order nonlinear effects such as self-steepening, self-induced Raman scattering and higher order dispersion effects such as third and fourth order dispersion play a decisive role in ultra short pulse generation. In chapter three the conditions for the occurrence of cross phase modulational instability, which occur as a result of a group velocity mismatch between the linearly polarized eigen states in the normal dispersion regime for an elliptically birefringent single mode optical fiber modelled by the coupled higher order nonlinear Schrödinger equation which includes all the above mentioned higher order dispersion and nonlinear effects, are obtained both analytically and numerically. In this case, different scenario for generation of ultra short pulses of various pulse widths, governed by the respective modulational instability conditions on including the higher order dispersive and nonlinear effects of the single mode optical fiber are discussed in detail.

A different phenomenon of modulational instability known as polarization modulation instability which involves a change of the polarization state of an incident pump wave as it traverses the circular birefringent optical fiber is discussed in detail in chapter four. The governing equation in this case pertains to generation of ultra short pulses of the order of 500 fs and above and hence is modelled by the the coupled higher order nonlinear Schrödinger equation which includes only the fourth order dispersion coefficient. Due to polarization modulation instability, the incident pump wave which is polarized on one axis of the fiber, would generate orthogonally polarized Stokes and anti-Stokes sidebands

and the unstable power gain is obtained. It is observed that the parametric gain curve virtually remains the same whenever the pump is rotated from the slow axis by a few degrees for both the regimes but when oriented close to the fast axis, the parametric gain curve is found to vary considerably for various values of the power thereby confirming the fact that the slow and the fast axes of a polarization preserving fiber are not equivalent when one considers the influence of the fourth order dispersion effects.

Chapter five deals with the case of soliton pulse compression in a single mode fiber with variable dispersion (decreasing dispersion) supporting both monomode and orthogonally polarized modes and with inline phase modulation and has been shown that there is exact balancing between the effective gain and the effecting phase modulation and as a result arrive at exact soliton solutions for the various dispersion profiles.

To make the soliton based communication systems highly competitive and economical when compared to the conventional systems, attenuation in a fiber must be avoided. In this context, erbium doped silica fibers play a prominent role in not only minimising the attenuation but also achieving the goal of all optical transmission. Chapter six concerns with the coherent soliton pulse propagation in an erbium doped fiber system associated with the self-induced transperancy phenomenon and which is characterized by the nonlinear Schrödinger-Maxwell-Bloch equations. The Lax pair for the system is determined. Now using the method of Darboux-Backlund transformation, soliton solutions are generated which throw light on the ultra-short pulse propagation through the erbium doped silica fibers with higher order dispersion, self-steepening and self-induced transparency effects.

Chapter seven deals with the overall conclusions presented in the thesis.

A part of these investigations has been published in/submitted to the following journals:

1. Soliton propagation in a birefringent optical fiber with fiber loss and frequency chirping, R. Ganapathy, V. C. Kuriakose and K. Porsezian, Optics Communications **194**, 299 (2001).

2. Polarization modulational instability in a birefringent optical with fourth order dispersion, R. Ganapathy and V. C. Kuriakose, Pramana-Journal of Physics **57**, 743 (2001).

3. Cross-phase modulational instability in an elliptical birefringent fiber with higher order nonlinearity and dispersion, R. Ganapathy and V. C. Kuriakose, Pramana-Journal of Physics **58**, 669 (2002).

4. Soliton interaction in a dispersion decreasing fiber with effective gain and effective phase modulation, R. Ganapathy and V. C. Kuriakose, Chaos, Solitons and Fractals **15**, 99 (2002).

5. Soliton pulse compression in a dispersion decreasing elliptic birefringent fiber with effective gain and effective phase modulation, R. Ganapathy and V. C. Kuriakose, Journal of Nonlinear Optical Physics and Materials **11**, 185 (2002).

A part of these investigations has been presented in the following seminars/workshops:

1. Cross-phase modulational instability in an elliptical birefringent fiber with higher order nonlinearity and dispersion, R. Ganapathy and V. C. Kuriakose, International Workshop on Optical Solitons:Theory and Experiments, Cochin University of Science and Technology, Cochin-682 022, January 24-29 (2002).

2. Soliton interaction in a dispersion decreasing fiber with effective gain and effective phase modulation, R. Ganapathy and V. C. Kuriakose, International Workshop on Optical Solitons:Theory and Experiments , Cochin University of Science and Technology, Cochin-682 022, January 24-29 (2002).

ACKNOWLEDGEMENTS

Table of Contents

viii

Chapter 1

Introduction

1.1 Introduction

Studies on pulse propagation in single mode optical fibers have attracted interest from a wide area of science and technology as they have laid down the foundation for an in-depth understanding of the underlying physical principles, especially in the field of optical communications [1]-[4]. Of the various types of nonlinear pulses propagating in a single mode optical fiber, the discovery of the optical soliton pulse is considered to be one of the most significant events of the twentieth century owing to its fantastic ability to propagate undistorted over long distances and to remain unaffected after collision with each other [5]. An optical soliton pulse manifests as a result of an interplay between the dispersive and nonlinear effects in optical fibers [5, 6]. The advent of high intense laser sources and optical fibers having very low fiber loss have further paved the way for efficient and fast transmission of ultrashort soliton pulses through single mode optical fibers that form the basis of high speed communication systems [7, 8]. Generation of ultra short soliton pulses have been experimentally achieved on employing dispersion-flattened fibers and fiber grating compressors [9, 10]. Recent developments in the

design of directional couplers, optical fiber Kerr gate, etc., have made possible the realization of extremely efficient optical switching devices by making use of the properties of inelastic collision of optical solitons [11, 12]. The important properties of the erbium doped optical fiber amplifiers such as high gain, low noise, wide band-width, polarization insensitive gain and high saturation output power have made them a competitive contender in the field of high speed optical communication [13]. It is no wonder that the erbium doped fiber amplifiers have been chosen as trans-ocean-cable network that connect all the major cities in the world. Here too the underlying phenomenon is based on optical solitons. Another interesting and useful application of the soliton formation capability of optical fibers is the development of soliton lasers [14]-[17]. These achievements have instigated extensive research in order to exploit the important properties of optical solitons and thus have paved the way for the need of innovative mathematical models which take into account of the proper physical properties of the single mode optical fibers.

This chapter is arranged as follows: In Sec.1.2, the characteristic properties of a single-mode optical fiber is dealt. Section 1.3 deals with the electric properties of the dielectric fiber. The master equation for information transfer in optical fibers is derived in Sec.1.4 and in Sec.1.5 the exact soliton solutions pertaining to the master equation are obtained.

1.2 Fiber characteristics

Depending on the number of modes that a fiber can support, fibers are generally classified as single mode and multi mode fibers [18]. A single mode fiber has only the fundamental transverse electric HE_{11} mode whereas a multi mode fiber

can support any number of modes. Further, depending on their refractive index profiles, both the single and multi mode fibers can be classified as step-index and graded-index fibers. As their name suggest, for a step-index fiber, the refractive index profile has the shape of a step whereas that for a graded index fiber has a parabolic shape [18] and is portrayed in Fig.(1.1).
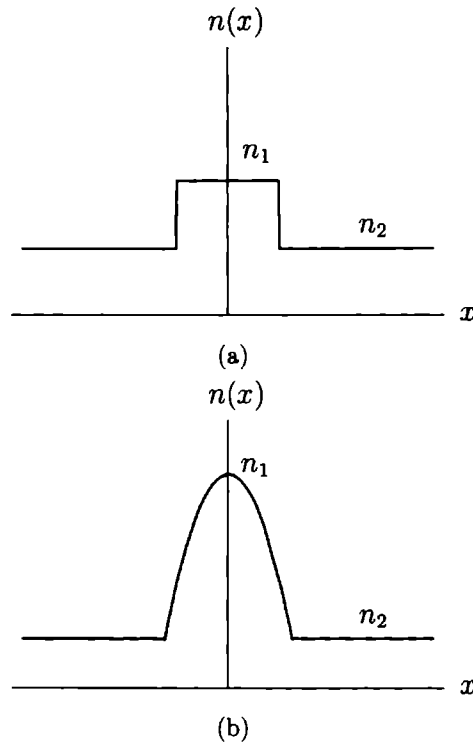
Fig. 1.1: Refractive index profiles for the (a) step index fiber; (b) graded index fiber. In both cases, n_1 is the refractive index of the core and n_2 that of the cladding with n_1 slightly greater than n_2.

A step-index single mode fiber (Fig.(1.2(a))) is a silica glass thread constituting of a central core of doped silica (SiO_2) surrounded by a cladding layer of pure silica. Its refractive index profile has a step shape, hence its name. The core radius is only of the order of several microns. The working principle of the optical fiber is based on the total internal reflection of light [18]. In order to enable this, the refractive index of the cladding (n_2) is arranged to be slightly
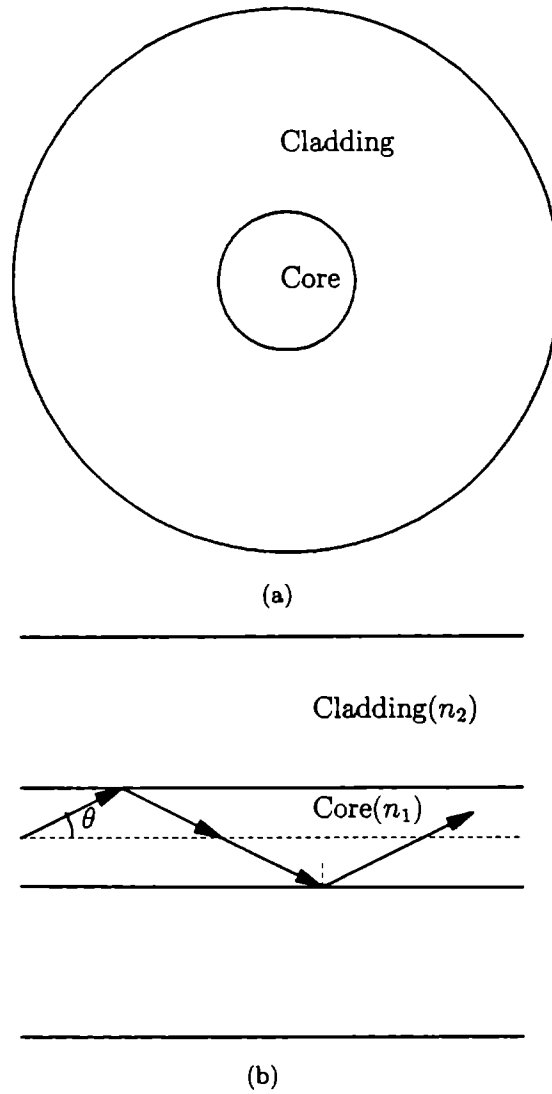
Fig. 1.2: (a) Cross- section of a step index fiber; (b) Light guidance taking place through the phenomenon of total internal reflection.

lower than that of the core (n_1). As a result, when light is directed into the core, it always gets reflected by the cladding wall, allowing it to propagate through the fiber core (Fig.(1.2(b))).

The step-index fiber is generally characterized by two main parameters, namely the numerical aperture given by $NA = \sqrt{n_1^2 - n_2^2}$ [18] which represents the ca-

pacity of the fiber to accept light and the normalized frequency V defined by $V = k_0 \, a \, \sqrt{n_1^2 - n_2^2}$ [18] which determines the number of modes supported by the fiber. k_0 is the propagation constant and 'a', the core radius. For a single mode fiber, $V < 2.4$ whereas for a multi mode fiber, $V > 2.4$ [18]

1.3   Electric properties of the dielectric fiber

A single mode fiber can be deciphered thoroughly by a knowledge of its linear and nonlinear properties which are discussed below in detail.

1.3.1   Fiber linear properties

Two main phenomena are to be taken into account regarding the description of the linear properties of a single mode fiber, namely i) fiber attenuation and ii) dispersion.

i) Fiber attenuation

The loss of energy in an optical fiber can be accounted either due to absorption or due to scattering. Absorption generally arises from the pure material forming the fiber, known as the intrinsic absorption [1] and also from the impurities such as Fe^{3+} or OH^- ions resulting from the production process, known as extrinsic absorption [19]. Another main factor that influences the fiber loss is scattering loss [19]. The loss due to scattering can further be distinguished into Rayleigh scattering loss [19], which is caused by the variations in the refractive index of the transmission medium over distances shorter than the wavelength and extrinsic scattering loss, that which is due to imperfections in the fiber or in the protective jacket. Scattering is the only type of loss in current commercially available fibers.
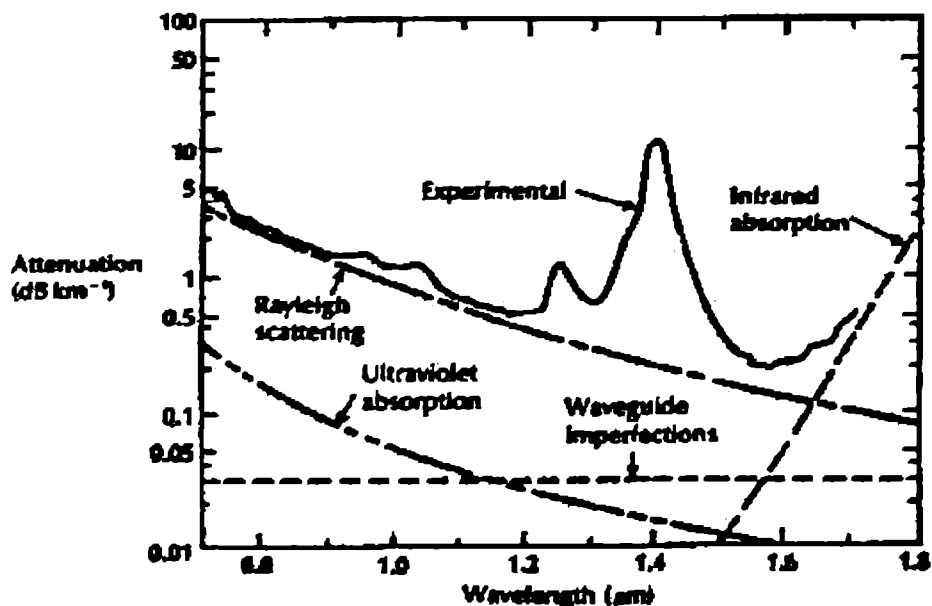
Fig. 1.3: Typical attenuation spectrum of an optical fiber [After Ref. [18]].

Figure 1.3 shows a plot of fiber attenuation versus wavelength for a commercially available fiber. The attenuation appears to be very close to the Rayleigh lower limit in the operating region. The presence of residual OH⁻ absorption limits the signal transmission to three transmission windows, namely, 0.85 μm, 1.3 μm and 1.55 μm. The fiber exhibits a minimum loss of about 0.2 dB/km near 1.55 μm which is due to Rayleigh scattering [19].

ii) Dispersion

Dispersion in a single mode optical fiber is generally characterized by its group velocity dispersion (GVD) [20]-[24] and its polarization mode dispersion (PMD) [25]-[29].

When a pulse propagates along the length of the fiber, its frequency components have different group velocities so that the pulse broadens during its propagation along the fiber. This spreading of the group velocity is known as GVD or chromatic dispersion [1, 4]. GVD essentially consists of two contributions, one due to the material of the fiber and the other due to the waveguide structure. Material dispersion [4] originates from the intrinsic properties of the fiber material, mainly from interaction of the light wave electric field with the bound electrons of the dielectric and can be described by the frequency dependence of the linear index of refraction $n_0(\omega)$. The resonance of bound electrons with the light wave frequency forms the major contributing factor to $n_0(\omega)$. Away from resonances, where the absorption rather than dispersion dominates, $n_0(\omega)$ can be expressed as $n_0(\omega) = 1 + \sum_{j=1}^{n} \frac{A_j \omega_j}{\omega_j^2 - \omega^2}$, where ω_j and A_j are respectively the resonant frequencies and their strengths. As regards the waveguide dispersion [1], it depends on guided propagation and is present even if material dispersion vanishes. The waveguide dispersion produces a positive GVD and the material dispersion produces a negative GVD at larger wavelengths [4]. The total dispersion is the sum of material and waveguide dispersions. Due to GVD, the instantaneous frequency of the pulse is found to vary with time and such a pulse is referred to as a chirped pulse [1, 4]. For a given fiber, the temporal broadening and chirping of the pulse are determined by the group delay parameter (dispersion coefficient) D [4] defined as $D = -\frac{2\pi c}{\lambda_0^2} k''$, where k'' is the GVD coefficient. D is measured by the delay of arrival time in picoseconds of two light pulses with the wavelength separation of one nanometer over a distance of a kilometer. $D < 0$ refers to the normal dispersion regime [4] and $D > 0$ refers to the anomalous dispersion regime [4]. In the normal dispersion regime, the instantaneous frequency within the dispersed pulse increases with time [4]. Thus the leading edge of the pulse is red shifted
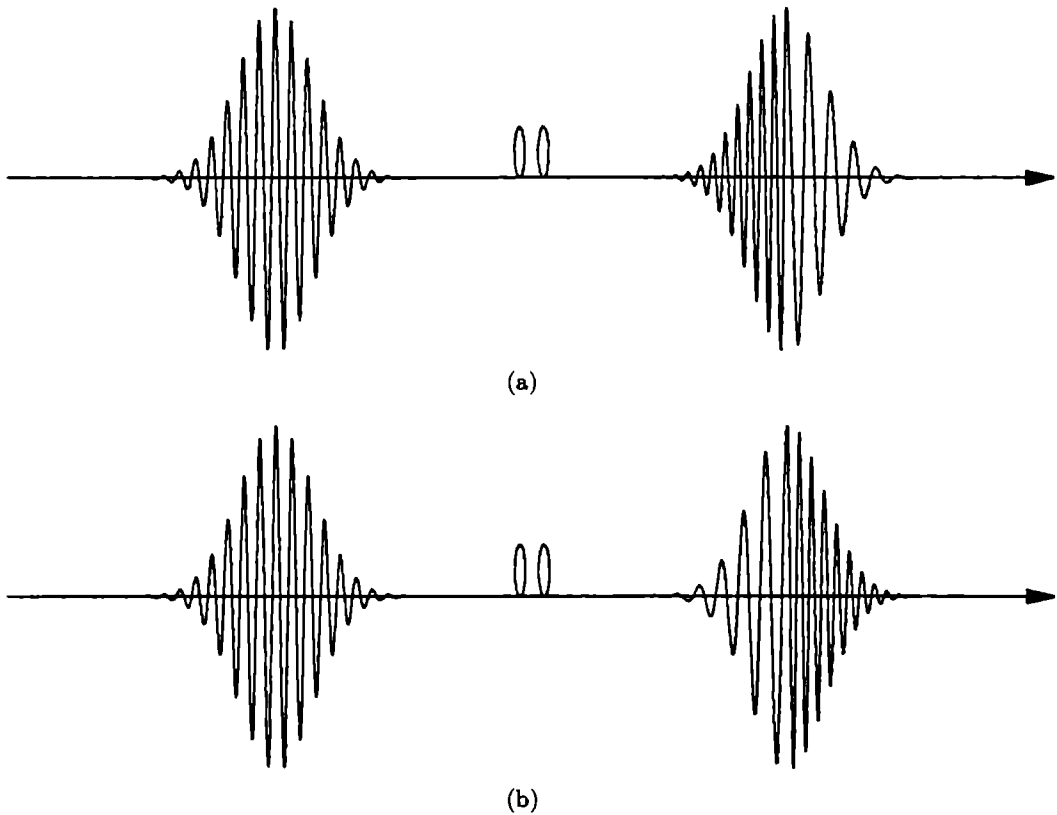
Fig. 1.4: Typical chirping caused in (a) the anomalous dispersion regime and (b) the normal dispersion regime when an unchirped pulse propagates through the fiber. The chirp is of opposite sign in the two cases.

and the trailing edge of the pulse is blue shifted. In the anomalous dispersion regime, as the instantaneous frequency decreases with time, the leading edge of the pulse is blue shifted and the trailing edge of the pulse is red shifted [4]. Figure 1.4 depicts the typical chirping caused in the anomalous and normal dispersion regimes.

It is possible for a single mode fiber to support two degenerate modes that are polarized in two orthogonal directions. Under ideal conditions of perfect cylindrical geometry and isotropic material, a mode excited with its polarization in one direction would not couple to the mode in the orthogonal direction. How-

ever small deviation from cylindrical geometry or small fluctuations in material anisotropy result in mixing up of the two polarization states and the mode degeneracy is thus broken. As a result, the mode-propagation constant k becomes slightly different for the modes polarized in orthogonal directions which is referred to as modal birefringence [25]. Due to modal birefringence, a group delay is induced between the two modes. As a result, the pulse broadens [25]. This pulse broadening is measured by a quantity called the differential group delay and the difference in dispersion between the two modes is called the PMD [25]-[29].

1.3.2   Fiber nonlinear properties

Fiber nonlinear properties are either due to changes in the refractive index with optical power or due to scattering phenomenon. The main nonlinear effects in a single mode optical fiber are i) Kerr effect [30]-[34], ii) Raman scattering [35]-[39], iii)Brillouin scattering [40, 41, 42] and iv) four wave mixing [43, 44].

i)Kerr effect

The origin of nonlinear response is related to non-harmonic motion of bound electrons under the influence of an applied field. Hence, the induced polarization $\mathbf{P}$ resulting from the electric dipoles is given by [1, 4]:

$$\mathbf{P} = \varepsilon_0 \left(\chi^{(1)} \cdot \mathbf{E} + \chi^{(2)} : \mathbf{EE} + \chi^{(3)} \vdots \mathbf{EEE} + \ldots \right)$$

where ε_0 is the vacuum permittivity and $\chi^{(j)}$, the jth order susceptibility tensor of rank j+1. The linear susceptibility tensor $\chi^{(1)}$ determines the linear refractive index n_0 and the attenuation coefficient γ. As silica glass has an inversion symmetry at the molecular level, even powered terms in $\mathbf{E}$ do not appear in the expression for $\mathbf{P}$ [1]. As a consequence, the nonlinear behavior of the fiber is

mainly due to the third order susceptibility tensor $\chi^{(3)}$ [1, 4]. In particular, the real part of $\chi^{(3)}$ is responsible for Kerr effect [1, 4], while the imaginary part for the Raman effect [1]. A light wave with frequency ω sees nonlinear response of the $\chi^{(3)}$ term through the interaction of ω, $-\omega$ and ω components. This response contributes to the nonlinear modification of index of refraction $n\left(\omega, |\mathbf{E}|^2\right)$ given by [1]:

$$n\left(\omega, |\mathbf{E}|^2\right) = n_0\left(\omega\right) + n_2\left(\omega\right)|\mathbf{E}|^2,$$

where the Kerr coefficient $n_2\left(\omega\right)$ is related to $\chi^{(3)}$ through the relation [1]

$$n_2\left(\omega\right) = \frac{3}{4n_0}\,\chi^{(3)}_{xxxx}.$$

Depending on the shape of the input signal, the Kerr nonlinearity manifests itself by different effects, such as self-phase modulation (SPM) [45]-[49], cross-phase modulation (XPM) [50]-[53], modulational instability (MI) [54]-[58], etc. SPM in a single mode optical fiber occurs when the refractive index of a light wave depends on the intensity of that light wave [2]. As a result, when the optical signal is intensity modulated, the resulting nonlinear phase-shift gives rise to a spurious phase-modulation. SPM leads to spectral broadening of optical pulses [45]. When a complex signal is put into a fiber, the time-dependent nonlinear phase-shift might result in a chirp in the transmitted field. This SPM-induced chirp will combine with the linear chirp resulting from GVD. Thus the effect of the interaction between SPM and GVD depends on the sign of the GVD coefficient [45]. Thus in the anomalous dispersion regime, where the fiber dispersion coefficient is negative, the linear and nonlinear chirps are of opposite signs as a result of which the pulse broadening is reduced. At a certain stage, these two effects balance exactly, thereby leading to a stable soliton pulse [45]. XPM is always accompanied by SPM and occurs when the effective refractive index of

a light wave depends not only on the intensity of that wave but also on the intensity of other copropagating waves in the optical fiber [50]. XPM is effective only when the interactive signals are superimposed in time. MI phenomena are also generated by the interplay between Kerr effect and GVD [54]. MI requires anomalous dispersion for the single-beam case and manifests itself as break-up of continuous wave or quasi-continuous wave radiation into a train of ultrashort pulses leading to an exponential growth or attenuation of the side bands with respect to the carrier of a modulated signal propagating through the fiber [54]. In the case of birefringent optical fibers MI can occur even in the normal dispersion regime [57].

ii)Raman scattering

When a light wave is incident in a fiber at the carrier frequency ω_0 in the presence of some resonance level ω_R of the fiber material, the incident light results in the downshift of the carrier frequency resulting in an entirely new frequency $\omega_0 - \omega_R$, known as the mode frequency. Such a process is known as Raman effect [1]. The principle of Raman scattering is that a lower wavelength pump-laser light travelling down an optical fiber along with the signal, scatters off atoms in the fiber, loses some energy to the atoms, and then continues its journey with the same wavelength as the signal. Therefore the signal has additional photons representing it and, hence, is amplified. This new photon can now be joined by many more from the pump, which continue to be scattered as they travel down the fiber in a cascading process. When the frequency beating between the incident and scattered waves collectively enhance the optical photon, the scattering process is stimulated and the amplitude of the scattered wave grows exponentially in the direction of propagation, a phenomenon known as the stimulated Raman

scattering (SRS) [37]. Raman gain, resulting from SRS, depends on the frequency separation between the pump and the Stokes modes, becomes zero when the frequency separation is zero and increases with frequency separation. As a result, the corresponding Raman gain spectrum spans over an extremely broad frequency range wider than about 20 THz [35]. Raman amplification [1, 2], one of the effects due to Raman scattering, aims to boost the power of signals. It is usually accomplished as "distributed amplification" i.e., it happens throughout the length of the actual transmission fiber. So into the same fiber that is carrying the signal, one can add a high-power pump wavelength (say of a few watts power), which will amplify the signal along many kilometers of fiber until the pump signal eventually fades away.

ii) Brillouin scattering

In Brillouin scattering, part of the energy of the electric field is transferred to the acoustic phonons [40]. At high power levels, it can induce stimulated effects and the intensity of the scattered light grows exponentially once the incident power exceeds a threshold value. The Brillouin-generated phonons are coherent, giving rise to a macroscopic acoustic wave in the fiber.

iv) Four wave mixing

Let ω_1, ω_2 and ω_3 be the frequencies of three waves incident in an optical fiber. The third order nonlinearity of the fiber, which is more predominant, would lead to the generation of a nonlinear polarization at a frequency, say ω_4 given by $\omega_4 = \omega_2 + \omega_3 - \omega_1$. This nonlinear polarization can, under some circumstances, lead to the generation of electromagnetic waves at the new frequency ω_4. This phenomenon is referred to as four wave mixing [43].

1.4 Master equation for information transfer in optical fibers

The nonlinear Schrödinger equation that describes the behavior of solitons in optical fibers is derived starting from first principles, i.e., Maxwell's equations in isotropic, dispersive and nonlinear dielectric material [60, 61]. The refractive index of the fiber is assumed to be axis symmetric such that only the fundamental HE_{11} mode is supported by the fiber [61]. The axis symmetry means that there is a one parameter family of such modes, parameterized by the direction of polarization, i.e., the ratio of the strengths in the transverse fields in, say the x and y directions and with the direction of propagation along the z axis. Moreover, the fiber is assumed to be polarization preserving also. With these assumptions, the derivation of the nonlinear Schrödinger equation is outlined below in the following stages. First, starting from the Maxwell's equations, the basic propagation equation for pulse propagation in a single mode weakly guided fiber is determined. Considering quasi monochromatic approximation, an expression for the slowly varying electric field envelope is developed in the second stage. In the third stage, the linear and nonlinear polarization components are determined upto $O(\varepsilon)$. Using the asymptotic expansion, the scalar nonlinear Schrödinger equation is derived in the fourth stage and finally correction terms are discussed.

i) Maxwell's equations

Let **E** and **H** respectively, be the electric and magnetic field vectors and **D** and **B**, the corresponding flux densities. The current density vector $\mathbf{J}_f$ and the charge density ρ_f represent the sources of electromagnetic field. Due to the absence of

free charges in an optical fiber, $\mathbf{J}_f = 0$ and $\rho_f = 0[1]$. Since the magnetic properties in silica can be ignored, the permeability is given by μ_0, namely the one for free space. The Maxwell's equations are [61]:

$$
\begin{aligned}
\nabla \times \mathbf{E} &= -\frac{\partial \mathbf{B}}{\partial t}, \\
\nabla \times \mathbf{B} &= \mu_0 \frac{\partial \mathbf{D}}{\partial t}, \\
\nabla \cdot \mathbf{D} &= 0 \quad \text{and} \\
\nabla \cdot \mathbf{B} &= 0.
\end{aligned}
\tag{1.4.1}
$$

The flux densities $\mathbf{D}$ and $\mathbf{B}$ are related to the electric and magnetic field vectors $\mathbf{E}$ and $\mathbf{H}$ respectively, via the relations [61]:

$$
\begin{aligned}
\mathbf{D} &= \varepsilon_0 \mathbf{E} + \mathbf{P} \quad \text{and} \\
\mathbf{B} &= \mu_0 \mathbf{H},
\end{aligned}
\tag{1.4.2}
$$

where $\mathbf{P}$ is the induced electric polarization. As silica exhibits linear and nonlinear response with retardation, the dielectric polarization $\mathbf{P}(\mathbf{r}, t)$ is expressed as the sum of linear part $\mathbf{P}_L(x, y, z, t)$ and nonlinear part $\mathbf{P}_{NL}(x, y, z, t)$ such that [1, 61]:

$$
\mathbf{P}(x, y, z, t) = \mathbf{P}_L(x, y, z, t) + \mathbf{P}_{NL}(x, y, z, t).
\tag{1.4.3}
$$

Both $\mathbf{P}_L(x, y, z, t)$ and $\mathbf{P}_{NL}(x, y, z, t)$ are in turn related to the electric field via the relation [60, 61]:

$$
\begin{aligned}
\mathbf{P}_L(x, y, z, t) &= \varepsilon_0 \int_{-\infty}^{+\infty} \chi^{(1)}(t - t') \cdot \mathbf{E}(x, y, z, t') \, dt' \quad \text{and} \\
\mathbf{P}_{NL}(x, y, z, t) &= \varepsilon_0 \int_{-\infty}^{+\infty} \int_{-\infty}^{+\infty} \int_{-\infty}^{+\infty} \chi^{(3)}(t - t_1, t - t_2, t - t_3) \vdots \mathbf{E}(x, y, z, t_1) \\
&\quad \mathbf{E}(x, y, z, t_2) \mathbf{E}(x, y, z, t_3) \, dt_1 dt_2 dt_3,
\end{aligned}
\tag{1.4.4}
$$

where $\chi^{(1)}$ and $\chi^{(3)}$ are the linear and third order nonlinear susceptibility tensors respectively, having the dependence of the spatial coordinates $\mathbf{r}$ of the material and having the form [61]:

$$\left(\chi^{(1)}.\mathbf{E}\right)_i \quad = \quad \sum_j \chi_{ij} E_j \quad \text{and}$$

$$\left(\chi^{(3)}:\mathbf{EEE}\right)_i \quad = \quad \sum_{jkl} \chi_{ijkl} E_j E_k E_l, \tag{1.4.5}$$

where $i = x, y, z$. Silica, being centro symmetric, does not exhibit the second order nonlinear effect [61]. For a weakly guided mode, $\nabla \cdot \mathbf{E} = 0$. Hence from Eqs. (1.4.1), (1.4.2) and (1.4.3), a relation of the form :

$$\nabla^2 \mathbf{E} - \frac{1}{c^2} \frac{\partial^2 \mathbf{E}}{\partial t^2} = \frac{1}{c^2 \varepsilon_0} \left(\frac{\partial^2 \mathbf{P}_L}{\partial t^2} + \frac{\partial^2 \mathbf{P}_{NL}}{\partial t^2} \right) \tag{1.4.6}$$

where $\mathbf{P}_L$ and $\mathbf{P}_{NL}$ are given by Eq.(1.4.4).

ii) Quasi-monochromatic approximation

In order to derive the nonlinear Schrödinger equation, the quasi- monochromatic approximation is considered i.e., the waveform is assumed to have a slowly varying envelope, or in the frequency domain, has a narrow spectrum with respect to its carrier frequency [61]. This approximation leads to slow variation of the light wave envelope with respect to time and distance [61]. The nonlinear Schrödinger equation is derived as the equation that describes long range evolution of the slowly varying envelope [61]. In the slowly varying envelope approximation, the electric field vector $\mathbf{E}(x, y, z, t)$ can be written in the form [61]:

$$\mathbf{E}(x, y, z, t) = \mathbf{U}(x, y, \omega_0) A \exp\left(i\left(k_0 z - \omega_0 t\right)\right) + \text{c.c.}, \tag{1.4.7}$$

where c.c denotes the complex conjugate. ω_0 and $k_0 \equiv k(\omega_0)$ represent the angular frequency and wave number of the carrier wave respectively and A is the

slowly varying wave envelope. $U(x, y, \omega_0)$ is a column vector representing the mode distribution over a cross-section in the fiber geometry. If $\tilde{E}(x, y, z, \omega)$ is the Fourier transform (F.T.) of the electric field vector $E(x, y, z, t)$, both of them are related to each other via the transformation:

$$E(x, y, z, t) = \frac{1}{2\pi} \int\limits_{-\infty}^{+\infty} \tilde{E}(x, y, z, \omega) \exp(-i\omega t) \, d\omega, \qquad (1.4.8)$$

and

$$\tilde{E}(x, y, z, \omega) = \int\limits_{-\infty}^{+\infty} E(x, y, z, t) \exp(i\omega t) \, dt. \qquad (1.4.9)$$

On substituting Eq.(1.4.7) in Eq.(1.4.9), the electric field in the frequency domain has the form :

$$\tilde{E}(x, y, z, \omega) = 2\pi\delta(\omega - \omega_0) \, AU(x, y, \omega_0) \exp(ik_0 z) + \text{c.c.} \qquad (1.4.10)$$

As long as the wave happens to be monochromatic, the wave envelope A remains a constant with respect to z and t, i.e., the spectrum is given by the delta function standing at the frequency $\omega = \pm\omega_0$. However, as a result of the quasi-monochromatic approximation, the envelope A acquires a sufficiently slow variation in time domain, whereas in frequency domain, it exhibits sufficiently small spectral broadening over the bandwidth $\Delta\omega$ in the vicinity of $\pm\omega_0$. A small parameter $\varepsilon \sim \Delta\omega/\omega_0$ is introduced as a factor characterizing the small scale of spectral broadening. Long range evolution of the envelope A is described in a small scale coordinate system given by $Z = \varepsilon z$. As a consequence of the long term amplitude modulation, $\tilde{E}(x, y, z, \omega)$ now has the form [61]:

$$\tilde{E}(x, y, z, \omega) = \tilde{A}(Z, \omega - \omega_0) \, U(x, y, \omega_0) \exp(ik_0 z) + \text{c.c.} \qquad (1.4.11)$$

The inverse Fourier transform (I.F.T.) of Eq.(1.4.11) yields:

$$
\begin{aligned}
\mathbf{E}\left(x,y,z,t\right) &= \frac{1}{2\pi}\int\limits_{-\infty}^{+\infty}\widetilde{\mathbf{E}}\left(x,y,z,\omega\right)\exp\left(-i\omega t\right)\,d\omega, \\
&= \frac{1}{2\pi}\int\limits_{-\infty}^{+\infty}\widetilde{A}\left(Z,\omega-\omega_0\right)\mathbf{U}\left(x,y,\omega_0\right)\exp\left(i\left(k_0 z-\omega t\right)\right)d\omega + \text{c.c.}, \\
&= \left(\frac{1}{2\pi}\int\limits_{-\infty}^{+\infty}\widetilde{A}\left(Z,\omega-\omega_0\right)\exp\left(-i\left(\omega-\omega_0\right)t\right)\,d\left(\omega-\omega_0\right)\right) \\
&\quad \mathbf{U}\left(x,y,\omega_0\right)\exp\left(i\left(k_0 z-\omega_0 t\right)\right) + \text{c.c.}
\end{aligned}
\tag{1.4.12}
$$

Let $\varepsilon\Omega \equiv \omega - \omega_0$ and $T = \varepsilon t$. Also let $A\left(Z,T;\varepsilon\right)$ be the I.F.T. of $\widetilde{A}\left(Z,\Omega;\varepsilon\right)$, which is of the form :

$$
A\left(Z,T;\varepsilon\right) = \frac{1}{2\pi}\int\limits_{-\infty}^{+\infty}\widetilde{A}\left(Z,\Omega;\varepsilon\right)\exp\left(-i\Omega T\right)\,d\Omega.
\tag{1.4.13}
$$

Using these in Eq.(1.4.12), the expression for $\mathbf{E}\left(x,y,z,t\right)$ simplifies to the form:

$$
\mathbf{E}\left(x,y,z,t\right) = \varepsilon A\left(Z,T;\varepsilon\right)\mathbf{U}\left(x,y,\omega_0\right)\exp\left(i\left(k_0 z-\omega_0 t\right)\right) + \text{c.c.}
\tag{1.4.14}
$$

From Eq.(1.4.13), the following relation is obtained :

$$
\left(i\varepsilon\frac{\partial}{\partial T}\right)^n A\left(Z,T;\varepsilon\right) = \frac{\varepsilon^n}{2\pi}\int\limits_{-\infty}^{+\infty}\Omega^n\widetilde{A}\left(Z,\Omega;\varepsilon\right)\exp\left(-i\Omega T\right)\,d\Omega,
\tag{1.4.15}
$$

where $n = 1, 2, \ldots$

iii) Linear and nonlinear polarization

The linear and nonlinear polarization vectors can be rewritten in the form [61]:

$$
\mathbf{P}_L\left(x,y,z,t\right) = \varepsilon_0\int\limits_{-\infty}^{+\infty}\chi^{(1)}\left(x,y,t-t'\right)\mathbf{E}\left(x,y,z,t'\right)\,dt',
$$

$$\mathbf{P}_{NL}(x,y,z,t) = \varepsilon_0 \int\limits_{-\infty}^{+\infty}\int\limits_{-\infty}^{+\infty}\int\limits_{-\infty}^{+\infty} \chi^{(3)}(x,y,t-t_1,t-t_2,t-t_3)$$

$$(\mathbf{E}(x,y,z,t_1)\cdot\mathbf{E}(x,y,z,t_2))$$

$$\mathbf{E}(x,y,z,t_3)\ dt_1 dt_2 dt_3, \tag{1.4.16}$$

where

$$\chi^{(1)}(x,y,t-t') \equiv \chi^{(1)}_{yy}(x,y,t-t') \quad \text{and}$$

$$\chi^{(3)}(x,y,t-t_1,t-t_2,t-t_3) \equiv \chi^{(3)}_{yyyy}(x,y,t-t_1,t-t_2,t-t_3). \tag{1.4.17}$$

On substituting Eq.(1.4.16) into Eq.(1.4.6), it takes the form [61]:

$$\nabla^2\mathbf{E} - \frac{1}{c^2}\frac{\partial^2\mathbf{E}}{\partial t^2} = \frac{1}{c^2}\left(\frac{\partial^2}{\partial t^2}\left[\int\limits_{-\infty}^{+\infty}\chi^{(1)}(x,y,t-t')\mathbf{E}(x,y,z,t')\ dt'\right]\right.$$

$$+\frac{\partial^2}{\partial t^2}\left[\int\limits_{-\infty}^{+\infty}\int\limits_{-\infty}^{+\infty}\int\limits_{-\infty}^{+\infty}\chi^{(3)}(x,y,t-t_1,t-t_2,t-t_3)\,(\mathbf{E}(x,y,z,t_1)\cdot\mathbf{E}(x,y,z,t_2))\right.$$

$$\left.\left.\mathbf{E}(x,y,z,t_3)\ dt_1 dt_2 dt_3\right]\right). \tag{1.4.18}$$

In order to study the behavior of the electric field in the vicinity of the stationary state (i.e.,$\varepsilon = 0$), an asymptotic expansion of $\mathbf{E}$ is considered with respect to ε and is given by [61] :

$$\mathbf{E} = \mathbf{E}_0 + \varepsilon\mathbf{E}_1 + \varepsilon^2\mathbf{E}_2 + \dots. \tag{1.4.19}$$

Considering right hand side of Eq.(1.4.18), the $O(\varepsilon)$ contribution in the linear polarization vector $\mathbf{P}_L$ and its Fourier transform yields the following expression [61]

$$\text{F.T.}\left(\frac{\partial^2}{\partial t^2}\left[\int\limits_{-\infty}^{+\infty}\chi^{(1)}(x,y,t-t')\mathbf{E}_0(x,y,z,t')\ dt'\right]\right) =$$

$$-\omega^2\widetilde{\chi}^{(1)}(x,y,\omega)\,\widetilde{A}(Z,\omega-\omega_0)\,\mathbf{U}(x,y,\omega_0)\exp(ik_0z) + \text{c.c.}, \tag{1.4.20}$$

where $\widetilde{\chi}^{(1)}(x,y,\omega) = \int\limits_{-\infty}^{+\infty} \chi^{(1)}(x,y,t)\exp(i\omega t)\ dt$. The inverse Fourier transform of Eq.(1.4.20) results in [61]:

$$\frac{\partial^2}{\partial t^2}\left[\int\limits_{-\infty}^{+\infty}\chi^{(1)}(x,y,t-t')\,\mathbf{E}_0(x,y,z,t')\ dt'\right] =$$

$$-\left(\frac{\varepsilon}{2\pi}\int\limits_{-\infty}^{+\infty}\left[(\omega_0+\varepsilon\Omega)^2\,\widetilde{\chi}^{(1)}(x,y,\omega_0+\varepsilon\Omega)\,\widetilde{A}(Z,\varepsilon\Omega)\exp(-i\varepsilon\Omega T)\right]d\Omega\right)$$

$$\mathbf{U}(x,y,\omega_0)\exp(i(k_0 z-\omega_0 t))+\text{c.c.}, \tag{1.4.21}$$

where the transformations $\varepsilon\Omega \equiv \omega-\omega_0$ and $T = \varepsilon t$ are used in the above equation. Equation (1.4.21) can be further simplified to the form [61]:

$$\frac{\partial^2}{\partial t^2}\left[\int\limits_{-\infty}^{+\infty}\chi^{(1)}(x,y,t-t')\,\mathbf{E}_0(x,y,z,t')\ dt'\right] =$$

$$-\varepsilon\left(\omega_0+i\varepsilon\frac{\partial}{\partial T}\right)^2\widetilde{\chi}^{(1)}\left(x,y,\omega_0+i\varepsilon\frac{\partial}{\partial T}\right)A(Z,T;\varepsilon)\,\mathbf{U}(x,y,\omega_0)$$

$$\exp(i(k_0 z-\omega_0 t))+\text{c.c.}, \tag{1.4.22}$$

where the relation given by Eq.(1.4.15) is considered. Now it can be easily verified that the higher order terms of $\mathbf{P}_L$ have a similar form to Eq.(1.4.22). The nonlinear contribution of the polarization vector appears only at ε^3. Once again considering right hand side of Eq.(1.4.18), the ε^3 contribution in the nonlinear polarization vector $\mathbf{P}_{NL}$ and its Fourier transform yields the following expression [61]:

$$F_1(x,y,z) =$$

$$-\left(\frac{1}{2\pi}\right)^3\int\limits_{-\infty}^{+\infty}\exp(i\omega t)\ dt\int\limits_{-\infty}^{+\infty}\int\limits_{-\infty}^{+\infty}\int\limits_{-\infty}^{+\infty}\left[(\omega_1+\omega_2+\omega_3)^2\,\widetilde{\chi}^{(3)}(x,y,\omega_1,\omega_2,\omega_3)\right.$$

$$\left.\left(\widetilde{\mathbf{E}}_0(x,y,z,\omega_1)\cdot\widetilde{\mathbf{E}}_0(x,y,z,\omega_2)\right)\widetilde{\mathbf{E}}_0(x,y,z,\omega_3)\exp(-i(\omega_1+\omega_2+\omega_3))\right]$$

$$d\omega_1 d\omega_2 d\omega_3+\text{c.c. }, \tag{1.4.23}$$

where

$$F_1(x, y, z) \equiv \text{F.T.} \left(\frac{\partial^2}{\partial t^2} \left[\int\limits_{-\infty}^{+\infty} \int\limits_{-\infty}^{+\infty} \int\limits_{-\infty}^{+\infty} \left\{ \chi^{(3)}(x, y, t - t_1, t - t_2, t - t_3) \right. \right. \right.$$

$$\left. \left. \left. (\mathbf{E}_0(x, y, z, t_1) \cdot \mathbf{E}_0(x, y, z, t_2)) \mathbf{E}_0(x, y, z, t_3) \right\} dt_1 dt_2 dt_3 \right] \right). \tag{1.4.24}$$

Now :

$$\widetilde{\mathbf{E}}_0(x, y, z, \omega_i) = \widetilde{A}(Z, \omega_i - \omega_0) \mathbf{U}(x, y, \omega_0) \exp(ik_0 z) + \text{c.c}, \tag{1.4.25}$$

where $i = 1, 2, 3$. Substitution of Eq.(1.4.25) into Eq.(1.4.23) yields a relation of the form [61]:

$$F_1(x, y, z) =$$

$$- \left(\frac{1}{2\pi} \right)^2 \int\limits_{-\infty}^{+\infty} \int\limits_{-\infty}^{+\infty} \int\limits_{-\infty}^{+\infty} \left[\delta(\omega - (\omega_1 + \omega_2 + \omega_3)) (\omega_1 + \omega_2 + \omega_3)^2 \, \widetilde{\chi}^{(3)}(x, y, \omega_1, \omega_2, \omega_3) \right.$$

$$\left\{ \left(\widetilde{A}(Z, \omega_1 - \omega_0) \mathbf{U}(x, y, \omega_0) \exp(ik_0 z) + \text{c.c} \right) \cdot \left(\widetilde{A}(Z, \omega_2 - \omega_0) \mathbf{U}(x, y, \omega_0) \right. \right.$$

$$\left. \left. \exp(ik_0 z) + \text{c.c} \right) \right\} \left(\widetilde{A}(Z, \omega_3 - \omega_0) \mathbf{U}(x, y, \omega_0) \exp(ik_0 z) + \text{c.c} \right) \right]$$

$$d\omega_1 d\omega_2 d\omega_3 + \text{c.c.} \tag{1.4.26}$$

On expanding the right hand side of Eq.(1.4.26), three terms proportional to each of $\exp(ik_0 z)$ and $\exp(-ik_0 z)$ and one term proportional to each of $\exp(3ik_0 z)$ and $\exp(-3ik_0 z)$ are obtained. Thus all together eight terms are obtained. In this case, only those terms which are proportional to $\exp(\pm ik_0 z)$ are of interest [61]. This is due to the fact that only these terms give rise to a resonant long distance effect. The coefficient of $\exp(-ik_0 z)$ is simply obtained by taking the complex conjugate of $\exp(ik_0 z)$. For example, one of the terms proportional to

$\exp\left(\pm ik_0 z\right)$ has the form [61]:

$$-\left(\frac{1}{2\pi}\right)^2 \int\limits_{-\infty}^{+\infty}\int\limits_{-\infty}^{+\infty}\int\limits_{-\infty}^{+\infty}\left[\delta\left(\omega-(\omega_1+\omega_2+\omega_3)\right)(\omega_1+\omega_2+\omega_3)^2\,\widetilde{\chi}^{(3)}\left(x,y,\omega_1,\omega_2,\omega_3\right)\right.$$

$$\left(\mathbf{U}\left(x,y,\omega_0\right)\cdot\mathbf{U}\left(x,y,\omega_0\right)\right)\mathbf{U}^*\left(x,y,-\omega_0\right)\widetilde{A}\left(Z,\omega_1-\omega_0\right)\widetilde{A}\left(Z,\omega_2-\omega_0\right)$$

$$\widetilde{A}^*\left(Z,-\omega_3-\omega_0\right)\exp\left(ik_0 z\right)\Bigg]\mathrm{d}\omega_1\mathrm{d}\omega_2\mathrm{d}\omega_3 + \text{c.c.} \tag{1.4.27}$$

Taylor expansion in the vicinity of $\omega_1 = \omega_0$, $\omega_2 = \omega_0$ and $\omega_3 = -\omega_0$ in Eq.(1.4.27) yields :

$$-\left(\frac{1}{2\pi}\right)^2 \int\limits_{-\infty}^{+\infty}\int\limits_{-\infty}^{+\infty}\int\limits_{-\infty}^{+\infty}\left[\delta\left(\omega-(\omega_1+\omega_2+\omega_3)\right)\left(\omega_0^2+2\omega_0\left(\omega_1-\omega_0\right)^2+2\omega_0\left(\omega_2-\omega_0\right)^2\right.\right.$$

$$\left.+ 2\omega_0\left(\omega_3+\omega_0\right)^2+\dots\right)\left(\widetilde{\chi}^{(3)}\left(x,y,\omega_0,\omega_0,-\omega_0\right)+\frac{\partial}{\partial\omega_1}\left[\widetilde{\chi}^{(3)}\left(x,y,\omega_0,\omega_0,-\omega_0\right)\right]\right.$$

$$\left(\omega_1-\omega_0\right)+\frac{\partial}{\partial\omega_2}\left[\widetilde{\chi}^{(3)}\left(x,y,\omega_0,\omega_0,-\omega_0\right)\right]\left(\omega_2-\omega_0\right)+\frac{\partial}{\partial\omega_3}\left[\widetilde{\chi}^{(3)}\left(x,y,\omega_0,\omega_0,-\omega_0\right)\right]$$

$$\left.\left(\omega_3+\omega_0\right)+\dots\right)\left(\mathbf{U}\left(x,y,\omega_0\right)\cdot\mathbf{U}\left(x,y,\omega_0\right)\right)\mathbf{U}^*\left(x,y,-\omega_0\right)\widetilde{A}\left(Z,\omega_1-\omega_0\right)$$

$$\widetilde{A}\left(Z,\omega_2-\omega_0\right)\widetilde{A}^*\left(Z,-\omega_3-\omega_0\right)\exp\left(ik_0 z\right)\Bigg]\mathrm{d}\omega_1\mathrm{d}\omega_2\mathrm{d}\omega_3. \tag{1.4.28}$$

Taking the inverse Fourier transform of Eq.(1.4.28) yields :

$$-\left(\frac{1}{2\pi}\right)^4 \int\limits_{-\infty}^{+\infty}\exp\left(-i\omega t\right)\,\mathrm{d}\omega\int\limits_{-\infty}^{+\infty}\exp\left(i\left(\omega-(\omega_1+\omega_2+\omega_3)\right)t'\right)\,\mathrm{d}t'$$

$$\int\limits_{-\infty}^{+\infty}\int\limits_{-\infty}^{+\infty}\int\limits_{-\infty}^{+\infty}\left\{\left(\mathbf{U}\left(x,y,\omega_0\right)\cdot\mathbf{U}\left(x,y,\omega_0\right)\right)\mathbf{U}^*\left(x,y,-\omega_0\right)\widetilde{A}\left(Z,\omega_1-\omega_0\right)\widetilde{A}\left(Z,\omega_2-\omega_0\right)\right.$$

$$\widetilde{A}^*\left(Z,-\omega_3-\omega_0\right)\exp\left(ik_0 z\right)\,\omega_0^2\left(\widetilde{\chi}^{(3)}\left(x,y,\omega_0,\omega_0,-\omega_0\right)+\frac{\partial}{\partial\omega_1}\left[\widetilde{\chi}^{(3)}\left(x,y,\omega_0,\omega_0,-\omega_0\right)\right]\right.$$

$$\left(\omega_1-\omega_0\right)+\frac{\partial}{\partial\omega_2}\left[\widetilde{\chi}^{(3)}\left(x,y,\omega_0,\omega_0,-\omega_0\right)\right]\left(\omega_2-\omega_0\right)+\frac{\partial}{\partial\omega_3}\left[\widetilde{\chi}^{(3)}\left(x,y,\omega_0,\omega_0,-\omega_0\right)\right]$$

$$\left.\left.\left(\omega_3+\omega_0\right)+\dots\right)\right\}\mathrm{d}\omega_1\mathrm{d}\omega_2\mathrm{d}\omega_3. \tag{1.4.29}$$

Equation (1.4.29) further simplifies to [61]:

$$
-\left(\frac{1}{2\pi}\right)^4 \int\limits_{-\infty}^{+\infty}\int\limits_{-\infty}^{+\infty}\int\limits_{-\infty}^{+\infty}\int\limits_{-\infty}^{+\infty}\int\limits_{-\infty}^{+\infty} \Bigg\{ \left(\mathbf{U}\left(x,y,\omega_0\right)\cdot\mathbf{U}\left(x,y,\omega_0\right)\right)\mathbf{U}^*\left(x,y,-\omega_0\right)\tilde{A}\left(Z,\omega_1-\omega_0\right)
$$

$$
\tilde{A}\left(Z,\omega_2-\omega_0\right)\tilde{A}^*\left(Z,-\omega_3-\omega_0\right)\exp\left(ik_0z\right)\,\omega_0^2\Big(\tilde{\chi}^{(3)}\left(x,y,\,\omega_0,\omega_0,-\omega_0\right)
$$

$$
+\frac{\partial}{\partial\omega_1}\left[\tilde{\chi}^{(3)}\left(x,y,\,\omega_0,\omega_0,-\omega_0\right)\right]\left(\omega_1-\omega_0\right)+\frac{\partial}{\partial\omega_2}\left[\tilde{\chi}^{(3)}\left(x,y,\,\omega_0,\omega_0,-\omega_0\right)\right]\left(\omega_2-\omega_0\right)
$$

$$
+\frac{\partial}{\partial\omega_3}\left[\tilde{\chi}^{(3)}\left(x,y,\,\omega_0,\omega_0,-\omega_0\right)\right]\left(\omega_3+\omega_0\right)+\ldots\Big)\exp\left(-i\omega\left(t-t'\right)\right)
$$

$$
\exp\left(-i\left(\omega_1+\omega_2+\omega_3\right)t'\right)\Bigg\}\mathrm{d}\omega\mathrm{d}\omega_1\mathrm{d}\omega_2\mathrm{d}\omega_3\mathrm{d}t'. \tag{1.4.30}
$$

Further, it can be noted that integration over ω in Eq.(1.4.30) can be written as

$$
\int\limits_{-\infty}^{+\infty}\exp\left(-i\omega\left(t-t'\right)\right)\,\mathrm{d}\omega = 2\pi\delta\left(t-t'\right), \tag{1.4.31}
$$

and thus the integration over t' is equivalent to replacing t' with t. It is also convenient to write $\exp\left(-i\left(\omega_1+\omega_2+\omega_3\right)t'\right)$ in the following form :

$$
\exp\left(-i\left(\omega_1+\omega_2+\omega_3\right)t'\right) = \exp\left(-i\omega_0t'\right)\exp\left(-i\Omega_1T'\right)\exp\left(-i\Omega_2T'\right)
$$

$$
\exp\left(-i\Omega_3T'\right), \tag{1.4.32}
$$

where $\varepsilon\Omega_1 \equiv \omega_1-\omega_0$, $\varepsilon\Omega_2 \equiv \omega_2-\omega_0$ and $\varepsilon\Omega_3 \equiv \omega_3+\omega_0$. Considering terms only up to the leading order in Eq.(1.4.30), i.e., considering only the effect due to $\omega_0^2\tilde{\chi}^{(3)}\left(x,y,\,\omega_0,\omega_0,-\omega_0\right)$ in Eq.(1.4.30), the following form is given as [61]:

$$
-\left(\frac{\varepsilon}{2\pi}\right)^3\exp\left(i\left(k_0z-\omega_0t\right)\right)\omega_0^2\tilde{\chi}^{(3)}\left(x,y,\,\omega_0,\omega_0,-\omega_0\right)\left(\mathbf{U}\left(x,y,\omega_0\right)\cdot\mathbf{U}\left(x,y,\omega_0\right)\right)
$$

$$
\mathbf{U}^*\left(x,y,-\omega_0\right)\int\limits_{-\infty}^{+\infty}\tilde{A}\left(Z,\varepsilon\Omega_1\right)\exp\left(-i\Omega_1T\right)\mathrm{d}\Omega_1\int\limits_{-\infty}^{+\infty}\tilde{A}\left(Z,\varepsilon\Omega_2\right)\exp\left(-i\Omega_2T\right)\mathrm{d}\Omega_2
$$

$$
\int\limits_{-\infty}^{+\infty}\tilde{A}\left(Z,-\varepsilon\Omega_3\right)\exp\left(-i\Omega_3T\right)\mathrm{d}\Omega_3. \tag{1.4.33}
$$

Substitution of Eq.(1.4.13) to Eq.(1.4.33) further reduces it to the form :

$$- \varepsilon^3 \exp\left(i\left(k_0 z - \omega_0 t\right)\right) \omega_0^2 \widetilde{\chi}^{(3)}\left(x, y, \omega_0, \omega_0, -\omega_0\right)\left(\mathbf{U}\left(x, y, \omega_0\right) \cdot \mathbf{U}\left(x, y, \omega_0\right)\right)$$

$$\mathbf{U}^*\left(x, y, -\omega_0\right) A^2\left(Z, T; \varepsilon\right) A^*\left(Z, T; \varepsilon\right). \tag{1.4.34}$$

Equation (1.4.34) is only one of the six terms of the nonlinear polarization proportional to $\exp\left(\pm i k_0 z\right)$ obtained, starting from the simplification of Eq.(1.4.26). The other five terms can be simplified by a similar procedure. The final form of the nonlinear polarization proportional to $\exp\left(\pm i k_0 z\right)$ is thus obtained as [61]:

$$- \varepsilon^3 \omega_0^2 \Bigg(\exp\left(i\left(k_0 z - \omega_0 t\right)\right) A^2\left(Z, T; \varepsilon\right) A^*\left(Z, T; \varepsilon\right) + \exp\left(-i\left(k_0 z - \omega_0 t\right)\right)$$

$$\left(A^*\left(Z, T; \varepsilon\right)\right)^2 A\left(Z, T; \varepsilon\right) \Bigg) \Bigg(\widetilde{\chi}^{(3)}\left(x, y, \omega_0, \omega_0, -\omega_0\right)\left(\mathbf{U}\left(x, y, \omega_0\right) \cdot \mathbf{U}\left(x, y, \omega_0\right)\right)$$

$$\mathbf{U}^*\left(x, y, -\omega_0\right) + \widetilde{\chi}^{(3)}\left(x, y, \omega_0, -\omega_0, \omega_0\right)\left(\mathbf{U}\left(x, y, \omega_0\right) \cdot \mathbf{U}^*\left(x, y, \omega_0\right)\right) \mathbf{U}\left(x, y, -\omega_0\right)$$

$$+ \widetilde{\chi}^{(3)}\left(x, y, \omega_0, -\omega_0, \omega_0\right)\left(\mathbf{U}^*\left(x, y, \omega_0\right) \cdot \mathbf{U}\left(x, y, \omega_0\right)\right) \mathbf{U}\left(x, y, -\omega_0\right) \Bigg) \cdot A^2 A^*$$

$$\tag{1.4.35}$$

iv) Asymptotic expansion

Equation (1.4.18) can be rewritten in the form [61]:

$$\nabla^2 \mathbf{E} - \frac{1}{c^2} F_2(x, y, z, t) = \frac{1}{c^2} \frac{\partial^2}{\partial t^2} \Bigg[\int\limits_{-\infty}^{+\infty} \int\limits_{-\infty}^{+\infty} \int\limits_{-\infty}^{+\infty} \Big\{ \chi^{(3)}\left(x, y, t - t_1, t - t_2, t - t_3\right)$$

$$\left(\mathbf{E}\left(x, y, z, t_1\right) \cdot \mathbf{E}\left(x, y, z, t_2\right)\right) \mathbf{E}\left(x, y, z, t_3\right) \Big\} dt_1 dt_2 dt_3 \Bigg),$$

$$\tag{1.4.36}$$

where :

$$F_2(x, y, z, t) \equiv \frac{\partial^2 \mathbf{E}}{\partial t^2} + \frac{\partial^2}{\partial t^2} \Bigg[\int\limits_{-\infty}^{+\infty} \Big\{ \chi^{(1)}\left(x, y, t - t'\right) \mathbf{E}\left(x, y, z, t'\right) \Big\} dt' \Bigg].$$

Asymptotic expansions of $\mathbf{E}$ and $\dfrac{\partial A}{\partial Z}$ are considered separately with respect to ε and are given by [61]:

$$
\begin{aligned}
\mathbf{E} &= \mathbf{E}_0 + \varepsilon \mathbf{E}_1 + \varepsilon^2 \mathbf{E}_2 + \ldots \qquad \text{and} \\
\frac{\partial A}{\partial Z} &= \frac{\partial A}{\partial Z_1} + \varepsilon \frac{\partial A}{\partial Z_2} + \varepsilon^2 \frac{\partial A}{\partial Z_3} + \ldots,
\end{aligned}
\qquad (1.4.37)
$$

where multiple scales with respect to z are introduced in the form [61]:

$$
Z_1 \equiv \varepsilon z, \; Z_2 \equiv \varepsilon^2 z, \ldots, Z_n \equiv \varepsilon^n z, \qquad (1.4.38)
$$

n being a positive integer. As the next step, Eq.(1.4.37) and Eq.(1.4.38) are substituted into Eq.(1.4.36) and analyzed for each ε^n. It can be noted from Eq.(1.4.36) that the lowest order ε simply gives the guiding mode of optical wave packets [61]. At the second lowest order ε^2, Eq.(1.4.36) gives rise to the long term behavior of the guided wave propagation along z with the group velocity of $\dfrac{1}{k_0'}$ where $k_0' \equiv \left.\dfrac{\partial k}{\partial \omega}\right|_{\omega=\omega_0}$. In order to represent the linear response of the electric field, a linear symmetric operator $\widehat{\mathbf{L}}$ is introduced which is a matrix having the form [61]:

$$
\widehat{\mathbf{L}}\left(\frac{\partial}{\partial x}, \frac{\partial}{\partial y}, ik, -i\omega \right) \equiv
\begin{pmatrix}
L_{11} & -\dfrac{\partial^2}{\partial x \partial y} & -ik\dfrac{\partial}{\partial x} \\[2mm]
-\dfrac{\partial^2}{\partial x \partial y} & L_{22} & -ik\dfrac{\partial}{\partial y} \\[2mm]
-ik\dfrac{\partial}{\partial x} & -ik\dfrac{\partial}{\partial y} & L_{33}
\end{pmatrix},
\qquad (1.4.39)
$$

where

$$
\begin{aligned}
L_{11} &= \frac{\partial^2}{\partial y^2} - k^2 + \left(\frac{n\omega}{c}\right)^2, \\[2mm]
L_{22} &= \frac{\partial^2}{\partial x^2} - k^2 + \left(\frac{n\omega}{c}\right)^2, \\[2mm]
L_{33} &= \frac{\partial^2}{\partial x^2} + \frac{\partial^2}{\partial y^2} + \left(\frac{n\omega}{c}\right)^2.
\end{aligned}
$$

Equation (1.4.36) can be written in terms of the linear operator $\widehat{\mathbf{L}}$ and is given by [61]:

$$
\begin{aligned}
\widehat{\mathbf{L}}\left(\frac{\partial}{\partial x}, \frac{\partial}{\partial y}, ik, -i\omega\right) \mathbf{E} &\equiv \nabla^2 \mathbf{E} - \frac{1}{c^2}\left(\frac{\partial^2 \mathbf{E}}{\partial t^2} + \frac{\partial^2}{\partial t^2}\left[\int\limits_{-\infty}^{+\infty}\left\{\chi^{(1)}\left(x, y, t - t'\right)\right.\right.\right. \\
&\qquad \left.\left.\left. \mathbf{E}\left(x, y, z, t'\right)\right\} dt'\right]\right) \\
&= \frac{1}{c^2}\frac{\partial^2}{\partial t^2}\left[\int\limits_{-\infty}^{+\infty}\int\limits_{-\infty}^{+\infty}\int\limits_{-\infty}^{+\infty}\left\{\chi^{(3)}\left(x, y, t - t_1, t - t_2, t - t_3\right)\right.\right. \\
&\qquad \left.\left. \left(\mathbf{E}\left(x, y, z, t_1\right)\cdot \mathbf{E}\left(x, y, z, t_2\right)\right)\mathbf{E}\left(x, y, z, t_3\right)\right\} dt_1 dt_2 dt_3\right].
\end{aligned}
$$

$$(1.4.40)$$

The mode distribution function $\mathbf{U}\left(x, y, \omega_0\right)$ is actually the solution that is to be determined from the relation [61]:

$$
\widehat{\mathbf{L}}\left(\frac{\partial}{\partial x}, \frac{\partial}{\partial y}, ik, -i\omega\right) \mathbf{U}\left(x, y, \omega_0\right) = 0. \tag{1.4.41}
$$

For a finite discrete set of values of $k = k_i\left(\omega\right)$, $\left(i = 1 \ldots N\right)$, Eq.(1.4.41) yield non trivial solutions $U_i\left(x, y, \omega_0\right)$, $\left(i = 1, 2, 3\right)$, that decay to zero as $x^2 + y^2 \to \infty$. $\mathbf{U}\left(x, y, \omega_0\right)$ is given by the column vector [61]:

$$
\mathbf{U}\left(x, y, \omega_0\right) \equiv \begin{pmatrix} U_1\left(x, y, \omega_0\right) \\ U_2\left(x, y, \omega_0\right) \\ U_3\left(x, y, \omega_0\right) \end{pmatrix}. \tag{1.4.42}
$$

The dispersion relation $D\left(\left[\mathbf{U}\right], k, \omega\right)$ is then determined by the relation [61]:

$$
D\left(\left[\mathbf{U}\right], k, \omega\right) \equiv \left\langle \mathbf{U}, \widehat{\mathbf{L}}\mathbf{U}\right\rangle = 0, \tag{1.4.43}
$$

where the inner product between two complex column vectors, say $\mathbf{a}$ and $\mathbf{b}$ is given by the Fredholm alternative theorem extended over a surface say dS and

are given by [61]:

$$\langle \mathbf{a}, \mathbf{b} \rangle = \int\limits_{-\infty}^{+\infty} (a_1^* b_1 + a_2^* b_2 + a_3^* b_3) \, d\mathbf{S}. \qquad (1.4.44)$$

From Eq.(1.4.43), the dispersion relation is given by [61]:

$$k^2 = \frac{\left(\dfrac{\omega}{c}\right)^2 \displaystyle\int\limits_{-\infty}^{+\infty} n^2 (x,y,\omega) \, |\mathbf{U}|^2 \, d\mathbf{S} - \displaystyle\int\limits_{-\infty}^{+\infty} \left| \left(\hat{\mathbf{x}} \dfrac{\partial}{\partial x} + \hat{\mathbf{y}} \dfrac{\partial}{\partial y} \right) \mathbf{U} \right|^2 d\mathbf{S}}{\displaystyle\int\limits_{-\infty}^{+\infty} |\mathbf{U}|^2 \, d\mathbf{S}}. \qquad (1.4.45)$$

ε contribution from Eq.(1.4.40) results in the transverse structure which is of the form [61]:

$$\widehat{\mathbf{L}} \left(\frac{\partial}{\partial x}, \frac{\partial}{\partial y}, ik, -i\omega \right) \mathbf{E}_0 = 0. \qquad (1.4.46)$$

The form for $\mathbf{E}_0$ which satisfies Eq.(1.4.46) is given by [61]:

$$\mathbf{E}_0 = \mathbf{U} \exp \left(i \left(k_0 z - \omega_0 t \right) \right) + \text{c.c.} \qquad (1.4.47)$$

Before studying the ε^2 contribution of Eq.(1.4.40), the following parameters are defined for convenience [61]:

$$
\begin{aligned}
X &\equiv \frac{\partial}{\partial x}, \\
Y &\equiv \frac{\partial}{\partial y}, \\
K - K_0 &\equiv i \left(k - k_0 \right), \\
&= \varepsilon \frac{\partial}{\partial Z_1} + \varepsilon^2 \frac{\partial}{\partial Z_2} + \ldots, \\
\Omega - \Omega_0 &\equiv -i \left(\omega - \omega_0 \right), \\
&= \varepsilon \frac{\partial}{\partial T}, \\
\widehat{\mathbf{L}}_1 &\equiv \widehat{\mathbf{L}} \left(X, Y, K_0, \Omega_0 \right), \\
\widehat{\mathbf{L}}_2 &\equiv \left. \frac{\partial \widehat{\mathbf{L}}}{\partial K} \right|_{K = K_0},
\end{aligned}
$$

$$\widehat{L}_3 \equiv \left.\frac{\partial \widehat{L}}{\partial \Omega}\right|_{\Omega=\Omega_0},$$

$$\widehat{L}_{22} \equiv \left.\frac{\partial^2 \widehat{L}}{\partial K^2}\right|_{K=K_0},$$

$$(1.4.48)$$

and so on. The linear symmetric operator $\widehat{L}\left(\dfrac{\partial}{\partial x}, \dfrac{\partial}{\partial y}, ik + \varepsilon\dfrac{\partial}{\partial Z_1} + \varepsilon^2\dfrac{\partial}{\partial Z_2} + \right.$

$\left. \ldots, -i\omega + \varepsilon\dfrac{\partial}{\partial T}\right)$ is expanded in a Taylor series, to give :

$$\widehat{L}\left(\frac{\partial}{\partial x}, \frac{\partial}{\partial y}, ik + \varepsilon\frac{\partial}{\partial Z_1} + \varepsilon^2\frac{\partial}{\partial Z_2} + \ldots, -i\omega + \varepsilon\frac{\partial}{\partial T}\right) \equiv$$

$$\widehat{L}_1 + \widehat{L}_2\left(\varepsilon\frac{\partial}{\partial Z_1}\right) + \widehat{L}_3\left(\varepsilon\frac{\partial}{\partial T}\right) + \widehat{L}_2\left(\varepsilon^2\frac{\partial}{\partial Z_2}\right) + \frac{1}{2}\widehat{L}_{22}\left(\varepsilon^2\frac{\partial^2}{\partial Z_1^2}\right)$$

$$+ \frac{1}{2}\widehat{L}_{33}\left(\varepsilon^2\frac{\partial^2}{\partial T^2}\right) + \widehat{L}_{23}\left(\varepsilon^2\frac{\partial^2}{\partial Z_1 \partial T}\right) + \ldots \qquad (1.4.49)$$

As a next step, differentiation with respect to ω of the dispersion relation given by Eq.(1.4.43) is carried out to obtain the certain inner products. Since Eq.(1.4.43) holds for all ω, the following result is obtained [61]:

$$\frac{dD}{d\omega} = \left\langle \frac{dU}{d\omega}, \widehat{L}U \right\rangle + \left\langle U, \widehat{L}\frac{dU}{d\omega} \right\rangle + \left\langle U, \frac{d\widehat{L}}{d\omega}U \right\rangle = 0. \qquad (1.4.50)$$

As $\widehat{L}$ is a self-adjoint operator, $\left\langle \dfrac{dU}{d\omega}, \widehat{L}U \right\rangle = \left\langle U, \widehat{L}\dfrac{dU}{d\omega} \right\rangle$. Hence from Eq.(1.4.50), the following relation is obtained to be [61]:

$$2\left\langle \frac{dU}{d\omega}, \widehat{L}U \right\rangle + \left\langle U, \frac{d\widehat{L}}{d\omega}U \right\rangle = 0. \qquad (1.4.51)$$

But, from the dispersion relation given by Eq.(1.4.43), $\left\langle \dfrac{dU}{d\omega}, \widehat{L}U \right\rangle = 0$. Now from Eq.(1.4.48),

$$\left.\frac{d\widehat{L}}{d\omega}\right|_{k_0,\omega_0} = \left.\frac{\partial \widehat{L}}{\partial(ik)}\frac{d(ik)}{d\omega}\right|_{k_0,\omega_0} + \left.\frac{\partial \widehat{L}}{\partial(-i\omega)}\frac{d(-i\omega)}{d\omega}\right|_{k_0,\omega_0},$$

$$= ik_0'\widehat{L}_2 - i\widehat{L}_3. \qquad (1.4.52)$$

Substituting this relation in Eq.(1.4.51) yields :

$$\left\langle \mathbf{U}, \widehat{\mathbf{L}}_3 \mathbf{U} \right\rangle = k_0' \left\langle \mathbf{U}, \widehat{\mathbf{L}}_2 \mathbf{U} \right\rangle. \tag{1.4.53}$$

ε^2 contribution from Eq.(1.4.40) results in the linear propagation equation for wave packets and is given by [61]:

$$\widehat{\mathbf{L}} \left(\frac{\partial}{\partial x}, \frac{\partial}{\partial y}, ik + \varepsilon \frac{\partial}{\partial Z_1} + \varepsilon^2 \frac{\partial}{\partial Z_2} + \ldots, -i\omega + \varepsilon \frac{\partial}{\partial T} \right) \varepsilon \mathbf{E}_1 = 0. \tag{1.4.54}$$

Using Eq.(1.4.49), Eq.(1.4.54) simplifies to the form :

$$\widehat{\mathbf{L}}_1 \left(\varepsilon \mathbf{E}_1 \right) + \varepsilon^2 \left(\widehat{\mathbf{L}}_2 \mathbf{U} \left(x, y, \omega_0 \right) \frac{\partial A}{\partial Z_1} + \widehat{\mathbf{L}}_3 \mathbf{U} \left(x, y, \omega_0 \right) \frac{\partial A}{\partial T} \right) \exp \left(i \left(k_0 z - \omega_0 t \right) \right) + \text{c.c.} = 0. \tag{1.4.55}$$

Let $\mathbf{E}_1 = \varepsilon \mathbf{U}_1 \exp \left(i \left(k_0 z - \omega_0 t \right) \right) + \text{c.c.}$ Hence Eq.(1.4.55) takes the form :

$$\mathbf{F}_1 \equiv \widehat{\mathbf{L}}_1 \mathbf{U}_1 = - \left(\widehat{\mathbf{L}}_2 \mathbf{U} \left(x, y, \omega_0 \right) \frac{\partial A}{\partial Z_1} + \widehat{\mathbf{L}}_3 \mathbf{U} \left(x, y, \omega_0 \right) \frac{\partial A}{\partial T} \right). \tag{1.4.56}$$

Solvability condition of $\mathbf{E}_1$ requires that the transverse solution of Eq.(1.4.41) be a smooth solution vanishing at the boundary $x^2 + y^2 \to \infty$ which is satisfied by the Fredholm alternative theorem. Hence for Eq.(1.4.56), Fredholm alternative theorem thereby demands [61]:

$$\left\langle \mathbf{U}, \mathbf{F}_1 \right\rangle = \left\langle \mathbf{U}, -\widehat{\mathbf{L}}_2 \mathbf{U} \right\rangle \frac{\partial A}{\partial Z_1} + \left\langle \mathbf{U}, -\widehat{\mathbf{L}}_3 \mathbf{U} \right\rangle \frac{\partial A}{\partial T} = 0. \tag{1.4.57}$$

But from Eq.(1.4.53),

$$\left\langle \mathbf{U}, -\widehat{\mathbf{L}}_2 \mathbf{U} \right\rangle \left(\frac{\partial A}{\partial Z_1} + k_0' \frac{\partial A}{\partial T} \right) = 0. \tag{1.4.58}$$

But $\left\langle \mathbf{U}, -\widehat{\mathbf{L}}_2 \mathbf{U} \right\rangle = -2ik_0 \left\langle \mathbf{U}, \mathbf{U} \right\rangle \neq 0.$ Hence from Eq.(1.4.58),

$$\frac{\partial A}{\partial Z_1} + k_0' \frac{\partial A}{\partial T} = 0. \tag{1.4.59}$$

Equation (1.4.59) represents the propagation of a wave packet at the group velocity of $\frac{1}{k_0'}$ [61]. Substitution of Eq.(1.4.59) into Eq.(1.4.56) yields :

$$
\begin{aligned}
\mathbf{F}_1 &= \left(\widehat{\mathbf{L}}_2 k_0' - \widehat{\mathbf{L}}_3\right) \mathbf{U}\frac{\partial A}{\partial T}, \\
&= \left(-i\widehat{\mathbf{L}}_2 k_0' + i\widehat{\mathbf{L}}_3\right) \mathbf{U} \left(i\frac{\partial A}{\partial T}\right), \\
&= -i\left.\frac{d\widehat{\mathbf{L}}}{d\omega}\right|_{k_0,\omega_0} \mathbf{U}\frac{\partial A}{\partial T}.
\end{aligned}
\tag{1.4.60}
$$

From the above equation, it is clear that the solvability condition gives rise to slow variation of the mode distribution U with respect to ω [61]. Now differentiation of Eq.(1.4.41) with respect to ω and evaluating the result at $\omega = \omega_0$ yield the relation [61]:

$$
\widehat{\mathbf{L}} \left.\frac{d\mathbf{U}}{d\omega}\right|_{k_0,\omega_0} = \left(-i\widehat{\mathbf{L}}_2 k_0' + i\widehat{\mathbf{L}}_3\right) \mathbf{U}.
\tag{1.4.61}
$$

Substitution of the above equation in Eq.(1.4.60) results in the relation :

$$
\mathbf{F}_1 = i\widehat{\mathbf{L}} \left.\frac{d\mathbf{U}}{d\omega}\right|_{k_0,\omega_0} \frac{\partial A}{\partial T}.
\tag{1.4.62}
$$

Thus from Eqs.(1.4.56) and (1.4.62), the following relation is obtained :

$$
\mathbf{U}_1 = i\left.\frac{d\mathbf{U}}{d\omega}\right|_{k_0,\omega_0} \frac{\partial A}{\partial T}.
\tag{1.4.63}
$$

Thus upto ε^2 [61],

$$
\mathbf{E}_0 + \varepsilon\mathbf{E}_1 = \varepsilon \left(\mathbf{U}\left(x,y,\omega_0\right) + i\varepsilon \left.\frac{d\mathbf{U}}{d\omega}\right|_{k_0,\omega_0} \frac{\partial}{\partial T}\right) A\left(Z,T\right)\exp\left(i\left(k_0 z - \omega_0 t\right)\right) + \text{c.c.}
\tag{1.4.64}
$$

Differentiating $\left.\dfrac{d\widehat{\mathbf{L}}}{d\omega}\right|_{k_0,\omega_0}$ in Eq.(1.4.52) once again with respect to ω and evaluating it at $\omega = \omega_0$, the following expression is obtained :

$$
\left.\frac{d^2\widehat{\mathbf{L}}}{d\omega^2}\right|_{k_0,\omega_0} = ik_0''\widehat{\mathbf{L}}_2 - k_0'^2\widehat{\mathbf{L}}_{22} + 2k_0'\widehat{\mathbf{L}}_{23} - \widehat{\mathbf{L}}_{33},
\tag{1.4.65}
$$

where the operators $\widehat{L}_{22}, \widehat{L}_{23}, \widehat{L}_{33}$ etc., are defined in Eq.(1.4.48). Hence the inner product between U and $\dfrac{d^2\widehat{L}}{d\omega^2}\bigg|_{k_0,\omega_0}$ U is given by :

$$\left\langle U, \frac{d^2\widehat{L}}{d\omega^2}\bigg|_{k_0,\omega_0} U \right\rangle = ik_0'' \left\langle U, \widehat{L}_2 U \right\rangle - k_0'^2 \left\langle U, \widehat{L}_{22} U \right\rangle + 2k_0' \left\langle U, \widehat{L}_{23} U \right\rangle - \left\langle U, \widehat{L}_{33} U \right\rangle .$$

$$(1.4.66)$$

Differentiating $\dfrac{dD}{d\omega}$ in Eq.(1.4.50) and equating it to zero yields :

$$\begin{aligned} \frac{d^2 D}{d\omega^2} &= 2\left\langle U, \left(ik_0'\widehat{L}_2 - i\widehat{L}_3\right) \frac{dU}{d\omega}\bigg|_{k_0,\omega_0} \right\rangle + ik_0'' \left\langle U, \widehat{L}_2 U \right\rangle - k_0'^2 \left\langle U, \widehat{L}_{22} U \right\rangle \\ &\quad + 2k_0' \left\langle U, \widehat{L}_{23} U \right\rangle - \left\langle U, \widehat{L}_{33} U \right\rangle \\ &= 0. \end{aligned}$$

$$(1.4.67)$$

ε^3 contribution from Eq.(1.4.40) results in the derivation of the scalar nonlinear Schrödinger equation and is given by [61]:

$$\begin{aligned} F_2 &\equiv \widehat{L}\left(\frac{\partial}{\partial x}, \frac{\partial}{\partial y}, ik + \varepsilon\frac{\partial}{\partial Z_1} + \varepsilon^2\frac{\partial}{\partial Z_2} + \ldots, -i\omega + \varepsilon\frac{\partial}{\partial T}\right) \varepsilon^2 E_2 \\ &= \frac{1}{c^2}\frac{\partial^2}{\partial t^2}\bigg[\int_{-\infty}^{+\infty}\int_{-\infty}^{+\infty}\int_{-\infty}^{+\infty} \Big\{\chi^{(3)}(x,y,t-t_1,t-t_2,t-t_3) \\ &\quad (E_0(x,y,z,t_1) \cdot E_0(x,y,z,t_2)) E_0(x,y,z,t_3)\Big\} \, dt_1 dt_2 dt_3\bigg] \end{aligned}$$

$$(1.4.68)$$

F_2 contains the following terms. They are a) the phase components of E_2 which are $\exp(\pm i(k_0 z \mp \omega_0 t))$ and $\exp(\pm 3i(k_0 z \mp \omega_0 t))$, and which can be explicitly represented as [61]:

$$E_2 = \varepsilon U_2 \exp(i(k_0 z - \omega_0 t)) + \varepsilon^3 V_2 \exp(3i(k_0 z - \omega_0 t)) + \text{c.c.} \qquad (1.4.69)$$

and b) the nonlinear polarization term [61] proportional to $\exp(\pm i(k_0 z - \omega_0 t))$ given by Eq.(1.4.34). Following a similar procedure used to determine the inner product $\langle U, F_1 \rangle$ in Eq.(1.4.57), the inner product $\langle U, F_2 \rangle$ is determined likewise.

Before determining the inner product, the expression for $\mathbf{F}_2$ is given as follows [61]:

$$\mathbf{F}_2 \equiv -\left(\widehat{\mathbf{L}}_2 \mathbf{U} \frac{\partial A}{\partial Z_2} + \frac{1}{2}\widehat{\mathbf{L}}_{22}\mathbf{U}\frac{\partial^2 A}{\partial Z_1^2} + \frac{1}{2}\widehat{\mathbf{L}}_{33}\mathbf{U}\frac{\partial^2 A}{\partial T^2} + \widehat{\mathbf{L}}_{23}\mathbf{U}\frac{\partial^2 A}{\partial Z_1 \partial T} \right)$$

$$- i\left(\widehat{\mathbf{L}}_2 \left.\frac{d\mathbf{U}}{d\omega}\right|_{k_0,\omega_0} \frac{\partial^2 A}{\partial Z_1 \partial T} + \widehat{\mathbf{L}}_3 \left.\frac{d\mathbf{U}}{d\omega}\right|_{k_0,\omega_0} \frac{\partial^2 A}{\partial T^2} \right)$$

$$- \left(\frac{\omega_0}{c}\right)^2 \left(\widetilde{\chi}^{(3)}\left(x,y,\omega_0,\omega_0,-\omega_0\right) \left(\mathbf{U}\left(x,y,\omega_0\right)\cdot\mathbf{U}\left(x,y,\omega_0\right)\right)\mathbf{U}^*\left(x,y,-\omega_0\right) \right.$$

$$+ \widetilde{\chi}^{(3)}\left(x,y,\omega_0,-\omega_0,\omega_0\right) \left(\mathbf{U}\left(x,y,\omega_0\right)\cdot\mathbf{U}^*\left(x,y,\omega_0\right)\right)\mathbf{U}\left(x,y,-\omega_0\right)$$

$$\left. + \widetilde{\chi}^{(3)}\left(x,y,\omega_0,-\omega_0,\omega_0\right) \left(\mathbf{U}^*\left(x,y,\omega_0\right)\cdot\mathbf{U}\left(x,y,\omega_0\right)\right)\mathbf{U}\left(x,y,-\omega_0\right) \right)A^2 A^*,$$

$$(1.4.70)$$

where the terms within the first parenthesis originate from the $\varepsilon\mathbf{E}_0$ and ε^2 contributions of the linear operator $\widehat{\mathbf{L}}$, whereas those in the second parenthesis originate from the $\varepsilon^2\mathbf{E}_1$ and ε contributions of the linear operator $\widehat{\mathbf{L}}$ and those in the third parenthesis originate from the nonlinear polarization term proportional to $\exp\left(\pm i\left(k_0 z - \omega_0 t\right)\right)$ given by Eq.(1.4.34). Fredholm alternative theorem demands $\langle \mathbf{U}, \mathbf{F}_2 \rangle = 0$, where [61]:

$$\langle \mathbf{U}, \mathbf{F}_2 \rangle = \left\langle \mathbf{U}, -\widehat{\mathbf{L}}_2\mathbf{U} \right\rangle \frac{\partial A}{\partial Z_2} + i\frac{k_0''}{2k_0'}\left\langle \mathbf{U}, -\widehat{\mathbf{L}}_2\mathbf{U} \right\rangle \frac{\partial^2 A}{\partial Z_1 \partial T}$$

$$+ \frac{1}{2k_0'}\left\langle \mathbf{U}, -\widehat{\mathbf{L}}_{33}\mathbf{U} \right\rangle \left(\frac{\partial^2 A}{\partial Z_1 \partial T} + k_0'\frac{\partial^2 A}{\partial T^2} \right)$$

$$- \frac{\omega_0^2}{c^2}\left\langle \left\{ \mathbf{U}, \left(\widetilde{\chi}^{(3)}\left(x,y,\omega_0,\omega_0,-\omega_0\right) \left(\mathbf{U}\left(x,y,\omega_0\right)\cdot\mathbf{U}\left(x,y,\omega_0\right)\right)\mathbf{U}^*\left(x,y,-\omega_0\right) \right. \right.\right.$$

$$+ \widetilde{\chi}^{(3)}\left(x,y,\omega_0,-\omega_0,\omega_0\right) \left(\mathbf{U}\left(x,y,\omega_0\right)\cdot\mathbf{U}^*\left(x,y,\omega_0\right)\right)\mathbf{U}\left(x,y,-\omega_0\right)$$

$$\left.\left.\left.+ \widetilde{\chi}^{(3)}\left(x,y,\omega_0,-\omega_0,\omega_0\right) \left(\mathbf{U}^*\left(x,y,\omega_0\right)\cdot\mathbf{U}\left(x,y,\omega_0\right)\right)\mathbf{U}\left(x,y,-\omega_0\right) \right) \right\} \right\rangle A^2 A^*.$$

$$(1.4.71)$$

Equation (1.4.71) is obtained by considering the following relation [61]:

$$\frac{k_0'}{2}\left\langle \mathbf{U},\widehat{\mathbf{L}}_{22}\mathbf{U}\right\rangle - \left\langle \mathbf{U},\widehat{\mathbf{L}}_{23}\mathbf{U}\right\rangle = \frac{1}{k_0'}\left\langle \mathbf{U},\left(ik_0'\widehat{\mathbf{L}}_2 - i\widehat{\mathbf{L}}_3\right)\frac{d\mathbf{U}}{d\omega}\bigg|_{k_0,\omega_0}\right\rangle$$
$$- \left\langle \mathbf{U},\widehat{\mathbf{L}}_{33}\mathbf{U}\right\rangle - i\frac{k_0''}{k_0'}\left\langle \mathbf{U},-\widehat{\mathbf{L}}_2\mathbf{U}\right\rangle \quad (1.4.72)$$

which in turn is obtained from Eq.(1.4.67). Substitution of Eq.(1.4.58) into Eq.(1.4.71) further simplifies it to :

$$\left\langle \mathbf{U},-\widehat{\mathbf{L}}_2\mathbf{U}\right\rangle \left(\frac{\partial A}{\partial Z_2} + \frac{i}{2}k_0''\frac{\partial^2 A}{\partial T^2}\right) = \frac{\omega_0^2}{c^2}\left\langle \left\{\mathbf{U},\left(\widetilde{\chi}^{(3)}\left(x,y,\omega_0,\omega_0,-\omega_0\right)\right.\right.\right.$$

$$\left(\mathbf{U}\left(x,y,\omega_0\right)\cdot\mathbf{U}\left(x,y,\omega_0\right)\right)\mathbf{U}^*\left(x,y,-\omega_0\right) + \widetilde{\chi}^{(3)}\left(x,y,\omega_0,-\omega_0,\omega_0\right)$$

$$\left(\mathbf{U}\left(x,y,\omega_0\right)\cdot\mathbf{U}^*\left(x,y,\omega_0\right)\right)\mathbf{U}\left(x,y,-\omega_0\right) + \widetilde{\chi}^{(3)}\left(x,y,\omega_0,-\omega_0,\omega_0\right)$$

$$\left.\left.\left(\mathbf{U}^*\left(x,y,\omega_0\right)\cdot\mathbf{U}\left(x,y,\omega_0\right)\right)\mathbf{U}\left(x,y,-\omega_0\right)\right)\right\}\right\rangle A^2 A^*. \quad (1.4.73)$$

In the above equation due to symmetry [61],

$$\widetilde{\chi}^{(3)}\left(x,y,\omega_0,\omega_0,-\omega_0\right) \approx \widetilde{\chi}^{(3)}\left(x,y,\omega_0,-\omega_0,\omega_0\right) \quad \text{and}$$

$$\mathbf{U}\left(x,y,\omega_0\right)\cdot\mathbf{U}^*\left(x,y,\omega_0\right) \approx \mathbf{U}^*\left(x,y,\omega_0\right)\cdot\mathbf{U}\left(x,y,\omega_0\right).$$

Thus Eq.(1.4.73) can be rewritten as :

$$\left(\frac{\partial A}{\partial Z_2} + \frac{i}{2}k_0''\frac{\partial^2 A}{\partial T^2}\right) - \frac{\omega_0^2}{c^2\left\langle \mathbf{U},-\widehat{\mathbf{L}}_2\mathbf{U}\right\rangle}\left\langle \mathbf{U},\left(\widetilde{\chi}^{(3)}\left[\left(\mathbf{U}\cdot\mathbf{U}\right)\mathbf{U}^* + 2\left(\mathbf{U}\cdot\mathbf{U}^*\right)\mathbf{U}\right]\right)\right\rangle A^2 A^* = 0.$$

$$(1.4.74)$$

Now

$$\left\langle \mathbf{U},-\widehat{\mathbf{L}}_2\mathbf{U}\right\rangle = -2ik_0\left\langle \mathbf{U},\mathbf{U}\right\rangle,$$
$$= -2ik_0\int|\mathbf{U}|^2\,\mathrm{d}\mathbf{S}, \quad (1.4.75)$$

and

$$\left\langle \mathbf{U},\left(\widetilde{\chi}^{(3)}\left[\left(\mathbf{U}\cdot\mathbf{U}\right)\mathbf{U}^* + 2\left(\mathbf{U}\cdot\mathbf{U}^*\right)\mathbf{U}\right]\right)\right\rangle \approx 3\widetilde{\chi}^{(3)}\left\langle \mathbf{U},|\mathbf{U}|^2\mathbf{U}\right\rangle,$$
$$= 3\widetilde{\chi}^{(3)}\left(\omega_0\right)\int|\mathbf{U}|^4\,\mathrm{d}\mathbf{S}, \quad (1.4.76)$$

where for simplicity, $\widetilde{\chi}^{(3)}$ is assumed to have negligible dependence on the transverse coordinates x and y and hence is out of the surface integral [61]. Also let

$$n_0 \equiv \frac{ck_0}{\omega_0},$$

$$n_2 \equiv \frac{3\widetilde{\chi}^{(3)}(\omega_0)}{2n_0} \quad \text{and}$$

$$g \equiv \frac{\int |U|^4 \, dS}{\int |U|^2 \, dS}. \tag{1.4.77}$$

Substitution of Eq.(1.4.77) into Eq.(1.4.74) yields [61, 30]

$$i\frac{\partial A}{\partial Z_2} - \frac{k_0''}{2}\frac{\partial^2 A}{\partial T^2} + \frac{gn_2\omega_0}{c}|A|^2 A = 0. \tag{1.4.78}$$

Therefore, from Eq.(1.4.37) [61, 30]

$$\frac{\partial A}{\partial Z} = \frac{\partial A}{\partial Z_1} + \varepsilon \frac{\partial A}{\partial Z_2},$$

$$= -k_0'\frac{\partial A}{\partial T} + i\varepsilon\left(-\frac{k_0''}{2}\frac{\partial^2 A}{\partial T^2} + \frac{gn_2\omega_0}{c}|A|^2 A\right), \tag{1.4.79}$$

which can be rewritten as [61, 30]:

$$i\left(\frac{\partial A}{\partial Z} + k_0'\frac{\partial A}{\partial T}\right) + \varepsilon\left(-\frac{k_0''}{2}\frac{\partial^2 A}{\partial T^2} + \frac{gn_2\omega_0}{c}|A|^2 A\right) = 0. \tag{1.4.80}$$

Let

$$u \equiv \sqrt{\frac{\gamma T_0^2}{|k_0''|}}A,$$

$$\zeta \equiv \frac{\varepsilon |k_0''|}{T_0^2}Z \quad \text{and}$$

$$\tau \equiv \frac{T - k_0'Z}{T_0}, \tag{1.4.81}$$

where $\gamma = \dfrac{gn_2\omega_0}{c}$ and T_0 is the initial pulse width. On substituting Eq.(1.4.81) into Eq.(1.4.80), the propagation equation governing pulse propagation in a single mode optical fiber is obtained as [61, 30]:

$$i\frac{\partial u}{\partial \zeta} - \frac{\text{sgn}(k_0'')}{2}\frac{\partial^2 u}{\partial \tau^2} + |u|^2 u = 0, \tag{1.4.82}$$

where sgn(k_0'') stands for the sign of the group velocity dispersion parameter k_0''. When sgn(k_0'')is negative (positive), Eq.(1.4.82) represents pulse propagation in the anomalous (normal) dispersion regime for a single mode optical fiber [60] and the governing equation is called the scalar nonlinear Schrödinger equation (NLSE) [60].

v) Correction factors

So far, the above equation has been derived by omitting some important physical aspects. In order to bring the equation into closer contact with reality, the following aspects have to be considered : a) attenuation, linear and nonlinear [1, 4], b) higher-order linear dispersion [62] and nonlinear dispersion [63] and an effective Raman scattering due to delay in $\tilde{\chi}^{(3)}$ [64]. They are as follows :

a)Attenuation correction

One of the major corrections required is the effect of material absorption [60] which originates from the imaginary part of the linear and nonlinear suscepti-bilities represented by $\text{Im}[\chi^{(1)}]$ and $\text{Im}[\chi^{(3)}]$ respectively. Including the former contribution in the linear polarization,

$$
\begin{aligned}
\mathbf{P}_L\,(x,y,z,t) &= \varepsilon_0 \int_{-\infty}^{+\infty} \chi^{(1)}\,(t-t') \cdot \mathbf{E}\,(x,y,z,t')\ \mathrm{d}t', \\
&\equiv \varepsilon_0 \int_{-\infty}^{+\infty} \left(\chi_R^{(1)}\,(t-t') + i\chi_I^{(1)}\,(t-t') \right) \cdot \mathbf{E}\,(\mathrm{x,y,z},t')\ \mathrm{d}t',
\end{aligned}
$$

$$(1.4.83)$$

where the suffix R stands for the real term while the suffix I stands for the imag-inary term of the linear susceptibility tensor. As a result, the $O\,(\varepsilon)$ contribution

in Eq.(1.4.20) has an additional term in the form given by [61]

$$-\omega_0^2 \widetilde{\chi}_I^{(1)}(x, y, \omega_0) \, \widetilde{A}(Z, \omega - \omega_0) \, \mathbf{U}(x, y, \omega_0) \exp(ik_0 z) + \text{c.c.} \qquad (1.4.84)$$

Further, it is assumed that $\widetilde{\chi}_I^{(1)}(x, y, \omega_0) \sim O(\varepsilon^2)$ and hence Eq.(1.4.84) has $O(\varepsilon^3)$ contribution as a result of the quasi monochromatic approximation [61]. By taking the inverse Fourier transform of Eq.(1.4.84) and considering the quasi monochromatic approximation, $\mathbf{F}_2$ in Eq.(1.4.70) has an additional term which is given by [61]

$$-i\frac{\omega_0^2}{\varepsilon^2 c^2} \widetilde{\chi}_I^{(1)}(x, y, \omega_0) \, A(Z, T) \, \mathbf{U}(x, y, \omega_0). \qquad (1.4.85)$$

This results in an additional term in the solvability condition $\langle \mathbf{U}, \mathbf{F}_2 \rangle = 0$ given by Eq.(1.4.71) and which is of the form [61]:

$$-i\frac{\omega_0^2}{\varepsilon^2 c^2} A(Z, T) \int \widetilde{\chi}_I^{(1)} |\mathbf{U}|^2 \, d\mathbf{S}. \qquad (1.4.86)$$

Due to this additional term, the new modified nonlinear Schrödinger equation which includes the effect due to material absorption also, takes the form [60, 61]:

$$i\left(\frac{\partial A}{\partial Z} + k_0'\frac{\partial A}{\partial T}\right) + \varepsilon\left(-\frac{k_0''}{2}\frac{\partial^2 A}{\partial T^2} + \frac{g n_2 \omega_0}{c}|A|^2 A + i\frac{\alpha}{2}A\right) = 0, \qquad (1.4.87)$$

where the absorption coefficient, $\alpha = \dfrac{\widetilde{\chi}_I^{(1)} \omega_0}{\varepsilon^2 n_0 c}$. In the dimensionless form, the above equation can be written as [60, 61]:

$$i\frac{\partial u}{\partial \zeta} - \frac{\text{sgn}(k_0'')}{2}\frac{\partial^2 u}{\partial \tau^2} + |u|^2 u + i\Gamma u = 0, \qquad (1.4.88)$$

where $\Gamma = \dfrac{\alpha |k_0''|}{2T_0^2}$. In a similar way, the nonlinear attenuation correction can be calculated, but its contribution is found to be negligible in practice.

b)Higher order corrections

The linear part of the nonlinear Schrödinger equation is generated by expanding the dispersion relation $D([\mathbf{U}], k, \omega) \equiv \left\langle \mathbf{U}, \widehat{L}\mathbf{U} \right\rangle = 0$ or the mode propagation

constant $k = k(\omega)$ in a Taylor series as [61]:

$$k\left(\omega_0 + i\varepsilon\frac{\partial}{\partial T}\right) A(Z,T) = k(\omega_0) A + i\varepsilon k_0'\frac{\partial A}{\partial T} - \frac{\varepsilon^2 k_0''}{2}\frac{\partial^2 A}{\partial T^2} + \dots . \qquad (1.4.89)$$

The next term in the series is [61]:

$$-\frac{i\varepsilon^3 k_0'''}{6}\frac{\partial^3 A}{\partial T^3},$$

and this gives rise to the higher order correction [61]:

$$-\frac{i\varepsilon k_0'''}{6}\frac{\partial^3 A}{\partial T^3},$$

in Eq.(1.4.87). As $\mathbf{E} = \varepsilon\mathbf{E}_0$, this higher order dispersion term appears at the ε^4 level.

To determine the effects of higher order nonlinear dispersion and of delay in $\chi^{(3)}$, the following procedure is considered. Eq.(1.4.33) is obtained by considering only the leading order terms. Now considering the next higher order terms also, which are given by [61]:

$$-\widetilde{A}(Z,\omega_1 - \omega_0)\,\widetilde{A}(Z,\omega_2 - \omega_0)\,\widetilde{A}^*(Z,-\omega_3 - \omega_0)\,\omega_0^2\left(\frac{\partial}{\partial\omega_1}\left[\widetilde{\chi}^{(3)}(x,y,\omega_0,\omega_0,-\omega_0)\right]\right.$$

$$(\omega_1 - \omega_0) + \frac{\partial}{\partial\omega_2}\left[\widetilde{\chi}^{(3)}(x,y,\omega_0,\omega_0,-\omega_0)\right](\omega_2 - \omega_0) + \frac{\partial}{\partial\omega_3}\left[\widetilde{\chi}^{(3)}(x,y,\omega_0,\omega_0,-\omega_0)\right]$$

$$\left.(\omega_3 + \omega_0) + \dots\right), \qquad (1.4.90)$$

and following the same steps used to obtain the nonlinear polarization terms in Eq.(1.4.35), the resultant equation will contain one additional term proportional to $A^2\dfrac{\partial A^*}{\partial T}$ and two additional terms proportional to $|A|^2\dfrac{\partial A}{\partial T}$.

The additional terms mentioned in cases a) and b) are contained in the ε^4 contribution from Eq.(1.4.40) given by :

$$\widehat{\mathbf{L}}\left(\frac{\partial}{\partial x},\frac{\partial}{\partial y},ik + \varepsilon\frac{\partial}{\partial Z_1} + \varepsilon^2\frac{\partial}{\partial Z_2} + \dots, -i\omega + \varepsilon\frac{\partial}{\partial T}\right)\varepsilon^3\mathbf{E}_3 = \mathbf{F}_3, \qquad (1.4.91)$$

where $\mathbf{F}_3$ contains the nonlinear terms discussed earlier as well as the linear terms discussed in cases a) and b). When the solvability condition [61]:

$$\langle \mathbf{U}, \mathbf{F}_3 \rangle = 0, \qquad (1.4.92)$$

is applied to Eq.(1.4.92), the final form for the slowly varying envelope $A(Z,T)$ in ε^4 is given by [61]:

$$\frac{\partial A}{\partial Z_3} = \varepsilon \left(\frac{k_0'''}{6} \frac{\partial^3 A}{\partial T^3} - \beta_1 \frac{\partial |A|^2 A}{\partial T} - \beta_2 A \frac{\partial |A|^2}{\partial T} \right), \qquad (1.4.93)$$

where $\dfrac{k_0'''}{6} \dfrac{\partial^3 A}{\partial T^3}$ results from including the cubic term in the expansion of the mode propagation constant, $\beta_1 \dfrac{\partial |A|^2 A}{\partial T}$ arises from including the first derivative of the slowly varying part of the nonlinear polarization given by Eq.(1.4.90)the correction due to nonlinear dispersion and the term $\beta_2 A \dfrac{\partial |A|^2}{\partial T}$ has its origin in the delayed Raman response [60, 61, 64]. Moreover :

$$\begin{aligned} \beta_1 &= \frac{\gamma}{\omega_0} \qquad \text{and} \\ \beta_2 &= i\gamma T_R, \end{aligned} \qquad (1.4.94)$$

where $\gamma = \dfrac{g n_2 \omega_0}{c}$ and T_R is related to the slope of the Raman gain. Therefore from Eq.(1.4.37) [61],

$$\begin{aligned} \frac{\partial A}{\partial Z} &= \frac{\partial A}{\partial Z_1} + \varepsilon \frac{\partial A}{\partial Z_2} + \varepsilon^2 \frac{\partial A}{\partial Z_3}, \\ &= -k_0' \frac{\partial A}{\partial T} + i\varepsilon \left(-\frac{k_0''}{2} \frac{\partial^2 A}{\partial T^2} + \gamma |A|^2 A + i\frac{\alpha}{2} A \right) \\ &\quad + i\varepsilon^2 \left(-i\frac{k_0'''}{6} \frac{\partial^3 A}{\partial T^3} + i\frac{\gamma}{\omega_0} \frac{\partial |A|^2 A}{\partial T} - \gamma T_R A \frac{\partial |A|^2}{\partial T} \right), \quad (1.4.95) \end{aligned}$$

The above equation can be rewritten as [61]:

$$\begin{aligned} i\frac{\partial A}{\partial Z} + \varepsilon \left(-\frac{k_0''}{2} \frac{\partial^2 A}{\partial T^2} + \gamma |A|^2 A + i\frac{\alpha}{2} A \right) + \varepsilon^2 \left(-i\frac{k_0'''}{6} \frac{\partial^3 A}{\partial T^3} + i\frac{\gamma}{\omega_0} \frac{\partial |A|^2 A}{\partial T} \right. \\ \left. - \gamma T_R A \frac{\partial |A|^2}{\partial T} \right) = 0. \qquad (1.4.96) \end{aligned}$$

Let

$$\beta_1 = \frac{k_0'''}{6\,|k_0''|\,T_0},$$

$$\beta_2 = \frac{1}{\omega_0 T_0} \quad \text{and}$$

$$\beta_3 = \frac{T_R}{T_0}. \tag{1.4.97}$$

Considering Eqs.(1.4.81) and (1.4.97), Eq.(1.4.96) can be written in the dimensionless form as [60, 61, 63]:

$$i\frac{\partial u}{\partial \zeta} - \frac{\operatorname{sgn}(k_0'')}{2}\frac{\partial^2 u}{\partial \tau^2} + |u|^2\,u + i\Gamma u + \varepsilon\left(-i\beta_1\frac{\partial^3 u}{\partial \tau^3} + i\beta_2\frac{\partial\,|u|^2\,u}{\partial \tau} - \beta_3 u\frac{\partial\,|u|^2}{\partial \tau}\right) = 0. \tag{1.4.98}$$

The term $-i\beta_1\dfrac{\partial^3 u}{\partial \tau^3}$ includes the effects of higher order dispersion that become important for ultra short pulses because of their wide bandwidth even when their wavelength is relatively far off from the zero-dispersion wavelength [60, 61, 63]. The term $i\beta_2\dfrac{\partial\,|u|^2\,u}{\partial \tau}$ is responsible for self-steepening and shock formation at a pulse edge [60]. The term $-\beta_3 u\dfrac{\partial\,|u|^2}{\partial \tau}$ is responsible for self-frequency shift [60].

1.5 Soliton solution for the nonlinear Schrödinger equation

Solution for the NLSE given by Eq.(1.4.82) in the anomalous dispersion regime can be obtained by using the auto-Bäcklund transformation technique [65].

Let $\Psi \equiv \begin{pmatrix} \Psi_1 \\ \Psi_2 \end{pmatrix}$ be a two-component wave function of the Zakharov-Shabat-Ablowitz-Kaup-Newell-Segur (ZS/AKNS) scattering problem for the nonlinear Schrödinger equation. The space and time evolutions of the wavefunction Ψ are

defined by the linear eigen value problem given by [65] :

$$\Psi_\tau = Q_1 \Psi,$$

$$\Psi_\zeta = Q_2 \Psi \quad \text{and}$$

$$\Psi = (\Psi_1, \Psi_2)^T, \tag{1.5.1}$$

where:

$$Q_1 = \begin{pmatrix} -i\,\lambda & u \\ -u^* & i\,\lambda \end{pmatrix}, \tag{1.5.2}$$

and

$$Q_2 = i\,\lambda^2 \begin{pmatrix} -1 & 0 \\ 0 & 1 \end{pmatrix}$$

$$+\lambda \begin{pmatrix} 0 & u \\ -u^* & 0 \end{pmatrix}$$

$$+\frac{i}{2} \begin{pmatrix} |u|^2 & u_\tau \\ u_\tau^* & -|u|^2 \end{pmatrix}, \tag{1.5.3}$$

such that the relation [65]:

$$Q_{1\zeta} - Q_{2\tau} + [Q_1, Q_2] = 0, \tag{1.5.4}$$

gives back the NLSE and where $[Q_1, Q_2] = Q_1 Q_2 - Q_2 Q_1$. Thus in effect, the NLSE is presented as a linear eigen value problem with eigen value λ [65]. The above mentioned wave function and potential refer to the $(n-1)^{\text{th}}$ −soliton problem [65], i.e.,

$$\Psi_1 \equiv \Psi_1 (n-1),$$

$$\Psi_2 \equiv \Psi_2 (n-1) \quad \text{and}$$

$$u \equiv u(n-1). \tag{1.5.5}$$

In a similar way, the $(n)^{\text{th}}$ −soliton problem can be represented in the form [65],

$$\Psi'_1 \equiv \Psi_1(n),$$

$$\Psi'_2 \equiv \Psi_2(n) \quad \text{and}$$

$$u' \equiv u(n). \tag{1.5.6}$$

and have the same form as Eqs.(1.5.1) and (1.5.2) and where all the terms are primed. Darboux's method [65] is employed to expand the $(n)^{\text{th}}$-soliton wave function

$$\Psi' \equiv \begin{pmatrix} \Psi'_1 \\ \Psi'_2 \end{pmatrix} \quad \text{in terms of the } (n-1)^{\text{th}}\text{-soliton solution } \Psi \equiv \begin{pmatrix} \Psi_1 \\ \Psi_2 \end{pmatrix} \quad \text{and is}$$

given by [65]:

$$\Psi'_1 = A\,\Psi_1 + B\,\Psi_2 \quad \text{and}$$

$$\Psi'_2 = C\,\Psi_1 + D\,\Psi_2, \tag{1.5.7}$$

where A, B, C and D are functions of ζ and τ having the form [65]:

$$A = a_0 + a_1\lambda,$$

$$B = b_0 + b_1\lambda,$$

$$C = c_0 + c_1\lambda \quad \text{and}$$

$$D = d_0 + d_1\lambda. \tag{1.5.8}$$

where a_i, b_i, c_i and d_i $(i = 0,1)$ are functions of ζ and τ through u and u'. Equation (1.5.8) suggests that Ψ' and Ψ differ by a linear function of the eigen value λ. From Eqs.(1.5.1) and (1.5.7), A, B, C and D are found to satisfy the differential equations [65]:

$$A_\zeta = u'C + u^*B,$$

$$B_\zeta = -uA + u'D - i\lambda B,$$

$$C_\zeta = -u'^* A + u^* D + i\lambda C \qquad \text{and}$$

$$D_\zeta = -(uC + u'^* B). \qquad (1.5.9)$$

Substitution of Eq.(1.5.8) in Eq.(1.5.9) yields partial solutions for a_i, b_i, c_i and d_i given by $a_0 = i\ \mu' - \frac{1}{2}\ \sqrt{4\ \nu'^2 - |u + u'|^2}$, $a_1 = -i$, $b_0 = \frac{1}{2}\ (u + u')$, $b_1 = 0$, $c_0 = -\frac{1}{2}\ (u^* + u'^*)$, $c_1 = 0, d_0 = -i\ \mu' - \frac{1}{2}\ \sqrt{4\ \nu'^2 - |u + u'|^2}$ and $d_1 = i$, where μ' and ν' are real denoting the soliton velocity and amplitude parameters respectively and $\lambda \equiv \mu' + i\ \nu'$. Substituting these in Eq.(1.5.8) and hence in Eq.(1.5.7) results in the recurrence relations connecting the $(n)^{\text{th}}$ and $(n-1)^{\text{th}}$-soliton wave functions Ψ' and Ψ respectively and are of the form [65]

$$\Psi'_1 = \left(-i\ \lambda + i\ \mu' - \frac{1}{2}\ \sqrt{4\ \nu'^2 - |u + u'|^2}\right)\ \Psi_1 + \frac{1}{2}\ (u + u')\ \Psi_2 \qquad \text{and}$$

$$\Psi'_2 = -\frac{1}{2}\ (u^* + u'^*)\ \Psi_1 + \left(i\ \lambda - i\ \mu' - \frac{1}{2}\ \sqrt{4\ \nu'^2 - |u + u'|^2}\right)\ \Psi_2. \ (1.5.10)$$

Let

$$\Gamma \equiv \left.\frac{\Psi_1}{\Psi_2}\right|_{\lambda \equiv \mu' + i\ \nu'} \qquad \text{and}$$

$$\Gamma' \equiv \left.\frac{\Psi'_1}{\Psi'_2}\right|_{\lambda \equiv \mu' + i\ \nu'}. \qquad (1.5.11)$$

On integrating Γ and Γ' in Eq.(1.5.11) with respect to ζ, the Riccati equations for Γ and Γ' can be obtained which are of the form [65]

$$\Gamma_\zeta = -2i\lambda\Gamma + u + u^*\Gamma^2, \qquad (1.5.12)$$

and

$$\Gamma'_\zeta = -2i\lambda\Gamma' + u' + u'^*\Gamma'^2, \qquad (1.5.13)$$

From Eq.(1.5.12), an expression of the form

$$\Gamma^2\Gamma^*_\zeta - \Gamma_\zeta = 2i\Gamma\left(\lambda^*\ |\Gamma|^2 + \lambda\right) - u\left(1 - |\Gamma|^4\right), \qquad (1.5.14)$$

is obtained. Similarly, from Eq.(1.5.13), an expression of the form

$$\Gamma^2 \Gamma_\zeta^* - \Gamma_\zeta = 2i\Gamma \left(\lambda^* + \lambda |\Gamma|^2\right) + u' \left(1 - |\Gamma|^4\right), \qquad (1.5.15)$$

is obtained. Substituting $\lambda \equiv \mu' + i\,\nu'$ in Eq.(1.5.14) results in the equation

$$2i\Gamma\mu' \left(1 + |\Gamma|^2\right) = \Gamma^2 \Gamma_\zeta^* - \Gamma_\zeta + u \left(1 - |\Gamma|^4\right) + 2\Gamma\nu' \left(1 - |\Gamma|^2\right). \qquad (1.5.16)$$

The pseudopotentials Γ and Γ' are related via the equation [65, 66] :

$$\Gamma' = \frac{1}{\Gamma^*}. \qquad (1.5.17)$$

Substitution of Eq.(1.5.17) into Eq.(1.5.15) results in an expression of the form

$$\Gamma^2 \Gamma_\zeta^* - \Gamma_\zeta = 2i\Gamma\mu' \left(1 + |\Gamma|^2\right) + u' \left(1 - |\Gamma|^4\right) + 2\Gamma\nu' \left(1 - |\Gamma|^2\right). \qquad (1.5.18)$$

Substitution of Eq.(1.5.16) in Eq.(1.5.18) leads to the recurrence relation connecting the $(n)^{\text{th}}$ and $(n-1)^{\text{th}}$ soliton solutions of the form [65]:

$$u(n-1) + u(n) = \frac{-4\,\Gamma(n-1)\,\nu(n)}{1 + |\Gamma(n-1)|^2}. \qquad (1.5.19)$$

From the two recurrence relations given by Eqs.(1.5.10) and (1.5.19), the procedure for determining the soliton wave functions and multi-soliton solutions starting from the seed solution $u(0) = 0$ is outlined below. Using $u(0) = 0$ in Eq.(1.5.1) and after some manipulations, the pseudo potential $\Gamma(0)$ is determined which is of the form [65]:

$$\Gamma(0) = \exp\left(-2i\left(\delta_1 + i\nu_1\Delta_1 + (\mu_1 + i\,\nu_1)(\zeta + 2\tau(\mu_1 + i\,\nu_1))\right)\right), \qquad (1.5.20)$$

where δ_1 and Δ_1 are two arbitrary phase constants. Also, $\mu_1 \equiv \mu(1)$ and $\nu_1 \equiv \nu(1)$. Substituting the above expression for $\Gamma(0)$ in the equation [65]

$$u(1) = \frac{-4\,\Gamma(0)\,\nu(1)}{1 + |\Gamma(0)|^2}, \qquad (1.5.21)$$
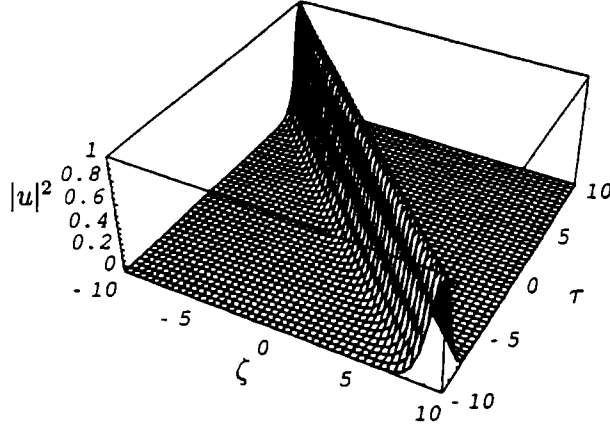
Fig. 1.5: Surface plot of the intensity of the single soliton solution given by Eq.(1.5.22)

determines the fundamental soliton solution for the NLSE in the anomalous dispersion regime and is given by [65, 66]:

$$u\,(1) \equiv u_1\,(\zeta, \tau) = -2\,\nu_1 \mathrm{sech}\,(f_1\,(\zeta, \tau))\,\exp\,(-i\,f_2\,(\zeta, \tau)\,) \qquad (1.5.22)$$

where

$$f_1\,(\zeta, \tau) \;=\; 2\,\nu_1\,(\,\tau + 2\,\mu_1\zeta + \Delta_1) \qquad \text{and}$$

$$f_2\,(\zeta, \tau) \;=\; 2\,\left(\mu_1\,\tau + \left(\mu_1^2 - \nu_1^2\right)\zeta + \delta_1\right). \qquad (1.5.23)$$

The single soliton solution is plotted in Fig.(1.5). The figure depicts the undistorted soliton propagation along the length of the fiber. This is mainly due to the balancing between the group velocity dispersion and self-phase nodulation terms in scalar nonlinear Schrödinger equation given by Eq.(1.4.82).

Once again on using the recurrence relations given by Eqs.(1.5.10) and (1.5.19), the two soliton solution for the NLSE is obtained and is of the form [65]:

$$u\,(2) \equiv u_2\,(\zeta, \tau) = \frac{N\,(\zeta, \tau)}{D\,(\zeta, \tau)}, \qquad (1.5.24)$$

where [65]:

$$
\begin{aligned}
N\left(\zeta, \tau\right) &= 2\,\nu_1\,\mathrm{sech}\left(\xi_1\right)\,\exp\left(-i\,\chi_1\right)\left(\Delta\mu\right)^2 \\
&\quad +4\,i\,\nu_1\,\mathrm{sech}\left(\xi_1\right)\,\exp\left(-i\,\chi_1\right)\,\nu_2\,\Delta\mu\;\tanh\left(\xi_2\right) \\
&\quad +2\,\nu_1\,\mathrm{sech}\left(\xi_1\right)\,\exp\left(-i\,\chi_1\right)\left(\nu_1^2 - \nu_2^2\right) \\
&\quad +2\,\nu_2\,\mathrm{sech}\left(\xi_2\right)\,\exp\left(-i\,\chi_2\right)\left(\Delta\mu\right)^2 \\
&\quad -4\,i\,\nu_2\,\mathrm{sech}\left(\xi_2\right)\,\exp\left(-i\,\chi_2\right)\,\nu_1\,\Delta\mu\;\tanh\left(\xi_1\right) \\
&\quad -2\,\nu_2\,\mathrm{sech}\left(\xi_2\right)\,\exp\left(-i\,\chi_2\right)\left(\nu_1^2 - \nu_2^2\right), \qquad \text{and} \\
D\left(\zeta, \tau\right) &= \left(\Delta\mu\right)^2 + \nu_1^2 + \nu_2^2 - 2\,\nu_1\,\nu_2\,\tanh\left(\xi_1\right)\,\tanh\left(\xi_2\right) \\
&\quad -2\;\nu_1\,\nu_2\,\mathrm{sech}\left(\xi_1\right)\,\mathrm{sech}\left(\xi_2\right)\,\cos\left(\chi_2 - \chi_1\right), \qquad (1.5.25)
\end{aligned}
$$

where [65]:

$$
\begin{aligned}
\xi_i &= 2\,\nu_i\left(\tau + 2\,\mu_i\zeta + \Delta_i\right) \qquad \text{and} \\
\chi_i &= 2\left(\mu_i\,\tau + \left(\mu_i^2 - \nu_i^2\right)\zeta + \delta_i\right) \qquad \text{with}\,i = 1, 2. \qquad (1.5.26)
\end{aligned}
$$

Also $\Delta\mu = \mu_2 - \mu_1$. Figure (1.6) shows the various interaction scenarios. In Fig.(1.6(a)), the off-phase injection of the two solitons with unequal amplitudes is shown. In this case, the two solitons remain separated as they propagate along the length of the fiber. Figure(1.6(b)) depicts the in-phase injection of the two solitons with equal amplitudes. Here, the two solitons collide with each other at $\zeta = 0$. These plots point out the fact that even after interaction process, soliton pulses propagate along the length of the fiber without any change in their shape.
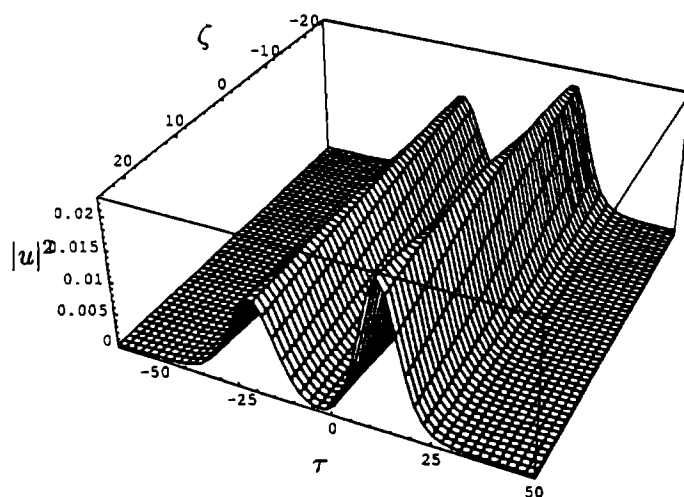
(a)
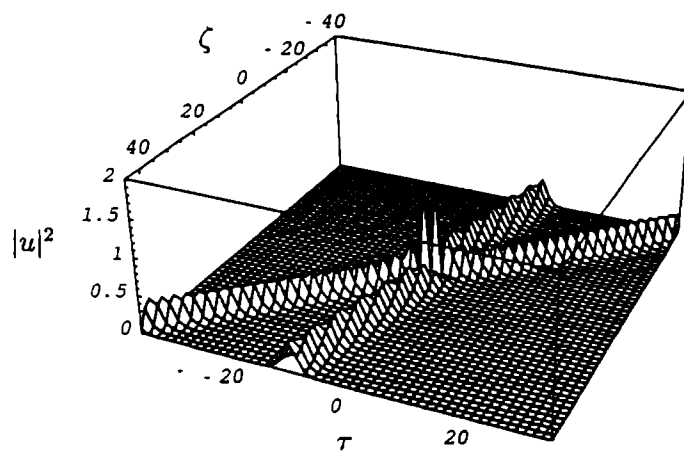
(b)

Fig. 1.6: Surface plots of the intensity of the two-soliton solution given by Eq.(1.5.24):
(a) Off-phase injection; (b) In-phase injection

Chapter 2

Travelling wave method for higher order cubic-quintic nonlinear Schrödinger equation

2.1 Introduction

Nonlinear pulse propagation in optical fibers has been a subject of extensive research primarily because of the possibility of transmitting undistorted pulses of high peak powers . In chapter one, the importance of nonlinear pulse propagation through single mode optical fibers have been discussed. In normal cases, the intensity dependent refractive index has the form $n = n_0(\omega) + n_2(|\mathbf{E}|^2)$, [1] whereby pulse propagation in the fiber is described by the scalar nonlinear Schrödinger equation having a cubic nonlinearity [1]. However when the nonlinear term happens to be smaller than the dispersion term, the refractive index coefficient takes the form $n = n_0(\omega) + n_2(|\mathbf{E}|^2) + n_4(|\mathbf{E}|^4)$ [3] as a result of which quintic nonlinearity should also be considered along with the cubic nonlinearity. In this chapter, various types of solutions in the form of algebraic bright and dark solitary wave solutions and periodic solutions are determined for the cubic-quintic nonlinear Schrödinger equation using the travelling wave method.

The chapter is arranged as follows : In Sec. 2.2, the basic equation is considered and using a travelling wave anstatz, the basic equation is reduced to a form which describes the dynamics of a particle moving in a potential well with a total energy equal to zero and mass equal to 2. Section 2.3 presents the various results obtained for the corresponding root distributions for the potential function and conclusion is made in Sec. 2.4.

2.2   Basic equation and travelling wave method

Pulse propagation in a single mode optical fiber whose nonlinear term happens to be smaller than the dispersion term is characterized by the cubic-quintic higher order nonlinear Schrödinger equation which is of the form [4]:

$$i\frac{\partial u}{\partial \zeta} - \frac{n}{2}\frac{\partial^2 u}{\partial \tau^2} + |u|^2 u + q_2 |u|^4 u + i\varepsilon_1 \frac{\partial |u|^2 u}{\partial \tau} = 0, \qquad (2.2.1)$$

where $n = \pm 1$, q_2-the coefficient of quintic term and ε_1-self-steepening coefficient. Self-steepening results from the intensity dependence of the group velocity, affecting self-phase modulation and resulting in spectral broadening [69, 70]. When $q_2 = \varepsilon_1 = 0$, Eq.(2.2.1) reduces to the scalar nonlinear Schrödinger equation and hence is completely integrable [66] and the corresponding multi solitons have been studied extensively [66]. In the present work, other types of solutions in the form of algebraic bright and dark solitary wave solutions and periodic solutions are determined using the "travelling wave method" [71]. For this $u\left(\zeta, \tau\right)$ is assumed to have the anstatz

$$u\left(\zeta, \tau\right) = r\left(\xi\right)\exp\left(i\theta\left(\xi\right)\right), \qquad (2.2.2)$$

where $r\left(\xi\right)$ and $\theta\left(\xi\right)$ are real and $\xi = \tau - v\zeta$. On substituting Eq.(2.2.2) in Eq.(2.2.1) and separating into real and imaginary parts, the following equations

are obtained :

$$-v\frac{\mathrm{d}r}{\mathrm{d}\xi} + \left(2\frac{\mathrm{d}r}{\mathrm{d}\xi}\frac{\mathrm{d}\theta}{\mathrm{d}\xi} + r\frac{\mathrm{d}^2\theta}{\mathrm{d}\xi^2}\right)\frac{n}{2} + 2\varepsilon_1 r^2\frac{\mathrm{d}r}{\mathrm{d}\xi} = 0, \tag{2.2.3}$$

and

$$vr\frac{\mathrm{d}\theta}{\mathrm{d}\xi} + \frac{n}{2}\left(\frac{\mathrm{d}^2 r}{\mathrm{d}\xi^2} - r\left(\frac{\mathrm{d}\theta}{\mathrm{d}\xi}\right)^2\right) + r^3 + q_2 r^5 - \varepsilon_1 r^3\frac{\mathrm{d}\theta}{\mathrm{d}\xi} = 0. \tag{2.2.4}$$

On multiplying Eq.(2.2.3) throughout by $2r$, it can be written in the form:

$$\frac{\mathrm{d}}{\mathrm{d}\xi}\left[-vr^2 + nr^2\frac{\mathrm{d}\theta}{\mathrm{d}\xi} + \varepsilon_1 r^4\right] = 0. \tag{2.2.5}$$

Equation (2.2.5) on integration, yields :

$$\frac{\mathrm{d}\theta}{\mathrm{d}\xi} = \frac{1}{n}\left(v + \frac{A}{r^2} - \varepsilon_1 r^2\right), \tag{2.2.6}$$

where A is an integration constant. Substituting Eq.(2.2.6) in Eq.(2.2.4) the following expression is obtained which is of the form :

$$\frac{\mathrm{d}^2 r}{\mathrm{d}\xi^2} + a_1 r^5 - a_2 r^3 + a_3 r - \frac{a_5}{r^3} = 0, \tag{2.2.7}$$

where :

$$
\begin{aligned}
a_1 &= \varepsilon_1^2 - 2nq_2, \\
a_2 &= 2\left(\varepsilon_1 v - n\right), \\
a_3 &= v^2 \quad \text{and} \\
a_5 &= A^2. \tag{2.2.8}
\end{aligned}
$$

Making the substitution,

$$S\left(\xi\right) = r^2\left(\xi\right), \tag{2.2.9}$$

in Eq.(2.2.7), it reduces to the form :

$$\left(\frac{dS}{d\xi}\right)^2 + V\left(S\right) = 0, \tag{2.2.10}$$

where the potential function $V(S)$ has the following expression in the polynomial form of order 4 :

$$V(S) = \frac{4a_1}{3}S^4 - 2a_2S^3 + 4a_3S^2 - a_4S + a_5, \qquad (2.2.11)$$

where a_4 is another integration constant. Equation (2.2.10) is analogous to the dynamics of a particle with a total energy equal to zero and mass equal to 2 in a potential well represented by $V(S)$. Depending on the different kinds of the potential function $V(S)$, a family of analytical solutions are obtained for Eq.(2.2.10) and hence Eq.(2.2.1) via the relation given by Eq.(2.2.2). As all the coefficients of the potential function $V(S)$ are assumed to be real, only those root distributions for $V(S)$ are considered for which $V(S)$ is negative. The following root distributions are as follows i) When $V(S)$ has a triple root $S = \alpha$ and a single root $S = \beta$, ii) When $V(S)$ has a double root $S = \alpha$ and two single roots $S = \beta$ and $S = \gamma$, iii) When $V(S)$ has a pair of equal and opposite roots $S = \pm\beta$ and a pair of complex conjugate roots $S = \pm i\alpha$ and iv) When $V(S)$ has a pair of equal and opposite roots $S = \pm\alpha$ and two single roots $S = \beta, \gamma$.

2.3   Results and discussion

i) When $V(S)$ has a triple root $S = \alpha$ and a single root $S = \beta$

In this case, the potential function $V(S)$ can be written in the form :

$$V(S) = \frac{4a_1}{3}(S - \alpha)^3(S - \beta). \qquad (2.3.1)$$

a) Bright solitary wave $(n = +1)$

On equating the coefficients of like powers of S between Eqs.(2.2.11) and (2.3.1), the following set of equations are obtained :

$$a_2 = \frac{2a_1}{3}\left(3\alpha + \beta\right), \qquad (2.3.2)$$

$$a_3 = a_1\alpha\left(\alpha + \beta\right), \qquad (2.3.3)$$

$$a_4 = \frac{4a_1}{3}\left(\alpha^2 + 3\beta\right), \qquad (2.3.4)$$

and

$$a_5 = \frac{4a_1}{3}\alpha^3\beta. \qquad (2.3.5)$$

From Eqs.(2.2.8) and (2.3.2), an expression for the dimensionless parameter v, which is the inverse of the soliton velocity, is obtained which is of the form :

$$v = \frac{1}{2\varepsilon_1}\left(\frac{2a_1}{3}\left(3\alpha + \beta\right) + 2\right). \qquad (2.3.6)$$

But from Eqs.(2.2.8) and (2.3.3),

$$v^2 = a_1\alpha\left(\alpha + \beta\right). \qquad (2.3.7)$$

Substituting Eqs.(2.3.3) and (2.3.7) in the relation $a_3 = v^2$ and considering the transformation:

$$\epsilon = \epsilon_1^2, \qquad (2.3.8)$$

a quadratic equation in ϵ is obtained which is of the form :

$$(\beta - 3\alpha)\,\beta\epsilon^2 - 2\left(3\left(\alpha q_2 - 1\right)\left(3\alpha + \beta\right) + 2\beta^2 q_2\right)\epsilon + \left(\left(6\alpha + 2\beta\right)q_2 - 3\right)^2 = 0.$$
$$(2.3.9)$$

The roots of the above quadratic equation are of the form :

$$\epsilon = \frac{1}{\beta\left(3\alpha - \beta\right)}\Bigg(3\left(3\alpha + \beta\right)\left(1 - \alpha q_2\right) - 2\beta^2 q_2$$
$$\pm 3\sqrt{3\alpha\left(\alpha + \beta\right)\left(3\alpha q_2^2\left(\alpha + \beta\right) - 2q_2\left(3\alpha + \beta\right) + 3\right)}\Bigg). \quad (2.3.10)$$

Therefore, from Eq.(2.3.8), the self-steepening coefficient, ε_1 can be obtained in terms of the roots α and β and is given by :

$$\varepsilon_1 = \pm\sqrt{\frac{1}{\beta(3\alpha-\beta)}\left(3(3\alpha+\beta)(1-\alpha q_2) - 2\beta^2 q_2 \pm 3r_1\right)}, \qquad (2.3.11)$$

where

$$r_1 = \sqrt{3\alpha(\alpha+\beta)(3\alpha q_2^2(\alpha+\beta) - 2q_2(3\alpha+\beta) + 3)} \qquad (2.3.12)$$

Only the positive root of Eq.(2.3.11) is taken into consideration and is given by :

$$\varepsilon_1 = \sqrt{\frac{1}{\beta(3\alpha-\beta)}\left(3(3\alpha+\beta)(1-\alpha q_2) - 2\beta^2 q_2 + 3r_1\right)}, \qquad (2.3.13)$$

On substituting Eq.(2.3.13) into Eq.(2.2.8), a_1 is determined and hence all the other coefficients, which are given by Eqs.(2.3.2)-(2.3.5).

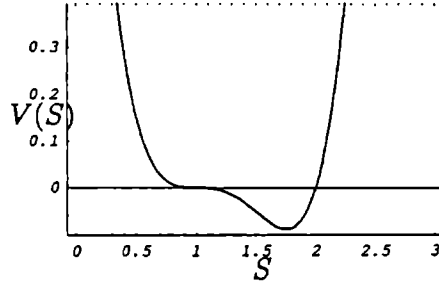The potential function $V(S)$ given by Eq.(2.3.1) has a minimum at

$$S = \frac{\alpha+3\beta}{4}, \qquad (2.3.14)$$

which is clear from Fig.(2.1(a)) where the potential function $V(S)$ is plotted against S. The nonlinear system given by Eq.(2.2.10) can now be written in the form

$$\left(\frac{dS}{d\xi}\right)^2 + \frac{4a_1}{3}(S-\alpha)^3(S-\beta) = 0. \qquad (2.3.15)$$

Since $V(S)$ has a minimum at the point given by Eq.(2.3.14), the nonlinear system represented by Eq.(2.3.15) has a center at the same point and hence is stable about that point. This is clearly represented in Fig.(2.1(b)) which portrays the phase diagram of the nonlinear system given by Eq.(2.3.15) in the phase space with coordinates $\left(S, \frac{dS}{d\xi}\right)$. The phase diagram given by Fig.(2.1(b)) suggests a solution as a homoclinic orbit. The corresponding explicit form is determined as given below. Equation (2.3.15) can be written in the form :

$$\frac{dS}{d\xi} = \sqrt{\frac{4a_1}{3}(S-\alpha)^3(\beta-S)}, \qquad (2.3.16)$$

(a)
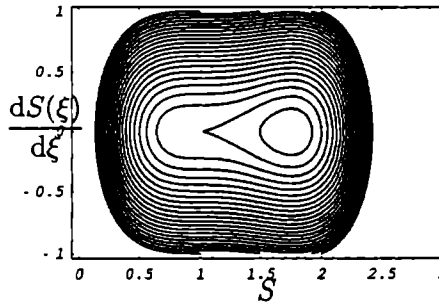
(b)

Fig. 2.1: (a) Plot of the potential function given by Eq.(2.3.1) with $\alpha = 1, \beta = 2, a_1 = 0.62, v = 1.36, q_2 = 0.8$; (b) Phase portrait of the nonlinear system given by Eq.(2.3.15) having a stable center at the point given by Eq.(2.3.14)

where $\beta > S \geq \alpha$. On taking the integral of Eq.(2.3.16) on both sides, it is written in the form :

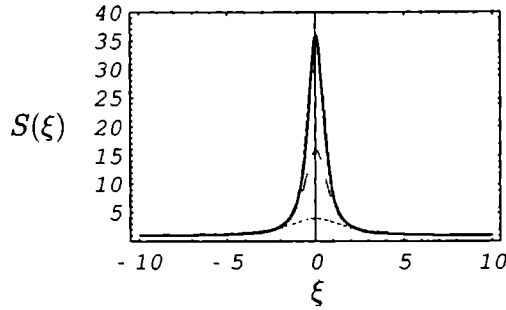$$\int \frac{dS}{\sqrt{(S-\alpha)^3 (\beta - S)}} = \sqrt{\frac{4a_1}{3}} \int d\xi. \qquad (2.3.17)$$

In order to simplify Eq.(2.3.17), the following substitution is considered :

$$t^2 = \frac{(\beta - S)}{(S - \alpha)}. \qquad (2.3.18)$$

After taking the differential of Eq.(2.3.18), it is written in the form :

$$dS = \frac{2(S-\alpha)^2 t}{(\alpha - \beta)} dt. \qquad (2.3.19)$$

(a)
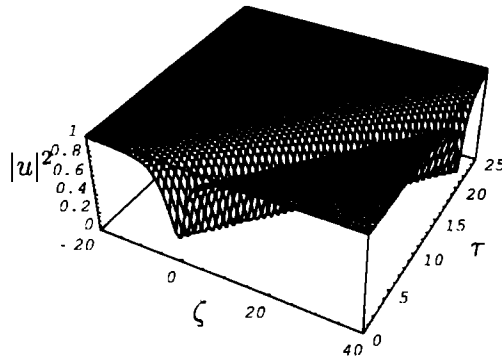
(b)

Fig. 2.2: (a) Plot of the bright solitary wave solution given by Eq.(2.3.21) for various values of β ($\beta = 2.0$(solid curve), 4.0(dashed curve)and6.0(dotted curve)) for the inequality condition $\beta > S \geq \alpha$; (b) Surface plot for the intensity of the dark solitary wave solution given by Eq.(2.3.21) for the inequality condition $\alpha > S \geq \beta$ where $|u|^2 = S(\xi)$

On substituting Eqs.(2.3.18) and (2.3.19) in Eq.(2.3.16) and on simplifying , a relation for t is obtained which is of the form :

$$t = \sqrt{\frac{a_1}{3}} \left(\alpha - \beta\right)\xi + c, \qquad (2.3.20)$$

where c is an arbitrary integration constant. $S\left(\xi\right)$ is retrieved from Eq.(2.3.20) via the relation (2.3.18) which yields a stable algebraic bright solitary wave solution for Eq.(2.3.15) and is given by :

$$S\left(\xi\right) = \frac{\beta + \alpha \left(\sqrt{\frac{a_1}{3}}\left(\alpha - \beta\right)\xi + c\right)^2}{1 + \left(\sqrt{\frac{a_1}{3}}\left(\alpha - \beta\right)\xi + c\right)^2}. \qquad (2.3.21)$$

For $\beta > S \geq \alpha$, Eq.(2.3.21) represents a bright solitary wave solution with an arbitrary background. For $c = 0$, $S(\xi)$ is symmetrically oriented about the axis origin and for $c \neq 0$, $S(\xi)$ is displaced from the axis origin. For various values of β such that $\beta > \alpha$ and $\beta \neq 3$ (for $\beta = 3$, $a_1 \rightarrow \infty$), it is observed that the full width at half maximum (FWHM) of the pulse gradually decreases with increasing β, while its amplitude increases with increasing β and is depicted in Fig.(2.2(a)).

b)Dark solitary wave ($n = -1$)

For the dark solitary wave case, the self-steepening term ε_1 has the form :

$$\varepsilon_1 = \sqrt{\frac{1}{\beta(3\alpha - \beta)}\left(3(3\alpha + \beta)(\alpha q_2 - 1) + 2\beta^2 q_2 + 3\,r_1\right)}, \qquad (2.3.22)$$

where r_1 is given by Eq.(2.3.12). For $n = -1$, the dark solitary wave solution is given by Eq.(2.3.21) where $\alpha > S \geq \beta$ and is plotted in Fig.(2.2(b)).

ii) When $V(S)$ has a double root $S = \alpha$ and two single roots $S = \beta$ and $S = \gamma$

The corresponding potential function $V(S)$ has the form :

$$V(S) = \frac{4a_1}{3}(S - \alpha)^2 (S - \beta)(S - \gamma). \qquad (2.3.23)$$

a) Bright solitary wave ($n = +1$)

On comparing Eq.(2.2.11) and Eq.(2.3.23), the following set of equations are obtained

$$a_2 = \frac{2a_1}{3}(2\alpha + \beta + \gamma), \qquad (2.3.24)$$

$$a_3 = \frac{a_1}{3}\left(\alpha^2 + \beta\gamma + 2\alpha(\beta + \gamma)\right), \qquad (2.3.25)$$

$$a_4 = \frac{4a_1}{3}\alpha\left(2\beta\gamma + \alpha\left(\beta + \gamma\right)\right), \qquad (2.3.26)$$

and

$$a_5 = \frac{4a_1}{3}\alpha^2\beta\gamma. \qquad (2.3.27)$$

Following a similar procedure in case i), ε_1 can be obtained in terms of the roots α, β and γ and is given by

$$\varepsilon_1 = \sqrt{\frac{\left(5\alpha^2 q_2 + 2q_2\left(\gamma^2 + \beta^2\right) + 2\alpha\left(\left(\beta + \gamma\right)q_2 - 3\right) + \beta\gamma q_2 - 3\left(\beta + \gamma\right) + 3\,r_2\right)}{\left(\left(\alpha - \beta\right)^2 - \gamma\left(2\alpha + \beta\right) + \gamma^2\right)}}, \qquad (2.3.28)$$

where

$$r_2 = \sqrt{\left(\left(\alpha q_2 - 1\right)\left(\left(\alpha + 2\beta\right)q_2 - 3\right) + \gamma q_2\left(\left(2\alpha + \beta\right)q_2 - 2\right)\right)\left(\alpha^2 + \beta\gamma + 2\alpha\left(\beta + \gamma\right)\right)} \qquad (2.3.29)$$

The potential function $V\left(S\right)$ given by Eq.(2.3.23) has a minimum at the points given by :

$$S = \frac{1}{8}\left(2\alpha + 3\left(\beta + \gamma\right) \pm \sqrt{\left(2\alpha + 3\left(\beta + \gamma\right)\right)^2 - 16\left(\alpha\left(\beta + \gamma\right) + 2\beta\gamma\right)}\right), \qquad (2.3.30)$$

and a maximum at the point :

$$S = \alpha. \qquad (2.3.31)$$

This scenario is depicted in Fig.(2.3(a)) where the potential function $V\left(S\right)$ is plotted against S. The nonlinear system given by Eq.(2.2.10) can now be written in the form :

$$\left(\frac{dS}{d\xi}\right)^2 + \frac{4a_1}{3}\left(S - \alpha\right)^2\left(S - \beta\right)\left(S - \gamma\right) = 0. \qquad (2.3.32)$$

Since $V\left(S\right)$ has a minimum at the points represented by Eq.(2.3.30), the above nonlinear system has a stable center at those points. Also the nonlinear system has a corresponding unstable saddle point at the point given by Eq.(2.3.31).

This scenario is in the phase diagram given by Fig.(2.3(b)) in the phase space with coordinates $\left(S, \frac{dS}{d\xi}\right)$. The phase diagram given by Fig.(2.3(b)) suggests a localized solution as a homoclinic orbit for the condition $\beta > S \geq \alpha > \gamma$. The
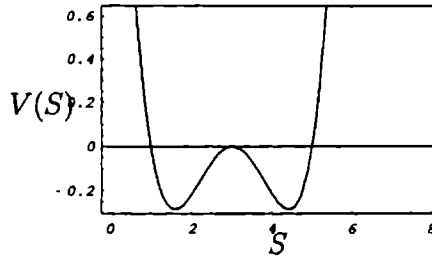
(a)
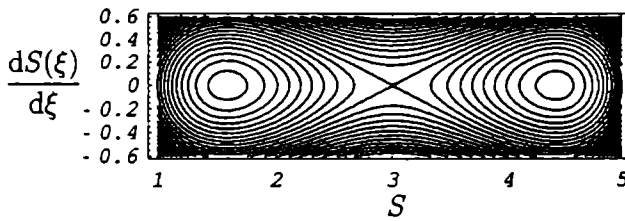
(b)

Fig. 2.3: (a) Plot of the potential function given by Eq.(2.3.23) with $\alpha = 3.0, \beta = 5.0, a_1 = 0.053, v = 0.94, q_2 = 0.8$; (b) Phase portrait of the nonlinear system given by Eq.(2.3.32) having two stable centers at the points given by Eq.(2.3.30) and an unstable saddle point at the point given by Eq.(2.3.31)

corresponding explicit form is determined as follows : Eq.(2.3.32) can be written in the form :

$$\frac{dS}{d\xi} = \sqrt{\frac{4a_1}{3} (S - \alpha)^2 (\beta - S)(S - \gamma)}, \qquad (2.3.33)$$

where $\beta > S \geq \alpha > \gamma$. On taking the integral of Eq.(2.3.33) on both sides, it is written in the form :

$$\int \frac{dS}{\sqrt{(S - \alpha)^2 (\beta - S)(S - \gamma)}} = \sqrt{\frac{4a_1}{3}} \int d\xi. \qquad (2.3.34)$$

Let :

$$t^2 = \frac{(\beta - S)}{(S - \gamma)}. \tag{2.3.35}$$

The differential of Eq.(2.3.35) is given by:

$$\mathrm{d}S = \frac{2 (S - \gamma)^2 t}{(\gamma - \beta)} \mathrm{d}t. \tag{2.3.36}$$

On substituting these in the integral equation given by Eq.(2.3.34), the corresponding integral equation simplifies to the form :

$$\sqrt{\frac{\alpha - \gamma}{\alpha - \beta}} \int \frac{\mathrm{d}t}{1 + \left(\sqrt{\frac{\alpha - \gamma}{\alpha - \beta}} t\right)^2} = \sqrt{\frac{a \gamma_1}{3} (\alpha - \beta)(\alpha - \gamma)} \mathrm{d}\xi. \tag{2.3.37}$$

Let :

$$\varsigma = \sqrt{\frac{\alpha - \gamma}{\alpha - \beta}} t. \tag{2.3.38}$$

On taking the differential of the above equation and on substituting in Eq.(2.3.37), the corresponding integral equation yields the solution given by :

$$\varsigma = \tan\left(\sqrt{\frac{a_1}{3} (\alpha - \beta)(\alpha - \gamma)} \xi + c\right), \tag{2.3.39}$$

where c is an arbitrary integration constant. Hence from Eq.(2.3.38) and then from Eq.(2.3.35), the analytical expression for the nonlinear system given by Eq.(2.3.32) is given by :

$$S(\xi) = \frac{\beta + \frac{(\alpha - \beta)\gamma}{(\alpha - \gamma)} \tan^2\left(\sqrt{\frac{a_1}{3} (\alpha - \beta)(\alpha - \gamma)} \xi + c\right)}{1 + \frac{(\alpha - \beta)}{(\alpha - \gamma)} \tan^2\left(\sqrt{\frac{a_1}{3} (\alpha - \beta)(\alpha - \gamma)} \xi + c\right)}. \tag{2.3.40}$$

For $c = 0$ and since $\beta > S \geq \alpha > \gamma$, the expression for $S(\xi)$ given by Eq.(2.3.40) simplifies to the form :

$$S(\xi) = \frac{\beta + \frac{(\beta - \alpha)\gamma}{(\alpha - \gamma)} \tanh^2\left(\sqrt{\frac{a_1}{3} (\beta - \alpha)(\alpha - \gamma)} \xi\right)}{1 + \frac{(\beta - \alpha)}{(\alpha - \gamma)} \tanh^2\left(\sqrt{\frac{a_1}{3} (\beta - \alpha)(\alpha - \gamma)} \xi\right)}. \tag{2.3.41}$$
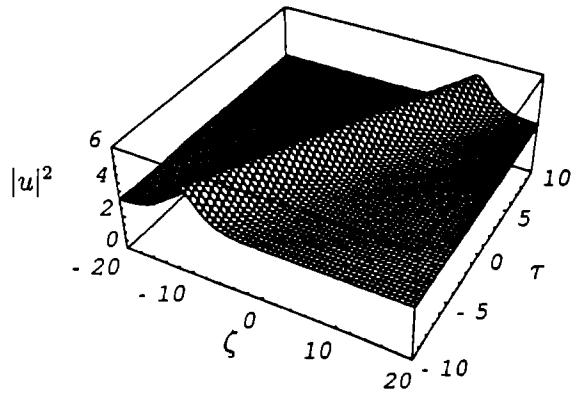
(a)
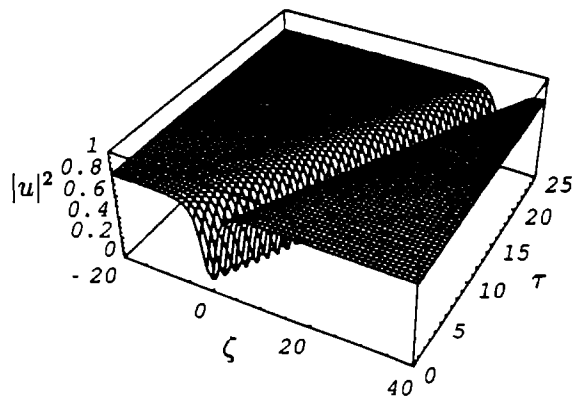
(b)

Fig. 2.4: (a) Surface plot for the intensity of the bright wave solution given by Eq.(2.3.41) for the inequality condition $\beta > S \geq \gamma > \alpha$ where $|u|^2 = S(\xi)$; (b) Surface plot for the intensity of the dark solitary wave solution given by Eq.(2.3.41) for the inequality condition $\gamma > S \geq \alpha > \beta$ where $|u|^2 = S(\xi)$

For $\beta > S \geq \alpha > \gamma$, Eq.(2.3.41) represents a bright solitary wave solution with an arbitrary background which is portrayed in Fig.(2.4(a)). Since the phase diagram given by Fig.(2.3(b)) has closed paths, there is a possibility for finding periodic solutions. This periodic solution is given by Eq.(2.3.40) for the condition $\alpha > S \geq \beta > \gamma$.

b) Dark solitary wave ($n = -1$)

In this case, ε_1 has the following form :

$$\varepsilon_1 = \sqrt{\frac{-\left(5\alpha^2 q_2 + 2q_2\left(\gamma^2 + \beta^2\right) + 2\alpha\left((\beta + \gamma)\,q_2 - 3\right) + \beta\gamma q_2 - 3\left(\beta + \gamma\right) + 3\,r_2\right)}{\left((\alpha - \beta)^2 - \gamma\left(2\alpha + \beta\right) + \gamma^2\right)}},$$

(2.3.42)

where r_2 is given by Eq.(2.3.29). The dark solitary wave solution is given by Eq.(2.3.41) where $\gamma > S \geq \alpha > \beta$ and is plotted in Fig.(2.4(b)).

iii) When $V(S)$ has a pair of equal and opposite roots $S = \pm\beta$ and a pair of complex conjugate roots $S = \pm i\alpha$

Here :

$$V(S) = \frac{4a_1}{3}\left(S^2 + \alpha^2\right)\left(S^2 - \beta^2\right).$$

(2.3.43)

On comparing Eq.(2.3.43) with Eq.(2.2.11), the following set of equations are obtained :

$$a_2 = 0,$$

(2.3.44)

$$a_3 = \frac{a_1}{3}\left(\alpha^2 - \beta^2\right),$$

(2.3.45)

$$a_4 = 0,$$

(2.3.46)

and

$$a_5 = -\frac{4a_1}{3}\alpha^2\beta^2.$$

(2.3.47)

In a similar fashion as in case i), ε_1 can be obtained in terms of the roots α and β and is given by :

$$\varepsilon_1 = \left(q_2^2 + \frac{3}{\left(\alpha^2 - \beta^2\right)}\right)^{\frac{1}{4}}.$$

(2.3.48)

In this case, $V(S)$ has a minimum at the critical point $S = 0$, which is a stable
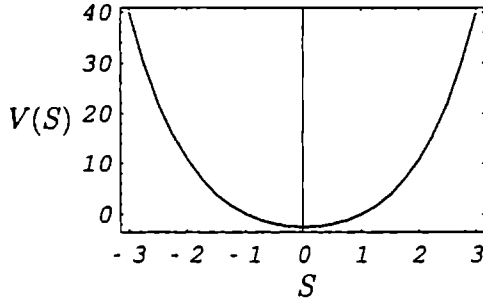
(a)
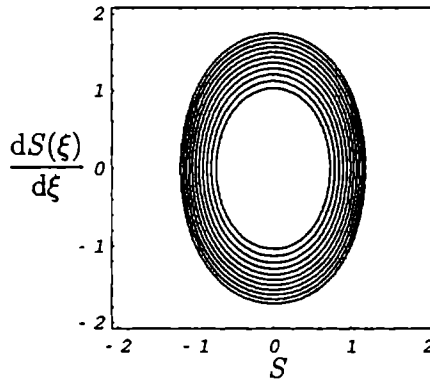
(b)

Fig. 2.5: (a) Plot of the potential function given by Eq.(2.3.43) with $\alpha = 3.0, \beta = 1.0, a_1 = 0.173, v = 0.743, q_2 = 0.8$; (b) Phase portrait of the nonlinear system given by Eq.(2.3.49) having a stable center at the axis origin

center and is plotted in Fig.(2.5(a)). The corresponding phase diagram is plotted in Fig.(2.5(b)). The nonlinear system can now be written in the form :

$$\left(\frac{\mathrm{d}S}{\mathrm{d}\xi}\right)^2 + \frac{4a_1}{3}\left(S^2 + \alpha^2\right)\left(S^2 - \beta^2\right) = 0. \tag{2.3.49}$$

The above equation can be rewritten as :

$$\frac{\mathrm{d}S}{\mathrm{d}\xi} = \sqrt{\frac{4a_1}{3} \left(S^2 + \alpha^2\right) \left(\beta^2 - S^2\right)},$$ (2.3.50)

where $\alpha > \beta > S$. On taking the integral of Eq.(2.3.50) on both sides, it is written in the form :

$$\int \frac{\mathrm{d}S}{\sqrt{\left(S^2 + \alpha^2\right) \left(\beta^2 - S^2\right)}} = \sqrt{\frac{4a_1}{3}} \int \mathrm{d}\xi.$$ (2.3.51)

Let

$$\Phi^2 = \frac{S^2}{\beta^2},$$ (2.3.52)

and let the Jacobian parameter m be of the form :

$$m = \frac{\beta^2}{\alpha^2 + \beta^2}.$$ (2.3.53)

On substituting Eqs.(2.3.52) and (2.3.53) in Eq.(2.3.51), the following integral takes the form :

$$\int \frac{\mathrm{d}\Phi}{\sqrt{\left(1 - \Phi^2\right) \left(1 - m\Phi^2\right)}} = \sqrt{\frac{4a_1 \left(\alpha^2 + \beta^2\right)}{3}} \int \mathrm{d}\xi.$$ (2.3.54)

The left hand side of Eq.(2.3.54) is the normal elliptic integral of first kind and the first form [72] and hence the solution of Eq.(2.3.54) can be readily obtained from the table of elliptic integrals and is given by :

$$\Phi^2 = \mathrm{cn}^2 \left(c + 2\sqrt{\frac{a_1 \left(\alpha^2 + \beta^2\right)}{3}}\xi, m\right),$$ (2.3.55)

where $\mathrm{cn}\left(u, m\right)$ is cosine amplitude Jacobian elliptic function [72]. Hence from Eq.(2.3.52), the periodic solution to Eq.(2.3.52) is of the form :

$$S\left(\xi\right) = \beta \mathrm{cn} \left(c + 2\sqrt{\frac{a_1 \left(\alpha^2 + \beta^2\right)}{3}}\xi, m\right).$$ (2.3.56)

and is plotted in Fig.(2.6).
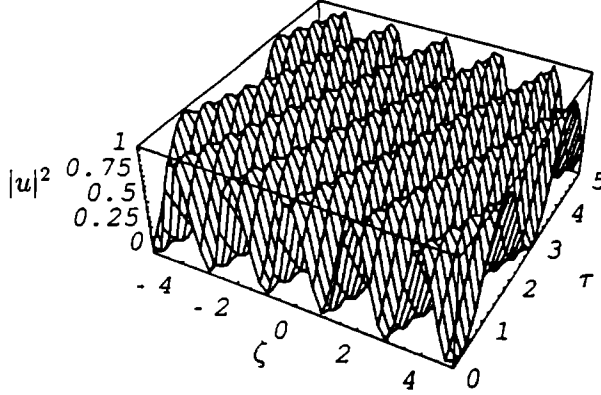
Fig. 2.6: Surface plot for the intensity of the periodic solitary wave solution given by Eq.(2.3.56) where $|u|^2 = S(\xi)$

iv) When $V(S)$ has a pair of equal and opposite roots $S = \pm\alpha$ and two single roots $S = \beta, \gamma$

The potential function $V(S)$ has the following expression given by:

$$V(S) = \frac{4a_1}{3}\left(S^2 - \alpha^2\right)(S - \beta)(S - \gamma).$$

(2.3.57)

The following set of equations are obtained on comparing Eq.(2.3.57) with Eq.(2.2.11)

$$a_2 = \frac{2a_1}{3}(\beta + \gamma),$$

(2.3.58)

$$a_3 = -\frac{a_1}{3}\left(\alpha^2 - \beta\gamma\right),$$

(2.3.59)

$$a_4 = -\frac{4a_1}{3}\alpha^2(\beta + \gamma),$$

(2.3.60)

and

$$a_5 = -\frac{4a_1}{3}\alpha^2\beta\gamma.$$

(2.3.61)

The extrema for the potential function $V(S)$ given by Eq.(2.3.57) can be determined from the cubic polynomial in S for various values of α, β and γ and is given by :

$$4S^3 - 3\left(\beta + \gamma\right)S^2 - 2\left(\alpha^2 - \beta\gamma\right)S + \alpha^2\left(\beta + \gamma\right) = 0. \qquad (2.3.62)$$

For $\alpha = 5$, $\beta = 0.2$ and $\gamma = 0.1$, $V(S)$ has a minimum at $S = 0.149985$ which
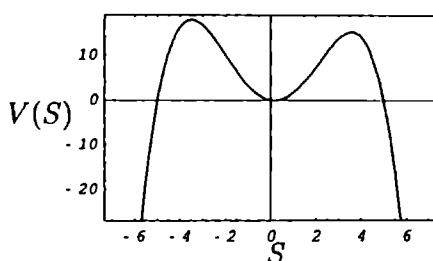
(a)
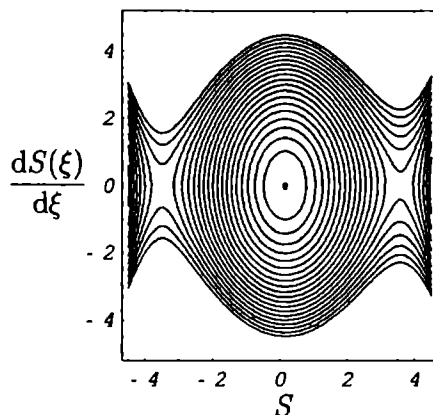
(b)

Fig. 2.7: (a) Plot of the potential function given by Eq.(2.3.57) with $\alpha = 5.0, \beta = 0.2, a_1 = -0.077, v = 0.804, q_2 = 0.8$; (b) Phase portrait having a stable center at $S = 0.149985$ and two unstable saddle points at $S = \pm 3.4984$

is a stable center and has two maxima at $S = -3.4984$ and $S = 3.57342$ which

are the unstable saddle points and are portrayed in Figs.(2.7(a)) and (2.7(b)). In order to obtain analytical expression for $S(\xi)$, the following equations are considered:

$$\lambda = \frac{1}{(\beta + \gamma)} \left(\beta\gamma + \alpha^2 + \sqrt{(\gamma^2 - \alpha^2)(\beta^2 - \alpha^2)} \right), \qquad (2.3.63)$$

$$\mu = \frac{1}{(\beta + \gamma)} \left(\beta\gamma + \alpha^2 - \sqrt{(\gamma^2 - \alpha^2)(\beta^2 - \alpha^2)} \right), \qquad (2.3.64)$$

$$b_1 = \frac{2}{\sqrt{(\gamma^2 - \alpha^2)(\beta^2 - \alpha^2)}} \left(\beta\gamma + \alpha^2 - \sqrt{(\gamma^2 - \alpha^2)(\beta^2 - \alpha^2)} \right), \qquad (2.3.65)$$

$$c_1 = \frac{-2}{\sqrt{(\gamma^2 - \alpha^2)(\beta^2 - \alpha^2)}} \left(\beta\gamma + \alpha^2 + \sqrt{(\gamma^2 - \alpha^2)(\beta^2 - \alpha^2)} \right), \qquad (2.3.66)$$

$$b_2 = \frac{-1}{\sqrt{(\gamma^2 - \alpha^2)(\beta^2 - \alpha^2)}} \left(\sqrt{(\gamma^2 - \alpha^2)} + \sqrt{(\beta^2 - \alpha^2)} \right)^2, \qquad (2.3.67)$$

$$c_2 = \frac{1}{\sqrt{(\gamma^2 - \alpha^2)(\beta^2 - \alpha^2)}} \left(\sqrt{(\gamma^2 - \alpha^2)} - \sqrt{(\beta^2 - \alpha^2)} \right)^2, \qquad (2.3.68)$$

and

$$T(\xi) = \frac{S(\xi) - \lambda}{S(\xi) - \mu}. \qquad (2.3.69)$$

Expressing the potential function $V(S)$ given by Eq.(2.3.57) in terms of $T(\xi)$ and λ, μ, b_1, c_1, b_2 and c_2, it takes the form :

$$V(S) = \frac{a_1 b_1 b_2}{12} (S - \mu)^4 (T^2 - a^2)(T^2 - b^2), \qquad (2.3.70)$$

where :

$$a^2 = -\frac{c_1}{b_1},$$

and $\qquad (2.3.71)$

$$b^2 = -\frac{c_2}{b_2}.$$

It can be easily verified that on substituting Eqs.(2.3.63)-(2.3.69) and Eq.(2.3.71) into Eq.(2.3.70), it gets simplified to Eq.(2.3.57). On differentiating Eq.(2.3.69) with respect to S on both sides, it takes the form :

$$\frac{dT}{dS} = \frac{\lambda - \mu}{(S - \mu)^2}. \qquad (2.3.72)$$

For the potential function given by Eq.(2.3.57), the nonlinear system has the form :

$$\frac{dS}{d\xi} = \sqrt{\frac{-4a_1}{3} \left(S^2 - \alpha^2\right) \left(S - \beta\right) \left(S - \gamma\right)}. \tag{2.3.73}$$

On substituting Eqs.(2.3.63)-(2.3.69) into Eq.(2.3.73), the following expression is obtained :

$$\begin{aligned} \frac{dT}{d\xi} &= \frac{dT}{dS} \sqrt{\frac{a_1' b_1 b_2}{12} \left(S - \mu\right)^4 \left(T^2 - a^2\right) \left(T^2 - b^2\right)} \\ &= \left(\lambda - \mu\right) \sqrt{\frac{a_1' b_1 b_2}{12} \left(T^2 - a^2\right) \left(T^2 - b^2\right)}, \end{aligned} \tag{2.3.74}$$

where $a_1 = -a_1'$, a_1' being positive always and $T^2 > (a^2, b^2)$. The above inequality is satisfied for the case $\alpha > \beta > \gamma$. On taking the integral of Eq.(2.3.74) on both sides, it is written in the form :

$$\int \frac{dT}{\sqrt{\left(T^2 - a^2\right)\left(T^2 - b^2\right)}} = a\left(\lambda - \mu\right)\sqrt{\frac{a_1' b_1 b_2}{12}} \int d\xi. \tag{2.3.75}$$

Let

$$\Phi^2 = \frac{\left(T^2 - a^2\right)}{\left(T^2 - b^2\right)}, \tag{2.3.76}$$

and let the Jacobian parameter m be of the form :

$$m = \frac{b^2}{a^2}. \tag{2.3.77}$$

On substituting Eqs.(2.3.76) and (2.3.77) in Eq.(2.3.75), the following integral equation takes the form :

$$\int \frac{d\Phi}{\sqrt{\left(1 - \Phi^2\right)\left(1 - m\Phi^2\right)}} = a\left(\lambda - \mu\right)\sqrt{\frac{a_1' b_1 b_2}{12}} \int d\xi. \tag{2.3.78}$$

The left hand side of Eq.(2.3.78) is the normal elliptic integral of first kind and the first form [72] and hence its solution can be readily obtained from the table

of elliptic integrals [72] and is given by :

$$\Phi^2 = \text{sn}^2 \left(c + a \ (\lambda - \mu) \ \sqrt{\frac{a_1' b_1 b_2}{12}} \xi, m \right), \qquad (2.3.79)$$

where $\text{sn}\,(u, m)$ is sine amplitude Jacobian elliptic function [72]. Thus from Eqs.(2.3.76) and (2.3.69), the periodic solution has the form :

$$S\,(\xi) = \frac{\lambda \text{cn}\,(kk\xi, m) - a\mu \text{dn}\,(kk\xi, m)}{\text{cn}\,(kk\xi, m) - a\text{dn}\,(kk\xi, m)}, \qquad (2.3.80)$$

where $kk = c + a \ (\lambda - \mu) \ \sqrt{\frac{a_1' b_1 b_2}{12}}$. Equation (2.3.80) is plotted in Fig.(2.8).
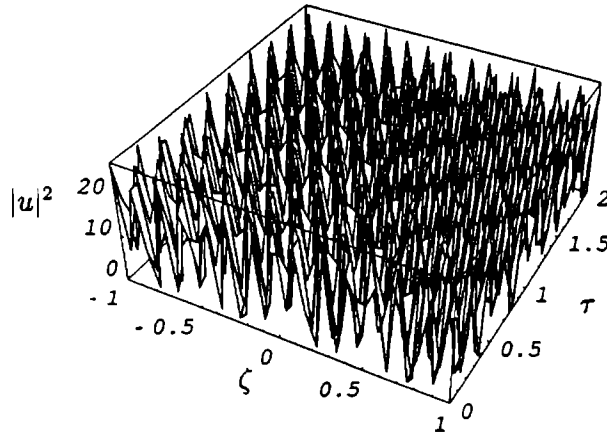
Fig. 2.8: Surface plot for the intensity of the periodic solitary wave solution given by Eq.(2.3.80) with $\alpha = 5.15$, $\beta = 20.0$, $\gamma = 15.0$, $v = 15.7$, $q_2 = 0.8$ and where $|u|^2 = S(\xi)$

2.4   Conclusions

Various analytical expressions in the form of algebraic bright and dark solitary wave solutions and periodic solutions are obtained for the higher order nonlinear Schrödinger equation by considering various forms for the potential function given

by Eq.(2.2.11). Moreover, as the total energy in this case is equal to zero, all the solutions for the corresponding potentials represent closed contours around stable centers and hence are stable.

Chapter 3

Cross-phase modulational instability in an elliptical birefringent fiber with higher order nonlinearity and dispersion

3.1 Introduction

In chapters one and two, the derivation for the higher order nonlinear Schrödinger equations were carried out by following a perturbative approach under the assumption that the fiber has negligible birefringence, both linear and nonlinear. However, small departures from cylindrical geometry or small fluctuations in material anisotropy compels the inclusion of the modal birefringence effect causing the mixing up of the two orthogonal polarization states by breaking the mode degeneracy , as a result of which the single mode fiber will support two different modes in perpendicular directions. Such a fiber is called a birefringent optical fiber [73]-[76].

Extensive research has been carried out in the field of soliton propagation in birefringent optical fibers [77]-[84]. On par with the soliton propagation, continuous wave propagation in optical fibers have also demanded special attention [1].

A continuous wave with a cubic nonlinearity in an anomalous dispersion regime is known to develop instability with respect to small modulations in amplitude or in phase, called modulational instability (MI) [54]. The MI phenomenon was discovered in fluids [85], in nonlinear optics [86] and in plasmas [87]. MI of a light wave in an optical fiber was suggested by Hasegawa and Brinkman [88] as a means to generate a far infrared light source and since then has attracted extensive attention for both its fundamental and applied interests [1]-[3]. As regards applications, MI provides a natural means of generating ultra short pulses at ultra-high repetition rates and is thus potentially useful for the development of high speed optical communication systems in future and hence has been exploited a great deal in many theoretical and experimental studies for the realization of laser sources adapted to ultrahigh bit-rate optical transmissions [89]-[91]. MI phenomenon is accompanied by sideband evolution at a frequency separation from the carrier which is proportional to the optical pump power [92]. When two or more optical waves copropagate through a birefringent optical fiber, they interact with each other through the fiber nonlinearity in such a way that the effective refractive index of a wave depends not only on the intensity of that wave but also on the intensity of other copropagating waves, a phenomenon known as cross-phase modulation (XPM) [1, 93]. MI in a birefringent optical fiber can be experimentally observed via two techniques namely i) the single-frequency copropagation where two pump waves of identical frequency copropagate with orthogonal polarizations parallel to the two birefringence axes of the fiber [94] and ii) the two-frequency copropagation, where the two polarized wave copropagate with different frequencies [95]. Drummond et al. have demonstrated experimentally that MI can occur for the normal dispersion regime by using the

single frequency copropagation technique [96] and have pointed out that the appearance of MI in the normal dispersion regime for a highly birefringent fiber is due to the group velocity mismatch (GVM) between the two copropagating waves and termed the instability as cross-phase MI (XMI) [96] . When breakup of continuous wave and quasi-continuous wave radiates into a train of picosecond and femto second pulses in the fiber, higher-order nonlinear effects such as self-steepening, self-induced Raman scattering (SRS) and higher order dispersion effects such as third and fourth order dispersion should also be taken into account [1, 97]. The influence of cross-phase modulation (XPM), higher order nonlinear effects such as self-steepening, self-induced Raman scattering (SRS) and higher order dispersion effects such as third and fourth order dispersion on XMI for a highly elliptical birefringent optical fiber is studied in this chapter and conditions for the occurrence of XMI in the normal dispersion regime are obtained.

The outline of the chapter is as follows. In Sec.3.2, the basic equation is presented. MI conditions for the basic equation are determined in Sec. 3.3. In Sec. 3.4 the derivation of the coupled linearized equations for the four side band amplitudes in the two orthogonal linear polarization components of the pump wave is presented and the MI conditions corresponding to the same are determined and are compared with those in Sec. 3.3. In Sec. 3.5, the conclusions are presented.

3.2   Mathematical formulation of the problem

In this chapter, the case of XPM-induced coupling of two waves having the same frequency but different polarizations is studied . In this regard, the basic equation will have two orthogonal polarization modes say P_x and P_y and hence the

nonlinear polarization vector $\mathbf{P}_{NL}$ has the form [1]

$$\mathbf{P}_{NL} = \frac{1}{2}\left(\widehat{e}_1 P_x + \widehat{e}_2 P_y\right)\exp\left(-i\omega_0 t\right) + \text{c.c.} \qquad (3.2.1)$$

where $\widehat{e}_1$ and $\widehat{e}_2$ denote the orthonormal polarization eigenvectors related to the unit vectors $\widehat{x}$ and $\widehat{y}$ oriented along the major and minor axes of the birefringence ellipse and are given by the expression [1] :

$$\widehat{e}_1 = \frac{\widehat{x} + ir\widehat{y}}{\sqrt{1+r^2}}, \qquad (3.2.2)$$

and

$$\widehat{e}_2 = \frac{r\widehat{x} - i\widehat{y}}{\sqrt{1+r^2}}, \qquad (3.2.3)$$

r representing the extent of ellipticity. Considering the slowly varying envelope approximation, the electric field has the form [1] :

$$\mathbf{E} = \frac{1}{2}\left(\widehat{e}_1 U + \widehat{e}_2 V\right)\exp\left(-i\omega_0 t\right) + \text{c.c.}, \qquad (3.2.4)$$

where U and V are the slowly varying electric field envelopes.

Malomed and Tasgal have derived the equation for the elliptically birefringent fiber pertaining to self-induced Raman scattering for arbitrary ellipticity angle [98, 99]. In this chapter, the important steps leading to the derivation of the coupled higher order nonlinear Schrödinger equation (CHNSE) model are outlined below from Refs. [98, 99]. Starting from the slowly varying envelope approximation, the final governing equations between the slowly varying electric field envelopes U and V and the two orthogonal polarization modes P_x and P_y are given by

$$iU_z = -\frac{\omega_0^2}{c^2}\left(P_x^{\text{Raman}} + P_x^{\text{non-Raman}}\right) \quad \text{and}$$
$$iV_z = -\frac{\omega_0^2}{c^2}\left(P_y^{\text{Raman}} + P_y^{\text{non-Raman}}\right) \qquad (3.2.5)$$

The equations for the Raman effect in an optical fiber in the case of arbitrary ellipticity have been derived in Ref. [99] where casuality [99] and nonlinear isotropy restrict the Raman contribution to the form [99]:

$$
\mathbf{P}^{\text{Raman}}(z,T) = \mathbf{E}(z,T) \int\limits_{-\infty}^{+\infty} F_1(T - T')\mathbf{E}(z,T') \cdot \mathbf{E}(z,T') dT'
$$

$$
\mathbf{E}(z,T) \cdot \int\limits_{-\infty}^{+\infty} \mathbf{E}(z,T')F_2(T - T')\mathbf{E}(z,T')dT', \quad (3.2.6)
$$

where $\mathbf{E}$ is the electric field and F_1 and F_2 are material functions. Under the slowly varying envelope approximation, as the electric field envelopes U and V and the polarization components P_x and P_y are assumed to vary slowly, the rapidly oscillatory out-of-phase terms may be dropped, provided the Raman time scales are much longer than the oscillation period of the electric field. The polarization envelopes-the terms which remain after rapidly oscillating terms are dropped from Eq.(3.2.6)-are thus given by [99] :

$$
P_x^{\text{Raman}} = U(z,T) \int\limits_{-\infty}^{+\infty} \left[2F_1(T - T') + \left(1 + \cos^2\theta\right) F_2(T - T') \right] |U(z,T)|^2 dT'
$$

$$
+U(z,T) \int\limits_{-\infty}^{+\infty} \left[2F_1(T - T') + \left(1 + \sin^2\theta\right) F_2(T - T') \right] |V(z,T)|^2 dT'
$$

$$
+V(z,T) \int\limits_{-\infty}^{+\infty} \left(1 + \sin^2\theta\right) F_2(T - T')U(z,T')V^*(z,T')dT'
$$

$$
P_y^{\text{Raman}} = V(z,T) \int\limits_{-\infty}^{+\infty} \left[2F_1(T - T') + \left(1 + \cos^2\theta\right) F_2(T - T') \right] |V(z,T)|^2 dT'
$$

$$
+V(z,T) \int\limits_{-\infty}^{+\infty} \left[2F_1(T - T') + \left(1 + \sin^2\theta\right) F_2(T - T') \right] |U(z,T)|^2 dT'
$$

$$
+U(z,T) \int\limits_{-\infty}^{+\infty} \left(1 + \sin^2\theta\right) F_2(T - T')U^*(z,T')V(z,T')dT', \quad (3.2.7)
$$

where the ellipticity angle θ defines the relations :

$$\widehat{e}_1 \cdot \widehat{e}_1 = \widehat{e}_2 \cdot \widehat{e}_2 = \cos\theta \qquad \text{and}$$

$$\widehat{e}_1 \cdot \widehat{e}_2 = \sin\theta. \tag{3.2.8}$$

Then, making the connection to the evolution equations, the Raman contribution to the evolution equations takes the form

$$iU_z|_{\text{Raman}} = P_x^{\text{Raman}} \qquad \text{and}$$

$$iV_z|_{\text{Raman}} = P_y^{\text{Raman}} \tag{3.2.9}$$

In the quasi-instantaneous limit, the functions F_1 and F_2 may be split into an instantaneous part and a quasi-instantaneous part, i.e.

$$F(T) = (F_{\text{inst}})\delta(T) + (F_{\text{quasi-inst}})\delta(T'). \tag{3.2.10}$$

The quasi-instantaneous part gives [99]

$$iU_z|_{\text{Raman}} = \gamma \left(U \left[\varepsilon_3' |U|^2 + \varepsilon_4' |V|^2 \right]_T + \varepsilon_5' V [U V^*]_T \right),$$

$$iV_z|_{\text{Raman}} = \gamma \left(V \left[\varepsilon_4' |U|^2 + \varepsilon_3' |V|^2 \right]_T + \varepsilon_5' U [U^* V]_T \right), \tag{3.2.11}$$

where γ is the nonlinearity coefficient. The Raman coefficients $\varepsilon_3', \varepsilon_4'$ and ε_5' are given by [99]:

$$\varepsilon_3' = \left[2(F_{\text{quasi-inst}})_1 + \left(1 + \cos^2\theta\right)(F_{\text{quasi-inst}})_2 \right],$$

$$\varepsilon_4' = \left[2(F_{\text{quasi-inst}})_1 + \sin^2\theta(F_{\text{quasi-inst}})_2 \right] \qquad \text{and}$$

$$\varepsilon_5' = \left(1 + \sin^2\theta\right)(F_{\text{quasi-inst}})_2. \tag{3.2.12}$$

Hence the relation between the three Raman coefficients can be written as :

$$\varepsilon_3' = \varepsilon_4' + \frac{2\,\cos^2\theta}{1 + \sin^2\theta}\,\varepsilon_5'. \tag{3.2.13}$$

The contributions due to the non-Raman terms can be derived in the same way as those due to the Raman terms [99] presented in this chapter and also by following a similar procedure for both of the slowly varying electric field envelopes U and V, as in the case for deriving the scalar nonlinear Schrödinger equation in chapter one. Furthermore, Menyuk has devised an easy method for deriving the coupled nonlinear Schrödinger equation [1]-[3]. Finally, the non-Raman contributions to the evolution equations take the form [99]:

$$iU_z|_{\text{non-Raman}} = -\left(\gamma \left(|U|^2 + B \, |V|^2 \right) U + i \, \frac{\gamma}{\omega_0} \left[\left(\varepsilon_1' \, |U|^2 + \varepsilon_2' \, |V|^2 \right) U \right]_T \right),$$

$$iV_z|_{\text{non-Raman}} = -\left(\gamma \left(B \, |U|^2 + |V|^2 \right) V + i \, \frac{\gamma}{\omega_0} \left[\left(\varepsilon_2' \, |U|^2 + \varepsilon_1' \, |V|^2 \right) V \right]_T \right),$$

$$(3.2.14)$$

where the terms in the square parenthesis denote the effect due to self-steepening [97]. ε_1' and ε_2' are constants and are the coefficients of the self-steepening terms. The cross-phase modulation coefficient B is a function of ellipticity and is given by [78]

$$B = \frac{2 + 2\sin^2\theta}{2 + \cos^2\theta} \qquad (3.2.15)$$

This gives $B = \dfrac{2}{3}$ for linear ellipticity $\theta = 0$; $B = 2$ for circular ellipticity $\theta = 90°$ and $B = 1$ for ideal birefringence case, for which $\theta \approx 35.3°$. Finally, the linear contributions to the evolution equations yield:

$$iU_z|_{\text{Linear}} = \left(-i\frac{\delta}{2} U_T + \frac{\beta_2}{2} U_{TT} + i \frac{\beta_3}{6} U_{TTT} + \frac{\beta_4}{24} U_{TTTT} \right),$$

$$iV_z|_{\text{Linear}} = \left(i\frac{\delta}{2} V_T + \frac{\beta_2}{2} V_{TT} + i \frac{\beta_3}{6} V_{TTT} + \frac{\beta_4}{24} V_{TTTT} \right), \qquad (3.2.16)$$

where β_2, β_3 and β_4 are the second, third and fourth order dispersion coefficients respectively. Considering both these higher order dispersion and nonlinear effects, the coupled higher order nonlinear Schrödinger equation (CHNSE) model [97]-[99] with the addition of self-steepening, SRS, third and fourth order dispersion

effects is given by:

$$i \left(U_z + \frac{\delta}{2} U_T \right) - \frac{\beta_2}{2} U_{TT} + \gamma \left(|U|^2 + B \, |V|^2 \right) U - i \frac{\beta_3}{6} U_{TTT} - \frac{\beta_4}{24} U_{TTTT}$$

$$+ i \frac{\gamma}{\omega_0} \left[(\varepsilon_1' \, |U|^2 + \varepsilon_2' \, |V|^2) U \right]_T - \gamma \left(U \, \left[\varepsilon_3' \, |U|^2 + \varepsilon_4' \, |V|^2 \right]_T + \varepsilon_5' \, V \right.$$

$$\left. [U \, V^*]_T \right) = 0,$$

$$i \left(V_z - \frac{\delta}{2} V_T \right) - \frac{\beta_2}{2} V_{TT} + \gamma \left(B \, |U|^2 + |V|^2 \right) V - i \frac{\beta_3}{6} V_{TTT} - \frac{\beta_4}{24} V_{TTTT}$$

$$+ i \frac{\gamma}{\omega_0} \left[(\varepsilon_2' \, |U|^2 + \varepsilon_1' \, |V|^2) V \right]_T - \gamma \left(V \, \left[\varepsilon_4' \, |U|^2 + \varepsilon_3' \, |V|^2 \right]_T + \varepsilon_5' \, U \right.$$

$$\left. [U^* \, V]_T \right) = 0, \tag{3.2.17}$$

where z is the longitudinal distance, $T = t - \dfrac{z}{v_g}$ is the retarded time.

In the dimensionless form, the above equation becomes [97]

$$i \left(u_\varsigma' + \Delta \, u_\tau' \right) - S_1 \, u_{\tau\tau}' + \left[\left| u' \right|^2 + B \left| v' \right|^2 \right] u' - i \, S_2 \, u_{\tau\tau\tau}' - S_3 \, u_{\tau\tau\tau\tau}'$$

$$+ i \left[\left(\varepsilon_1 \, |u'|^2 + \varepsilon_2 \, |v'|^2 \right) u' \right]_\tau - \left(u' \left[\varepsilon_3 \, |u'|^2 + \varepsilon_4 \, |v'|^2 \right]_\tau + \varepsilon_5 \, v' \, [u' \, v'^*]_\tau \right) = 0,$$

$$i \left(v_\varsigma' - \Delta \, v_\tau' \right) - S_1 \, v_{\tau\tau}' + \left[B \left| u' \right|^2 + \left| v' \right|^2 \right] v' - i \, S_2 \, v_{\tau\tau\tau}' - S_3 \, v_{\tau\tau\tau\tau}'$$

$$+ i \left[\left(\varepsilon_2 \, |u'|^2 + \varepsilon_1 \, |v'|^2 \right) v' \right]_\tau - \left(v' \left[\varepsilon_4 \, |u'|^2 + \varepsilon_3 \, |v'|^2 \right]_\tau + \varepsilon_5 \, u' \, [u'^* \, v']_\tau \right) = 0,$$

$$\tag{3.2.18}$$

where $\varsigma = \dfrac{z}{T_0^2} \, |\beta_2|$; $\tau = \dfrac{T}{T_0}$; $\Delta = \dfrac{T_0 \, \delta}{2 \, |\beta_2|}$; $S_1 = \dfrac{s_1}{2}$; $S_2 = \dfrac{s_2 \, |\beta_3|}{6 \, T_0 \, |\beta_2|}$;

$S_3 = \dfrac{s_3 \, |\beta_4|}{24 \, T_0^2 \, |\beta_2|}$; $U = \sqrt{\dfrac{|\beta_2|}{\gamma \, T_0^2}} \, u'$; $V = \sqrt{\dfrac{|\beta_2|}{\gamma \, T_0^2}} \, v'$; $\varepsilon_1 = \dfrac{\varepsilon_1'}{\omega_0 \, T_0}$; $\varepsilon_2 = \dfrac{\varepsilon_2'}{\omega_0 \, T_0}$;

$\varepsilon_3 = \dfrac{\varepsilon_3'}{T_0}$; $\varepsilon_4 = \dfrac{\varepsilon_4'}{T_0}$; $\varepsilon_5 = \dfrac{\varepsilon_5'}{T_0}$, where T_0 is an arbitrary timescale and

$s_i = \pm 1$ $(i = 1, 2, 3)$. In this chapter, three different scenarios for generation of

ultra short pulses of various pulse widths, governed by the respective MI con-

ditions are considered, namely: (i) generation of ultra short pulses of the order

of 500 fs and above [100] where all the higher order nonlinear terms can be neglected [101, 102] i.e., $\varepsilon_1 = \varepsilon_2 = \varepsilon_3 = \varepsilon_4 = \varepsilon_5 = 0$ with only the third and fourth order dispersion terms remaining in Eq.(3.2.18), (ii) generation of ultra short pulses in the femto second region below 500 fs where the influence of SRS and self-steepening should be considered along with the higher order dispersion terms [1, 2, 103], (iii) generation of ultra short pulses in the sub-pico femto second region containing terms in Eq.(3.2.18) other than the self-steepening and fourth order dispersion terms, which can be safely neglected [1, 3, 103].

3.3 Stability analysis and modulational instability conditions

In the case of continuous wave or quasi-continuous wave radiations, the orthogonally polarized amplitudes u' and v' are independent of τ at the input end of the fiber at $\zeta = 0$. Considering the case for a linearly polarized pump oriented at an arbitrary angle with respect to either the slow or the fast axis of the birefringent fiber and assuming that both $u'(\zeta, \tau)$ and $v'(\zeta, \tau)$ remain time independent during propagation inside the fiber, Eq.(3.2.18) admits steady-state solutions of the form [1]:

$$
\begin{aligned}
u' &= \sqrt{P_1} \, \exp\left(i\,\zeta\,\left(P_1 + B\,P_2\right)\right), \\
v' &= \sqrt{P_2} \, \exp\left(i\,\zeta\,\left(P_2 + B\,P_1\right)\right),
\end{aligned}
\tag{3.3.1}
$$

where $P_{1,2}$ are proportional to input powers along the principal axes. These steady-state solutions imply that light propagates through the birefringent fiber unchanged except for acquiring a power-dependent phase shift. The stability of the steady state solution is examined by looking into the system in the presence

of small amplitude perturbations $u\left(\zeta,\tau\right)$ and $v\left(\zeta,\tau\right)$ given by:

$$u' = \left(\sqrt{P_1} + u\right) \exp\left(i\,\zeta\,\left(P_1 + B\,P_2\right)\right),$$

$$v' = \left(\sqrt{P_2} + v\right) \exp\left(i\,\zeta\,\left(P_2 + B\,P_1\right)\right), \tag{3.3.2}$$

On substituting Eq.(3.3.2) into Eq.(3.2.18) and on linearizing in $u\left(\zeta,\tau\right)$ and $v\left(\zeta,\tau\right)$, the following linearized equations in $u\left(\zeta,\tau\right)$ and $v\left(\zeta,\tau\right)$ are obtained:

$$i\,(u_\zeta + \Delta\,u_\tau) - S_1\,u_{\tau\tau} + \left(P_1\,(u+u^*) + B\,\sqrt{P_1\,P_2}\,(v+v^*)\right) - i\,S_2\,u_{\tau\tau\tau}$$

$$- S_3\,u_{\tau\tau\tau\tau} + i\,\left(\varepsilon_1\,P_1\,[u^* + 2\,u]_\tau + \varepsilon_2\,\left[P_2\,u + \sqrt{P_1\,P_2}\,(v+v^*)\right]_\tau\right)$$

$$- \left(\varepsilon_3\,P_1\,[u+u^*]_\tau + \varepsilon_4\,\sqrt{P_1\,P_2}\,[v+v^*]_\tau + \varepsilon_5\,\left[P_2\,u + \sqrt{P_1\,P_2}\,v^*\right]_\tau\right) = 0,$$

$$i\,(v_\zeta - \Delta\,v_\tau) - S_1\,v_{\tau\tau} + \left(B\,\sqrt{P_1\,P_2}\,(u+u^*) + P_2\,(v+v^*)\right) - i\,S_2\,v_{\tau\tau\tau}$$

$$- S_3\,v_{\tau\tau\tau\tau} + i\,\left(\varepsilon_1\,P_2\,[v^* + 2\,v]_\tau + \varepsilon_2\,\left[P_1\,v + \sqrt{P_1\,P_2}\,(u+u^*)\right]_\tau\right)$$

$$- \left(\varepsilon_3\,P_2\,[v+v^*]_\tau + \varepsilon_4\,\sqrt{P_1\,P_2}\,[u+u^*]_\tau + \varepsilon_5\,\left[\sqrt{P_1\,P_2}\,u^* + P_1\,v\right]_\tau\right) = 0. $$

$$\tag{3.3.3}$$

The Fourier transforms of $u\left(\zeta,\tau\right)$ and $v\left(\zeta,\tau\right)$ are:

$$A_1\left(\zeta,\omega\right) = \frac{1}{\sqrt{2\,\pi}} \int_{-\infty}^{+\infty} u\left(\zeta,\tau\right) \exp\left(i\,\omega\,\tau\right)\,d\tau,$$

$$A_2\left(\zeta,\omega\right) = \frac{1}{\sqrt{2\,\pi}} \int_{-\infty}^{+\infty} v\left(\zeta,\tau\right) \exp\left(i\,\omega\,\tau\right)\,d\tau, \tag{3.3.4}$$

which yield the inverse Fourier transforms

$$u\left(\zeta,\tau\right) = \frac{1}{\sqrt{2\,\pi}} \int_{-\infty}^{+\infty} A_1\left(\zeta,\omega\right) \exp\left(-i\omega\tau\right)\,d\omega$$

$$= \frac{1}{\sqrt{2\,\pi}} \int_{-\infty}^{+\infty} A_1\left(\zeta,-\omega\right) \exp\left(i\omega\tau\right)\,d\omega, \tag{3.3.5}$$

$$v\left(\zeta, \tau\right) = \frac{1}{\sqrt{2\,\pi}} \int\limits_{-\infty}^{+\infty} A_2\left(\zeta, \omega\right) \exp\left(-i\omega\tau\right) \, d\omega$$

$$= \frac{1}{\sqrt{2\,\pi}} \int\limits_{-\infty}^{+\infty} A_2\left(\zeta, -\omega\right) \exp\left(i\omega\tau\right) \, d\omega. \qquad (3.3.6)$$

On substituting Eqs.(3.3.5) and (3.3.6)into Eq.(3.3.3) and on considering the relation given by

$$A_i^\dagger\left(\zeta, \omega\right) = A_i^*\left(\zeta, -\omega\right), \qquad (3.3.7)$$

where $i = 1, 2$, Eq.(3.3.5) gets transformed to the following set of equations [97]:

$$\frac{1}{\sqrt{2\,\pi}} \int\limits_{-\infty}^{+\infty} \left(i\frac{\partial A_1}{\partial\zeta} + N_{11}A_1 + N_{12}A_1^\dagger + N_{13}A_2 + N_{14}A_2^\dagger\right) \exp\left(-i\omega\tau\right) \, d\omega = 0,$$

$$(3.3.8)$$

and

$$\frac{1}{\sqrt{2\,\pi}} \int\limits_{-\infty}^{+\infty} \left(i\frac{\partial A_2}{\partial\zeta} + N_{21}A_1 + N_{22}A_1^\dagger + N_{23}A_2 + N_{24}A_2^\dagger\right) \exp\left(-i\omega\tau\right) \, d\omega = 0.$$

$$(3.3.9)$$

where [97]

$$N_{11} = \Delta\omega + S_2\omega^3 + P_1 + S_1\omega^2 + 2\varepsilon_1 P_1\omega + \varepsilon_1 P_2\omega + i\varepsilon_3 P_1\omega + i\varepsilon_5 P_2\omega - S_3\omega^4,$$

$$N_{12} = P_1 + \varepsilon_1 P_1\omega + i\varepsilon_3 P_1\omega,$$

$$N_{13} = B\sqrt{P_1 P_2} + i\varepsilon_4\sqrt{P_1 P_2}\omega + \varepsilon_2\sqrt{P_1 P_2}\omega,$$

$$N_{14} = B\sqrt{P_1 P_2} + \varepsilon_2\sqrt{P_1 P_2}\omega + i\varepsilon_4\sqrt{P_1 P_2}\omega + i\varepsilon_5\sqrt{P_1 P_2}\omega,$$

$$N_{21} = N_{13},$$

$$N_{22} = N_{14},$$

$$N_{23} = -\Delta\omega + S_2\omega^3 + P_1 + S_1\omega^2 + 2\varepsilon_1 P_2\omega + \varepsilon_2 P_1\omega + i\varepsilon_3 P_2\omega + i\varepsilon_5 P_1\omega - S_3\omega^4,$$

$$N_{24} = P_2 + \varepsilon_1 P_2\omega + i\varepsilon_3 P_2\omega.$$

On taking the complex conjugate of Eq.(3.3.3) and proceeding as above, one more set of equations are obtained [97]

$$\frac{1}{\sqrt{2\,\pi}} \int\limits_{-\infty}^{+\infty} \left(i\frac{\partial A_1^\dagger}{\partial \zeta} + N_{31}A_1 + N_{32}A_1^\dagger + N_{33}A_2 + N_{34}A_2^\dagger \right) \exp\left(-i\omega\tau\right) \; d\omega = 0,$$

$$(3.3.10)$$

and

$$\frac{1}{\sqrt{2\,\pi}} \int\limits_{-\infty}^{+\infty} \left(i\frac{\partial A_2^\dagger}{\partial \zeta} + N_{41}A_1 + N_{42}A_1^\dagger + N_{43}A_2 + N_{44}A_2^\dagger \right) \exp\left(-i\omega\tau\right) \; d\omega = 0,$$

$$(3.3.11)$$

where [97]

$$N_{31} = -P_1 + \varepsilon_1 P_1\omega - i\varepsilon_3 P_1\omega,$$

$$N_{32} = \Delta\omega + S_2\omega^3 - P_1 - S_1\omega^2 + 2\varepsilon_1 P_1\omega + \varepsilon_2 P_2\omega - i\varepsilon_3 P_1\omega + i\varepsilon_5 P_2\omega + S_3\omega^4,$$

$$N_{33} = -B\sqrt{P_1 P_2} + \varepsilon_2\sqrt{P_1 P_2}\omega - i\varepsilon_4\sqrt{P_1 P_2}\omega - i\varepsilon_5\sqrt{P_1 P_2}\omega,$$

$$N_{34} = -B\sqrt{P_1 P_2} - i\varepsilon_4\sqrt{P_1 P_2}\omega + \varepsilon_2\sqrt{P_1 P_2}\omega,$$

$$N_{41} = N_{33},$$

$$N_{42} = N_{34},$$

$$N_{43} = -P_1 + \varepsilon_1 P_2\omega - i\varepsilon_3 P_2\omega,$$

$$N_{44} = -\Delta\omega + S_2\omega^3 - P_2 - S_1\omega^2 + 2\varepsilon_1 P_2\omega + \varepsilon_2 P_1\omega - i\varepsilon_3 P_{12}\omega + i\varepsilon_5 P_1\omega + S_3\omega^4.$$

On considering the case when the linearly polarized pump is oriented at 45° with respect to both the axes such that power is equally distributed along both axes, i.e., $P_1 = P_2 = P$ with the total input power being $2P$ and on equating the integrands in Eqs.(3.3.8)-(3.3.11) equal to zero and after some manipulation, four linearized equations in terms of $A_1 + A_1^\dagger$, $A_1 - A_1^\dagger$, $A_2 + A_2^\dagger$ and $A_2 - A_2^\dagger$ are

obtained which are of the form [97]:

$$i\frac{\partial\left(A_1+A_1^\dagger\right)}{\partial\zeta} = M_{11}\left(A_1+A_1^\dagger\right) + M_{12}\left(A_1-A_1^\dagger\right)$$
$$+M_{13}\left(A_2+A_2^\dagger\right) + M_{14}\left(A_2-A_2^\dagger\right),$$

$$i\frac{\partial\left(A_1-A_1^\dagger\right)}{\partial\zeta} = M_{21}\left(A_1+A_1^\dagger\right) + M_{22}\left(A_1-A_1^\dagger\right)$$
$$+M_{23}\left(A_2+A_2^\dagger\right) + M_{24}\left(A_2-A_2^\dagger\right),$$

$$i\frac{\partial\left(A_2+A_2^\dagger\right)}{\partial\zeta} = M_{31}\left(A_1+A_1^\dagger\right) + M_{32}\left(A_1-A_1^\dagger\right)$$
$$+M_{33}\left(A_2+A_2^\dagger\right) + M_{34}\left(A_2-A_2^\dagger\right),$$

$$i\frac{\partial\left(A_2-A_2^\dagger\right)}{\partial\zeta} = M_{41}\left(A_1+A_1^\dagger\right) + M_{42}\left(A_1-A_1^\dagger\right)$$
$$+M_{43}\left(A_2+A_2^\dagger\right) + M_{44}\left(A_2-A_2^\dagger\right),$$

where

$$M_{11} = \Delta\omega + S_2\,\omega^3 + P\,\omega\,(3\,\varepsilon_1+\varepsilon_2),$$
$$M_{12} = S_1\,\omega^2 - S_3\,\omega^4 + i\,\varepsilon_5\,P\,\omega,$$
$$M_{13} = 2\,\varepsilon_2\,P\,\omega,$$
$$M_{14} = -i\,\varepsilon_5\,P\,\omega,$$
$$M_{21} = S_1\,\omega^2 - S_3\,\omega^4 + 2\,P + i\,P\,\omega\,(2\,\varepsilon_3+\varepsilon_5),$$
$$M_{22} = \Delta\omega + S_2\,\omega^3 + P\,\omega\,(\varepsilon_1+\varepsilon_2),$$
$$M_{23} = 2\,BP + iP\omega\,(\varepsilon_4+\varepsilon_5),$$
$$M_{24} = 0,$$

$$M_{31} = 2\,\varepsilon_2\,P\,\omega,$$

$$M_{32} = -i\,\varepsilon_5\,P\,\omega,$$

$$M_{33} = -\Delta\,\omega + S_2\,\omega^3 + P\,\omega\,(3\,\varepsilon_1 + \varepsilon_2),$$

$$M_{34} = M_{12},$$

$$M_{41} = 2BP + iP\omega\,(2\,\varepsilon_4 + \varepsilon_5),$$

$$M_{42} = 0,$$

$$M_{43} = M_{21},$$

$$M_{44} = -\Delta\,\omega + S_2\,\omega^3 + P\,\omega\,(\varepsilon_1 + \varepsilon_2).$$

These equations can be brought into the following matrix form [97]

$$i\,\frac{\partial\,\mathbf{A}\,(\varsigma,\omega)}{\partial\,\zeta} = -\mathbf{M}\,(\omega)\,\mathbf{A}\,(\varsigma,\omega) \tag{3.3.12}$$

where:

$$\mathbf{A}\,(\varsigma,\omega) = \begin{pmatrix} A_1 + A_1^\dagger \\ A_1 - A_1^\dagger \\ A_2 + A_2^\dagger \\ A_2 - A_2^\dagger \end{pmatrix}, \tag{3.3.13}$$

and

$$\mathbf{M}\,(\omega) = \begin{pmatrix} M_{11} & M_{12} & M_{13} & M_{14} \\ M_{21} & M_{22} & M_{23} & 0 \\ M_{31} & M_{32} & M_{33} & M_{34} \\ M_{41} & 0 & M_{43} & M_{4.} \end{pmatrix}. \tag{3.3.14}$$

The eigen value equation is given by :

$$|\mathbf{M}\,(\omega) - k\,\mathbf{I}| = 0, \tag{3.3.15}$$

where **I** is the identity matrix . From Eq.(3.3.15), a dispersion relation in k is obtained which is a fourth order polynomial equation . As is well known, MI occurs when there is an exponential growth in the amplitude of the perturbed wave which implies the existence of a nonvanishing imaginary part in the complex eigen value k [1]. The MI phenomenon is measured by a gain given by $G = |\text{Im } k|$ where Im k denotes the imaginary part of k. The gain parameter G throws light on the MI conditions for the three different scenarios of pulse propagation mentioned in Sec. 3.2. The results obtained for the three different cases are discussed below [97]

(i) MI condition governing the generation of ultra short pulses in the femto second region of the order of 500 fs and above

This scenario has been experimentally studied by Cavalacanti et al. for the scalar nonlinear Schrödinger equation [100]. The case when the linearly polarized pump is oriented at 45° with respect to both the axes such that equal power is distributed along each axis, $i.e., P_1 = P_2 = P$ with the total input power being $2P$ is considered. From Eq.(3.3.15), the dispersion relation between k and ω is obtained which is of the form [97]

$$k^4 - 4\, S_2\, \omega^3\, k^3 - 2\, \omega^2\, L_1\, k^2 + 4\, S_2\, \omega^5\, L_2\, k + \omega^4\, L_3 = 0 \qquad (3.3.16)$$

where

$$L_1 = \Delta^2 + \omega^2\, \left(S_1^2 - 3\, S_2^2\, \omega^2 + S_3^2\, \omega^4\right) - S_1\, \left(2\, S_3\, \omega^4 - P\right),$$

$$L_2 = \Delta^2 + \omega^2\, \left(S_1^2 - S_2^2\, \omega^2 + S_3^2\, \omega^4 - S_3\, P\right) - S_1\, \left(2\, S_3\, \omega^4 - P\right),$$

and

$$L_3 = \Delta^4 + \omega^4 \left(-S_2^2\,\omega^2 + \left(S_1 - S_3\,\omega^2\right)^2\right)^2 + \left(1 - B^2\right)\left(S_1 - S_3\,\omega^2\right)^2 P^2$$
$$+2\,\omega^2\left(S_1 - S_3\,\omega^2\right)\left(-S_2^2\,\omega^2 + \left(S_1 - S_3\,\omega^2\right)^2\right)P$$
$$-2\,\Delta^2\left(\omega^2\left(S_1^2 + S_2^2\,\omega^2 + S_3^2\,\omega^4 - S_3\,P\right) - S_1\left(2\,S_3\,\omega^4 - P\right)\right)$$

$S_1 = -\frac{1}{2}$ portrays the case of MI in the anomalous dispersion regime which has been discussed in detail in Ref.[1, 96]. The normal dispersion regime denoted by $S_1 = \frac{1}{2}$ is now analyzed. In this case, the complex eigen value k obtained from the dispersion relation given by Eq.(3.3.16) has the form [97]

$$k = S_2\,\omega^3 \pm \omega\sqrt{L_4 \pm 2\,\sqrt{L_5}}\,, \qquad (3.3.17)$$

where

$$L_4 = \Delta^2 + \left(S_1 - S_3\,\omega^2\right)\left(S_1\,\omega^2 - S_3\,\omega^4 + 2\,P\right),$$
$$L_5 = \left(S_1 - S_3\,\omega^2\right)\left(B^2\left(S_1 - S_3\,\omega^2\right)P^2 + \Delta^2\left(S_1\,\omega^2 - S_3\,\omega^4 + 2\,P\right)\right)$$

Eq. (3.3.17) is found to possess a nonzero imaginary part only for the case given by [97]

$$k = S_2\,\omega^3 \pm \omega\sqrt{L_4 - 2\,\sqrt{L_5}}\,. \qquad (3.3.18)$$

Hence from the above equation, the condition for instability to occur is determined which is given by $L_4^2 < 4\,L_5$. From Eq. (3.3.18) it is clear that the instability condition is not affected irrespective of the presence or absence of S_2, the dimensionless third order dispersion coefficient. Figure(3.1(a)) shows the graphical relation between the frequency detuning ω, input power P and gain G for $B = \frac{2}{3}$ which depicts linear birefringence, $\Delta = 3.92512$, $S_1 = 0.5$, $S_2 = 2.6087 \times 10^{-6}$ and $S_3 = 1.69082 \times 10^{-6}$. This corresponds to the case when $|\beta_2| = 69.0$ ps^2/Km, $|\beta_3| = 0.54 \times 10^{-3}$ ps^3/Km and $|\beta_4| = 7.0 \times 10^{-4}$ ps^4/Km.
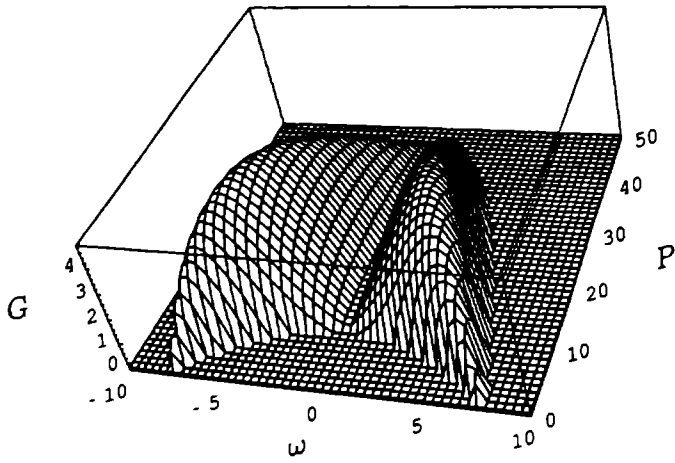
(a)
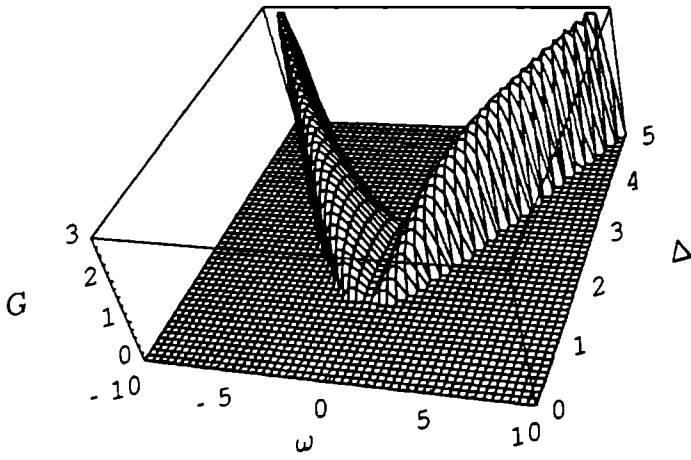
(b)

Fig. 3.1: Surface plots of the gain spectrum G for case (i) when $|\beta_2| = 69.0$ ps^2/Km, $|\beta_3| = 0.54 \times 10^{-3}$ ps^3/Km and $|\beta_4| = 7.0 \times 10^{-4}$ ps^4/Km: (a) Gain spectrum as a function of frequency detuning ω and input power P for $\Delta = 3.925$, $S_1 = 0.5$, $S_2 = 2.6087 \times 10^{-6}$ and $S_3 = 1.69082 \times 10^{-6}$; (b) Gain spectrum as a function of frequency detuning ω and group velocity mismatch Δ for $P = 5.0$ and having the same values for the rest of the parameters as in (a).
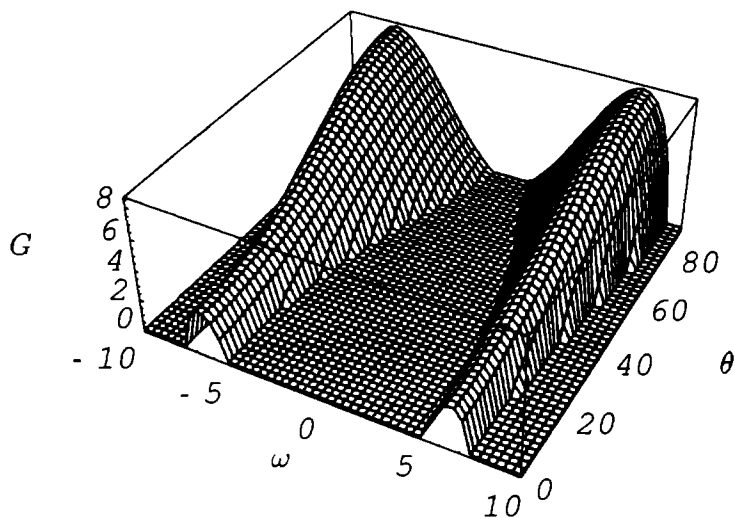
(a)
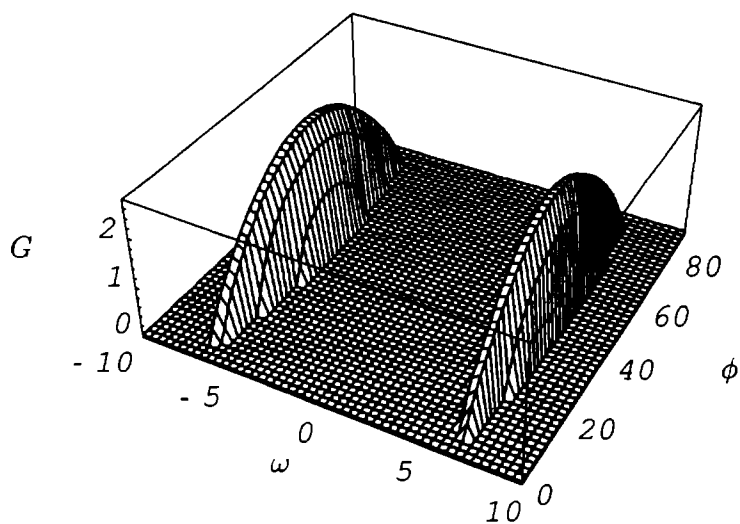
(b)

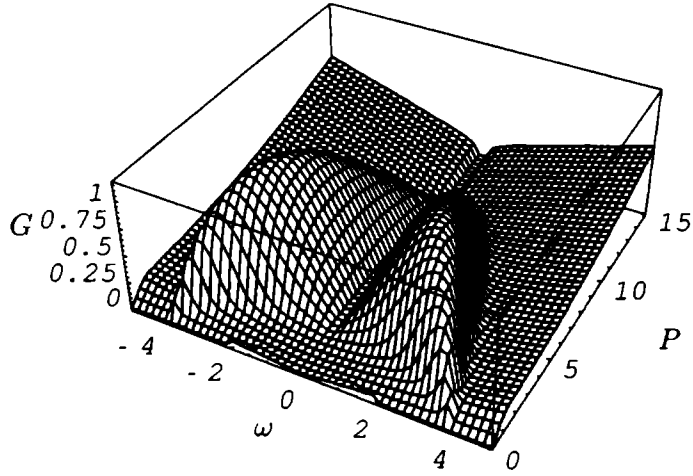Fig. 3.2: Surface plots of the gain spectrum G for case (i): (a) Gain spectrum as a function of frequency detuning ω and ellipticity angle θ for the same values as in Fig.(3.1) (b) Gain spectrum as a function of frequency detuning ω and polarization angle ϕ for the same values as in Fig.(3.1)

From Fig.(3.1(a)), it is evident that as the pump power is increased, the peaks of the gain curve move closer to the zero detuning frequency with the peak position changing relatively slowly when compared to the increase in the gain band width. This is the case of cross-phase MI (XMI) which occurs at a finite detuning from the carrier frequency [96]. A marked difference of the present results from the results obtained in Ref.[96] is that generation of ultra short pulses of the order of 500 fs and above requires a comparatively much wider range of input power and the region of MI spreads over a comparatively wider range of the frequency detuning ω, where the fourth order dispersion plays a dominant role. In Fig.(3.1(b)), which shows the graphical relation between gain G, group velocity mismatch Δ and frequency detuning ω for $P = 5.0$ and with the other parameters having the same values as in Fig.(3.1(a)), the instability occurs only for finite values of group velocity mismatch. As is well known, the XPM coupling factor B depends on the ellipticity angle θ and can vary from $\frac{2}{3}$ to 2 for values of θ in the range 0 to $\frac{\pi}{2}$ [1]-[3]. $\theta = 0$ corresponds to linear birefringence for which $B = \frac{2}{3}$ and $\theta = \frac{\pi}{2}$ corresponds to circular birefringence for which $B = 2$ [1]-[3]. For $\theta \approx 35°$, $B = 1.0$ which corresponds to the ideal birefringence case where the self and cross-phase coupling terms are identical [78]. Figure (3.2(a)) shows the variation of gain G with respect to the frequency detuning ω and the ellipticity angle θ for $P = 5.0$. In this case, the peaks of the gain curve increase with increasing θ. Furthermore it can be observed that as the pump power is steadily increased, the gap between the two sidebands decreases and finally approaches the zero detuning frequency. To study the effect of variations in the pump polarization wherein the pump power is not distributed equally along both the axes, the pump powers in terms of the polarization angle ϕ can be written in the form $P_1 = 2P\cos^2(\phi)$ and $P_2 = 2P\sin^2(\phi)$ such that the total

pump power is always equal to $2P$. On substituting these into the eigen value Eq.(3.3.15), the MI condition is determined numerically (Mathematica source code is given in Appendix A). Figure (3.2(b)) depicts the surface plot of the gain spectrum as a function of the frequency detuning ω and the polarization angle ϕ. As in Ref.[96], here too maximum gain occurs at $\phi = 45°$ and no XMI is observed when the linearly polarized pump is polarized on either principal axis.

(ii)MI condition governing the generation of ultra short pulses in the femto second region below 500 fs

It is not possible to neglect the influence of SRS and self-steepening on the MI in this regime as it is typically larger than other perturbations and unlike dispersion, the Raman effect is nonconservative and can thus cause a permanent redistribution of the pulses' internal energy [99]. For the same values of the dispersion parameters as considered in Fig.(3.1(a)) and with $\Delta = 1.963$, $S_1 = 0.5$, $S_2 = 5.217 \times 10^{-6}$, $S_3 = 6.763 \times 10^{-6}$, $\varepsilon_1 = \varepsilon_2 = 4.0 \times 10^{-6}$, $\varepsilon_3 = 0.03$, $\varepsilon_4 = \varepsilon_5 = 0.01$, the XMI condition is determined by numerically evaluating the eigen value Eq.(3.3.15) when the linearly polarized pump is polarized equally with respect to either axis. The corresponding gain spectrum as a function of frequency detuning ω and input power P is portrayed in Fig.(3.3(a)). From Fig.(3.3(a)), it is evident that for comparatively low values of ω, the gain spectrum is dominated more by XPM and GVD effects with the result that in that specific region, a gain spectrum similar to the case depicted in Fig.(3.1(a)) is obtained. Here too, the occurrence of MI requires a comparatively wider range of input power but lesser than that in case (i).

(a)
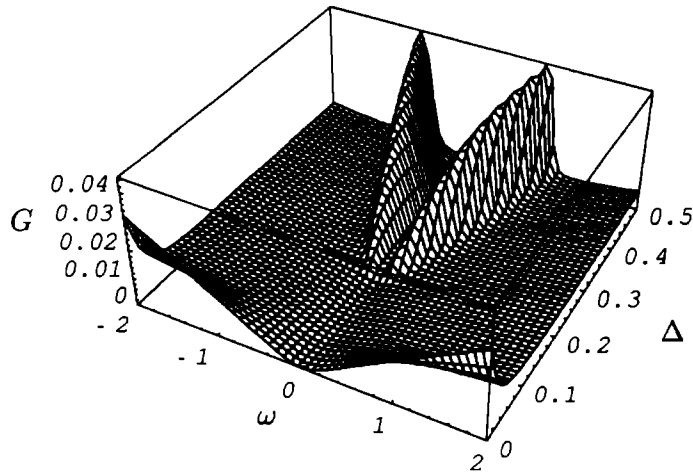
(b)

Fig. 3.3: Surface plots of the gain spectrum G for case (ii) with $S_1 = 0.5$, $S_2 = 5.217 \times 10^{-6}$, $S_3 = 6.763 \times 10^{-6}$, $\varepsilon_1 = \varepsilon_2 = 4.0 \times 10^{-6}$, $\varepsilon_3 = 0.03$, $\varepsilon_4 = \varepsilon_5 = 0.01$: (a) Gain spectrum as a function of frequency detuning ω and input power P for $\Delta = 1.963$ (b) Gain spectrum as a function of frequency detuning ω and group velocity mismatch Δ for $P = 0.1$
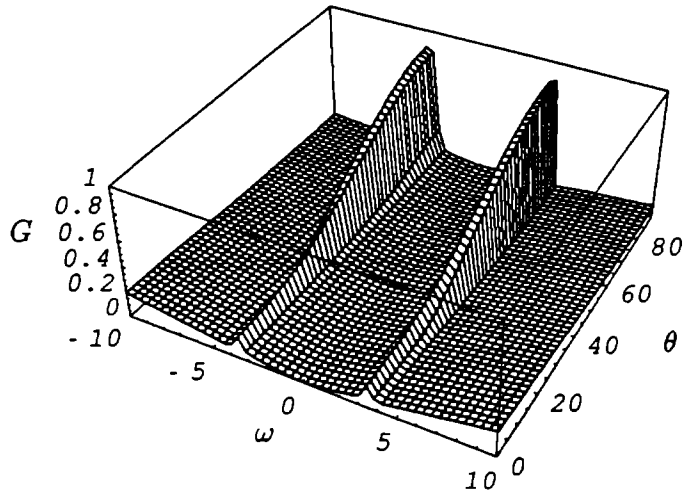
(a)
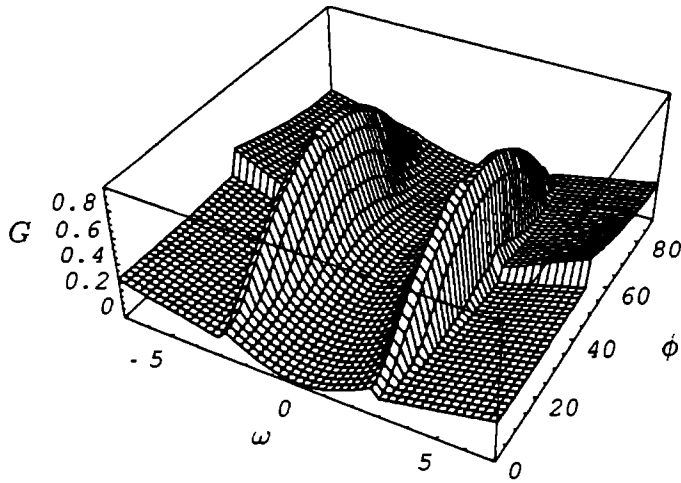
(b)

Fig. 3.4: Surface plots of the gain spectrum G for case (ii) with $\Delta = 1.963$ and $P = 0.1$. The rest of the parameters have the same values as in Fig.(3.3): (a) Gain spectrum as a function of frequency detuning ω and ellipticity angle θ (b) Gain spectrum as a function of frequency detuning ω and polarization angle ϕ

By suitably adjusting the various parameters, it can be inferred from Figs.(3.3) and (3.4) that while self-steepening reduces the maximum value of the gain spectrum, SRS enhances the region of MI. One effect dominates over the other depending on the values of the various parameters considered in this chapter. In most cases the SRS dominates over the self-steepening effect. Thus SRS has a hand in reducing the range of input power required for the instability to occur which nullifies to an extent the demand for a comparatively wider range of input power by fourth order dispersion and self-steepening . As a result, for comparatively higher values of ω and with increasing power, SRS effect becomes predominant with the result that the gain spectrum increases linearly with ω. In a nutshell, the effect of SRS widens the region of MI whereas the effect of self-steepening tries to reduce the maximum gain which is evident when one compares Fig.(3.1(a)) and Fig.(3.3(a)). A marked difference between cases (i) and (ii) is that in the latter case, the influence on MI due to the fourth order dispersion term is much less when compared with the former case. Figures (3.3(b)), (3.4(a)) and (3.4(b)) which portray the frequency dependent gain as functions of Δ, θ and ϕ respectively for an input power $P = 0.1$, bring forth similar effects of SRS on MI as portrayed in Fig.(3.3(a)) with the result that the gain parameter has non zero values everywhere except for the zero detuning frequency where the gain parameter vanishes.

(iii) MI condition governing the generation of ultrashort pulses in the sub- pico- femto second region

The MI condition which governs the generation of ultrashort pulses in the sub- pico- femto second regime is only influenced by the effect due to SRS and as a

result, the effects due to self-steepening and fourth order dispersion can be safely

neglected.

(a)
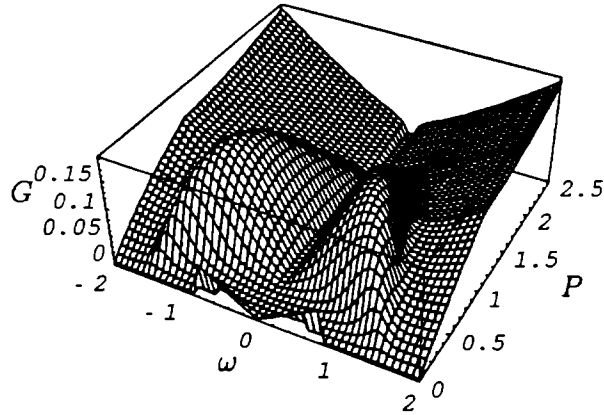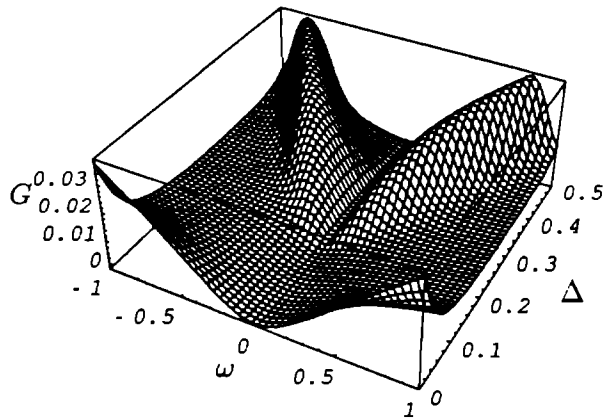

(b)

Fig. 3.5: Surface plots of the gain spectrum G for case (iii) with $S_1 = 0.5$, $S_2 = 1.304 \times 10^{-3}$, $S_3 = 0.0$, $\varepsilon_1 = \varepsilon_2 = 0.0$, $\varepsilon_3 = 0.075$, $\varepsilon_4 = \varepsilon_5 = 0.025$: (a) Gain spectrum as a function of frequency detuning ω and input power P for $\Delta = 0.785$; (b) Gain spectrum as a function of frequency detuning ω and group velocity mismatch Δ for $P = 0.1$
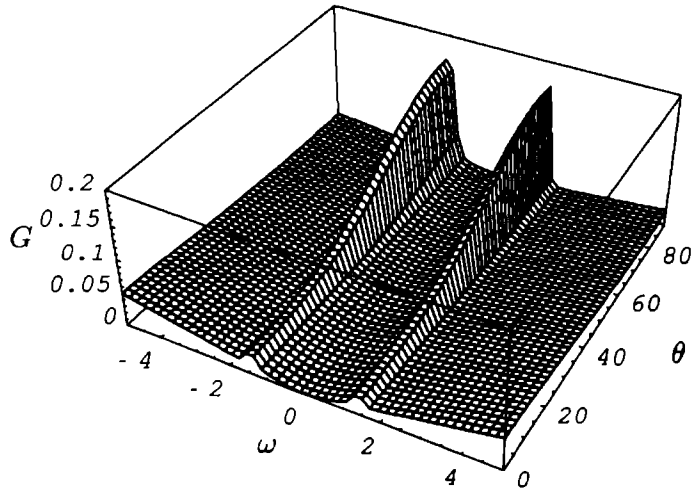
(a)
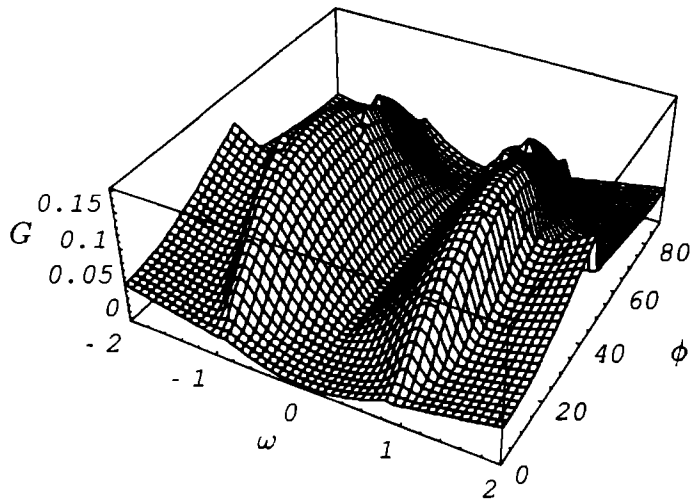
(b)

Fig. 3.6: Surface plots of the gain spectrum G for case (iii) with $\Delta = 0.785$ and $P = 0.1$. The rest of the parameters have the same values as in Fig.(3.5): (a) Gain spectrum as a function of frequency detuning ω and ellipticity angle θ; (b) Gain spectrum as a function of frequency detuning ω and polarization angle ϕ

The gain parameter is plotted in Fig.(3.5(a)) as a function of frequency detuning and input power. A marked difference in this case from that in (i) and (ii) is that the instability condition is achieved for a comparatively shorter range of input power. Moreover, SRS enhances the region of MI. These are clearly depicted in Figs. (3.5(b)), (3.6(a)) and (3.6(b)) which portray the frequency dependent gain as functions of Δ, θ and ϕ respectively for an input power $P = 0.1$.

3.4 MI phenomenon in terms of Stokes and antiStokes side band amplitudes

The regions of instability may also be understood as arising from a process in which the group-velocity dispersion of the down shifted sideband polarized on the slow axis and the up-shifted sideband on the fast axis, is balanced by the group velocity mismatch. This can be verified by assuming for perturbation, a modulation ansatz with wave number k and frequency ω of the form:

$$
\begin{aligned}
u\left(\varsigma,\tau\right) &= u_s\left(\varsigma\right)\exp\left(i\,\omega\,\tau\right)+u_a\left(\varsigma\right)\exp\left(-i\,\omega\,\tau\right), \\
v\left(\varsigma,\tau\right) &= v_s\left(\varsigma\right)\exp\left(i\,\omega\,\tau\right)+v_a\left(\varsigma\right)\exp\left(-i\,\omega\,\tau\right),
\end{aligned} \tag{3.4.1}
$$

where u_s and u_a can be regarded respectively, as the measures of the amplitudes of the Stokes and antiStokes sidebands for the slow axis whereas v_s and v_a represent those for the fast axis. On substituting the above expressions into Eq.(3.2.18) and on linearizing with respect to u_s, u_a^*, v_s and v_a^*, a set of coupled linear ordinary differential equations in terms of the perturbing fields u_s, u_a^*, v_s and v_a^* are obtained which can be written in the form of a matrix equation given by [97]

$$
-i\,\frac{d\,\mathbf{X}\left(\varsigma\right)}{d\,\varsigma} = \mathbf{L}\,\mathbf{X}\left(\varsigma\right) \tag{3.4.2}
$$

where the column matrix $\mathbf{X}(\varsigma) = \begin{pmatrix} u_s \\ u_a^* \\ v_s \\ v_a^* \end{pmatrix}$ and

$$\mathbf{L} = \begin{pmatrix} L_{11} & L_{12} & L_{13} & L_{14} \\ L_{21} & L_{22} & L_{23} & L_{24} \\ L_{31} & L_{32} & L_{33} & L_{34} \\ L_{41} & L_{42} & L_{43} & L_{44} \end{pmatrix}, \qquad (3.4.3)$$

where the elements of $\mathbf{L}$ take the form : $L_{11} = P_1 - \Delta\,\omega + S_1\,\omega^2 - S_3\,\omega^4 - S_2\,\omega^3 - \omega\,(2\,\varepsilon_1\,P_1 + \varepsilon_2\,P_2) - i\,\omega\,(\varepsilon_3\,P_1 + \varepsilon_5\,P_2)$;

$L_{12} = P_1\,(1 - \varepsilon_1\,\omega - i\,\varepsilon_3\,\omega)\,; L_{13} = \sqrt{P_1\,P_2}\,(B - \varepsilon_2\,\omega - i\,\varepsilon_4\,\omega)\,;$

$L_{14} = \sqrt{P_1\,P_2}\,(B - \varepsilon_2\,\omega - i\,\varepsilon_4\,\omega - i\,\varepsilon_5\,\omega)\,; L_{21} = P_1\,(-1 - \varepsilon_1\,\omega + i\,\varepsilon_3\,\omega)\,;$

$L_{22} = -P_1 - \Delta\,\omega - S_1\,\omega^2 + S_3\,\omega^4 - S_2\,\omega^3 - \omega\,(2\,\varepsilon_1\,P_1 + \varepsilon_2\,P_2) + i\,\omega\,(2\,\varepsilon_3\,P_1 + \varepsilon_5\,P_2)\,;$

$L_{23} = \sqrt{P_1\,P_2}\,(-B - \varepsilon_2\,\omega + i\,\varepsilon_4\,\omega + i\,\varepsilon_5\,\omega)\,; L_{24} = \sqrt{P_1\,P_2}\,(-B - \varepsilon_2\,\omega + i\,\varepsilon_4\,\omega)\,;$

$L_{31} = \sqrt{P_1\,P_2}\,(B - \varepsilon_2\,\omega)\,; L_{32} = \sqrt{P_1\,P_2}\,(B - i\,\varepsilon_4\,\omega - i\,\varepsilon_5\,\omega)\,;$

$L_{33} = P_2 + \Delta\,\omega + S_1\,\omega^2 - S_3\,\omega^4 - S_2\,\omega^3 - \omega\,(2\,\varepsilon_1\,P_2 + \varepsilon_2\,P_1) - i\,\omega\,(\varepsilon_3\,P_2 + \varepsilon_5\,P_1)\,;$

$L_{34} = P_2\,(1 - \varepsilon_1\,\omega - i\,\varepsilon_3\,\omega)\,; L_{41} = \sqrt{P_1\,P_2}\,(-B - \varepsilon_2\,\omega + i\,\varepsilon_4\,\omega + i\,\varepsilon_5\,\omega)\,;$

$L_{42} = \sqrt{P_1\,P_2}\,(-B - \varepsilon_2\,\omega)\,; L_{43} = P_2\,(-1 - \varepsilon_1\,\omega + i\,\varepsilon_3\,\omega)\,;$

$L_{44} = -P_2 + \Delta\,\omega - S_1\,\omega^2 + S_3\,\omega^4 - S_2\,\omega^3 - \omega\,(2\,\varepsilon_1\,P_2 + \varepsilon_2\,P_1) + i\,\omega\,(\varepsilon_3\,P_2 + \varepsilon_5\,P_1)\,;$

where $P_1 = 2P\cos^2(\phi)$ and $P_2 = 2P\sin^2(\phi)$, ϕ being the polarization angle. Now for achieving the MI condition required for the generation of ultra short pulses of the order of 500 fs and above, a similar procedure is followed as in case (i) of Sec. 3.3 to arrive at the dispersion relation from Eq.(3.3.15) which is of the form [97]

$$k = -S_2\,\omega^3 \pm \omega\sqrt{L_4 - 2\sqrt{L_5}}, \qquad (3.4.4)$$

where L_4 and L_5 have the same form as obtained in Sec. 3.3. Here too, the condition for instability to occur is $L_4^2 < 4\ L_5$ as is clear from Eq.(3.4.4) and hence we obtain the same gain parameter as in case (i) of Sec. 3.3 even though the eigen values are different in both cases. Hence all the results considered in case (i) of Sec. 3.3 can be arrived at.
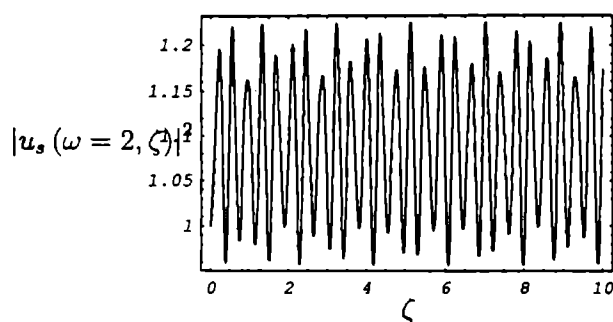

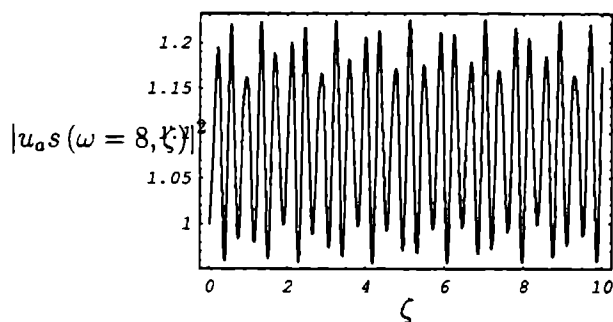Fig. 3.7: Intensity of the Stokes side band amplitude for the slow axis for $\omega = 2.0$.

Fig. 3.8: Intensity of the antiStokes side band amplitude for the slow axis for $\omega = 8.0$.

Likewise, the remaining two cases present in Sec. 3.3 are analyzed and arrive numerically at the same results as obtained in Sec. 3.3. Thus the modulational

ansatz given by Eq.(3.4.1) can also effectively portray the MI phenomenon in the single-frequency propagation regime. Eq.(3.4.2), being a linear homogenous ordinary differential equation, has a solution of the form:

$$\mathbf{X}(\varsigma) = \exp(i\,\mathbf{L}\,\varsigma)\,\mathbf{C}, \qquad (3.4.5)$$

where the constant column matrix $\mathbf{C}$ depends on the initial conditions of the four linearized side band amplitudes. Figures (3.7) and (3.8) show the graphical relation for the Stokes and antiStokes side band amplitudes respectively for the slow axis with respect to ς. For the Stokes case, $\omega = 2.0$ whereas for the antiStokes case, $\omega = 8.0$. Similar graphs can be obtained for the fast axis also.

3.5   Conclusions

The conditions for the occurrence of cross phase MI in the normal dispersion regime which occurs as a result of a group velocity mismatch between the linearly polarized eigen states when the linearly polarized pump is oriented at 45° with respect to the slow or fast axis are obtained. The instability conditions that govern the generation of ultra short pulses for the three cases mentioned in Sec. 3.3 are not affected irrespective of the presence or absence of S_2-the dimensionless third order dispersion coefficient. For variations in the pump polarization, maximum gain occurs for 45° polarization for all the cases considered in this chapter. The effect of SRS on MI is such that for comparative small values of the perturbation frequency, group velocity dispersion and cross-phase modulation terms dominate whereas for comparatively large values the perturbation frequency, the gain spectrum increases linearly with the result that the region of MI is widened due to SRS. Moreover the self-steepening effect reduce the maximum gain and

bandwidth. As one slowly approaches towards the zero group velocity dispersion regime, the condition for the cross phase MI requires sufficiently large values of the total input power over a wide range of frequency detuning ω. At the zero group velocity dispersion regime, one obtains only the original MI. Furthermore, a modulational anstatz given by Eq.(3.4.1) for the perturbation amplitudes is considered and have been able to retrieve all the results considered in Sec. 3.3 and thus the two methods discussed in Sec. 3.3 and Sec. 3.4 give the same values for the gain parameter.

Chapter 4

Polarization modulational instability in a birefringent optical fiber with fourth order dispersion

4.1 Introduction

The cross-phase modulational instability conditions pertaining to the generation of ultrashort pulses have been discussed in detail in chapter three. In this chapter, another modulational instability phenomenon known as polarization modulational instability (PMI) is dealt with. In polarization preserving birefringent optical fibers, MI may involve a change of the polarization state of an incident pump wave [104] as it traverses the fiber. This phenomenon is known as polarization MI (PMI) which is sensitive to the relative phase of the orthogonally polarized waves. Due to PMI, the incident pump wave which is polarized on one axis of the fiber, would generate orthogonally polarized Stokes and anti-Stokes sidebands. Trillo and Wabnitz, in their work, have analyzed the role of nonlinear polarization of the pump on parametric amplification [105]. They have shown that PMI manifests as large changes in the output state of polarization when the

input power or the polarization state is changed slightly. They attributed this phenomenon to the case when the linear beat length of the optical fiber becomes comparable to its nonlinear beat length for a specific input power. As the nonlinear polarization response of the birefringent optical fibers play a very crucial role in ultrashort pulse generation through pulse reshaping, a detailed analysis about PMI phenomenon is very much needed. MI phenomena in presence of higher order dispersion effects results in ultrashort pulses with very high repetition rates which find applications in ultrafast all-optical switches [106]. In this chapter, considering the single-frequency copropagation regime, the influence of fourth order dispersion effects on PMI gain spectra of a linearly polarized intense pump wave which experiences periodic nonlinear polarization rotation in a birefringent optical fiber in the normal dispersion regime is considered [107].

The remainder of the chapter is arranged as follows. In Sec. 4.2, the basic equation is discussed. The linear stability of a linearly polarized pump wave oriented at arbitrary angles with respect to the principal axes is carried out in Sec. 4.3. In Sec. 4.4, the conclusions are discussed.

4.2 Basic Equation

In chapter three, the coupled higher order nonlinear Schrödinger equation with the addition of self-steepening, SRS, third and fourth order dispersion effects has been studied in the context of cross-phase modulational instability. In this chapter, the instability condition required for the generation of ultrashort pulses of the order of 500 fs and above is considered. As a result, other than the fourth order dispersion term present in Eq.(3.2.18), the rest of the terms present in the same equation, that account for third order dispersion and all higher order

nonlinear effects, are equated to zero. Also, the group velocity mismatch between the two modes is neglected. Then the residual equation resulting from Eq.(3.2.18) takes the form :

$$i\, U_z - \frac{\beta_2}{2}\, U_{TT} + \gamma\, \left(|U|^2 + B\, |V|^2\right) U - \frac{\beta_4}{24}\, U_{TTTT} \ = \ 0,$$
$$i\, V_z - \frac{\beta_2}{2}\, V_{TT} + \gamma\, \left(B\, |U|^2 + |V|^2\right) V - \frac{\beta_4}{24}\, V_{TTTT} \ = \ 0. \qquad (4.2.1)$$

For obtaining Eq.(4.2.1), the carrier frequency of the propagation modes is chosen to be at the extremum of the group velocity dispersion as a result of which the third order dispersion vanishes. This can be achieved in a dispersion-flattened fiber [1]. Cavalcanti et. al. have demonstrated experimentally the MI phenomena for the scalar nonlinear Schrödinger equation [100] where they have considered the effect due to fourth order dispersion with the second and fourth order dispersion coefficients at -0.1 ps^2/Km and -7.0 ps^4/Km respectively at the wavelength λ = 1.32 μm. Equation (4.2.1) is an extension to the case for a birefringent medium. In chapter 3, the effect due to four-wave mixing [1, 3, 110] and that due to linear birefringence [1, 98] had been neglected. Considering these two effects for the low birefringence case, Eq.(4.2.1) takes the form :

$$i\, U_z - \frac{\beta_2}{2}\, U_{TT} + \gamma\, \left(|U|^2 + B\, |V|^2\right) U + \frac{\Delta\beta}{2}U + \gamma\,(1 - B)\, V^2 U^* - \frac{\beta_4}{24}\, U_{TTTT} \ = \ 0,$$
$$i\, V_z - \frac{\beta_2}{2}\, V_{TT} + \gamma\, \left(B\, |U|^2 + |V|^2\right) V - \frac{\Delta\beta}{2}V + \gamma\,(1 - B)\, U^2 V^* - \frac{\beta_4}{24}\, V_{TTTT} \ = \ 0,$$
$$(4.2.2)$$

where the coefficient $\Delta\beta$ accounts for the linear birefringence [110] and the terms $\gamma\,(1 - B)\, V^2 U^*$ and $\gamma\,(1 - B)\, U^2 V^*$ account for the four-wave mixing [3, 111]. For $B = \frac{2}{3}$, Eq.(4.2.2) represents the case for light propagation in a linearly birefringent fiber with U and V being the slowly varying electric field envelopes pertaining to linear polarization components. Hence Eq.(4.2.2) can be rewritten

in the form :

$$i\, U_z - \frac{\beta_2}{2}\, U_{TT} + \gamma\, \left(|U|^2 + \frac{2}{3}|V|^2\right) U + \frac{\Delta\beta}{2} U + \frac{\gamma}{3} V^2 U^* - \frac{\beta_4}{24}\, U_{TTTT} \;=\; 0,$$

$$i\, V_z - \frac{\beta_2}{2}\, V_{TT} + \gamma\, \left(\frac{2}{3}|U|^2 + |V|^2\right) V - \frac{\Delta\beta}{2} V + \frac{\gamma}{3} U^2 V^* - \frac{\beta_4}{24}\, V_{TTTT} \;=\; 0.$$

$$(4.2.3)$$

An optically active medium such as a twisted birefringent optical fiber supports circularly polarized waves [105] and its circular polarization components U' and V' can be related to the linear polarization components U and V by the relation [1, 3]:

$$U' \;=\; \frac{U + V}{\sqrt{2}} \quad \text{and}$$

$$V' \;=\; \frac{-i\,(U - V)}{\sqrt{2}} \qquad (4.2.4)$$

On substituting Eq.(4.2.4) in Eq.(4.2.3) and after some simplifications, Eq.(4.2.3) takes the form [107]:

$$i\, U'_z - \frac{\beta_2}{2}\, U'_{TT} + \frac{2\gamma}{3}\, \left(|U'|^2 + 2|V'|^2\right) U' + \frac{\Delta\beta}{2} V' - \frac{\beta_4}{24}\, U'_{TTTT} \;=\; 0,$$

$$i\, V'_z - \frac{\beta_2}{2}\, V'_{TT} + \frac{2\gamma}{3}\, \left(2|U'|^2 + |V'|^2\right) V' + \frac{\Delta\beta}{2} U' - \frac{\beta_4}{24}\, V'_{TTTT} \;=\; 0.$$

$$(4.2.5)$$

where U' and V' correspond to the representation of the field in terms of its right and left circular polarization components. In this context, $\Delta\beta$ is a measure of the periodic twist present in the birefringent fiber [98]. The total input power P for the system is given by $P = |U'|^2 + |V'|^2$. On considering the following transformations given by $U'(z, T) = \sqrt{P}\, u(\varsigma, \tau)$; $V'(z, T) = \sqrt{P}\, v(\varsigma, \tau)$; $\varsigma = \Delta\beta\, z$; $\tau = \sqrt{\dfrac{\Delta\beta}{|\beta_2|}}\, T$; $S_1 = \dfrac{s_1}{2}$; $S_3 = \dfrac{s_3}{24}\dfrac{|\beta_4|}{|\beta_2|}\dfrac{\Delta\beta}{}$; $p = \dfrac{\gamma P}{3\,\Delta\beta}$ and substituting

in Eq.(4.2.5), the corresponding equation in the dimensionless form becomes [107]

$$i\,u_\varsigma - S_1\,u_{\tau\tau} + 2\,p\,\left[|u|^2 + 2\,|v|^2\right]u - S_3\,u_{\tau\tau\tau\tau} + \frac{v}{2} = 0,$$

$$i\,v_\varsigma - S_1\,v_{\tau\tau} + 2\,p\,\left[|v|^2 + 2\,|u|^2\right]v - S_3\,v_{\tau\tau\tau\tau} + \frac{u}{2} = 0, \qquad (4.2.6)$$

where u and v are the normalized circular polarization components of the intensely polarized pump wave. ς is the dimensionless longitudinal distance and τ is the dimensionless retarded time. u_ς refers to partial derivative with respect to ς and so on. S_1 and S_3 denote group velocity dispersion and fourth order dispersion coefficients respectively. Since the single-frequency copropagation regime is considered, S_1 and S_3 are considered to have the same value on both the slow and fast axes [1-3]. Equation (4.2.6) represents the propagation in an optically active medium such as a twisted birefringent optical fiber which supports circularly polarized waves. In this chapter, the case where the carrier frequency of continuous wave is at the extremum of the group velocity dispersion as a result of which the third order dispersion vanishes, is considered. Furthermore, other nonlinear effects such as stimulated Raman scattering (SRS), self steepening, etc. have also been neglected as generation of ultrashort pulses of the order of 500 femto seconds and above as at this range, only the effects due to fourth order dispersion become high enough to influence the modulational instability (MI) phenomena [100]. The parameter p refers to normalized power.

4.3   Stability analysis and PMI phenomena

In this chapter, the case for a linearly polarized pump oriented at an arbitrary angle θ, known as the orientation angle, with respect to either the slow or the fast axis of the birefringent fiber is considered. In order to obtain the instability

conditions, as in chapter three, it is assumed for the case of continuous wave or quasi-continuous wave radiations that the orthogonally polarized amplitudes $u(\varsigma, \tau)$ and $v(\varsigma, \tau)$ remain time independent during propagation inside the fiber. Hence, the steady state solutions for Eq.(4.2.6) are of the form:

$$u(\varsigma) = |U(\varsigma)| \exp(i\,\phi_1(\varsigma)),$$
$$v(\varsigma) = |V(\varsigma)| \exp(i\,\phi_2(\varsigma)). \tag{4.3.1}$$

Let the nonlinear phase shift $\phi = \phi_1 - \phi_2$. The nonlinear phase shift is responsible for the power dependent ellipse rotation of the pump wave. On substituting Eq.(4.3.1) in Eq.(4.2.6) and separating into real and imaginary parts, the following expressions are obtained [107]:

$$\frac{d\,|U|}{d\varsigma} = \frac{|V|}{2}\,\sin\phi, \tag{4.3.2}$$

$$\frac{d\,|V|}{d\varsigma} = -\frac{|U|}{2}\,\sin\phi, \tag{4.3.3}$$

$$\frac{d\phi_1}{d\varsigma} = 2\,p\,\left(|U|^2 + 2\,|V|^2\right) + \frac{|V|}{2\,|U|}\,\cos\phi, \tag{4.3.4}$$

and

$$\frac{d\phi_2}{d\varsigma} = 2\,p\,\left(2\,|U|^2 + |V|^2\right) + \frac{|U|}{2\,|V|}\,\cos\phi. \tag{4.3.5}$$

From Eqs.(4.3.4) and (4.3.5), the variation of the nonlinear phase shift ϕ with respect to the nondimensional longitudinal distance ς is obtained as

$$\frac{d\phi}{d\varsigma} = 2\,p\,\left(|V|^2 - |U|^2\right) + \frac{\left(|V|^2 - |U|^2\right)}{2\,|U|\,|V|}\,\cos\phi. \tag{4.3.6}$$

As the state of polarization of a pump wave can be changed by introducing a phase shift between the two orthogonal polarization components of the pump wave [127], Eq.(4.3.6) throws light on the local state of polarization. The local state of polarization of the pump is duly represented by the normalized Stokes

parameters [1, 3, 105] (Details about the Stokes parameters is given in Appendix B) which are of the form:

$$S_0\left(\varsigma\right) = |U|^2 + |V|^2, \tag{4.3.7}$$

$$S_1\left(\varsigma\right) = 2\;|U|\;|V|\;\cos\;\phi, \tag{4.3.8}$$

$$S_2\left(\varsigma\right) = 2\;|U|\;|V|\;\sin\;\phi, \tag{4.3.9}$$

and

$$S_3\left(\varsigma\right) = |V|^2 - |U|^2, \tag{4.3.10}$$

such that $S_1^2\left(\varsigma\right) + S_2^2\left(\varsigma\right) + S_3^2\left(\varsigma\right) = 1$. On differentiating Eqs.(4.3.8), (4.3.9) and (4.3.9) throughout with respect to ς and by using Eqs.(4.3.2)-(4.3.5), the corresponding equations to the Stokes parameters are obtained which are of the form [107]:

$$\frac{\mathrm{d}\;S_1\left(\varsigma\right)}{\mathrm{d}\;\varsigma} = -2\,p\,S_2\left(\varsigma\right)\;S_3\left(\varsigma\right), \tag{4.3.11}$$

$$\frac{\mathrm{d}\;S_2\left(\varsigma\right)}{\mathrm{d}\;\varsigma} = S_3\left(\varsigma\right)\;(1 + 2\,p\;\;S_1\left(\varsigma\right)), \tag{4.3.12}$$

and

$$\frac{\mathrm{d}\;S_3\left(\varsigma\right)}{\mathrm{d}\;\varsigma} = -S_2\left(\varsigma\right). \tag{4.3.13}$$

From Eqs.(4.3.11) and (4.3.13), a relation of the form:

$$\frac{\mathrm{d}}{\mathrm{d}\;\varsigma}\left[S_1\left(\varsigma\right) - pS_3^2\left(\varsigma\right)\right] = 0, \tag{4.3.14}$$

is obtained. The above equation results in the expression,

$$S_1\left(\varsigma\right) - p\,S_3^2\left(\varsigma\right) = \mathrm{C}, \tag{4.3.15}$$

where the integration constant, $\mathrm{C} = S_{10} - p\,S_{30}^2$. S_{10} and S_{30} can be determined from the initial conditions. Making use of the relation,

$$
\begin{aligned}
S_2^2\left(\varsigma\right) &= 1 - \left(S_1^2\left(\varsigma\right) + S_3^2\left(\varsigma\right)\right) \\
&= 1 - \mathrm{C}^2 - (1 + 2\mathrm{C}p)\,S_3^2\left(\varsigma\right) - p^2 S_3^4\left(\varsigma\right), \tag{4.3.16}
\end{aligned}
$$

Eq.(4.3.13) can be written of the form

$$\left(\frac{d\,S_3\,(\varsigma)}{d\,\varsigma}\right)^2 = p^2 \left(\alpha_1 - S_3^2\,(\varsigma)\right)\left(\alpha_2 + S_3^2\,(\varsigma)\right), \qquad (4.3.17)$$

where

$$\alpha_1 = \frac{1}{2\,p^2}\left(-(1+2\,p\,S_{10}) + \sqrt{(1+2\,p\,S_{10})^2 + 4\,p^2\,S_{20}^2}\right) \qquad \text{and}$$

$$\alpha_2 = \frac{1}{2\,p^2}\left((1+2\,p\,S_{10}) + \sqrt{(1+2\,p\,S_{10})^2 + 4\,p^2\,S_{20}^2}\right). \qquad (4.3.18)$$

S_{20} can also be obtained from the initial conditions. Equation (4.3.17) can be solved using Jacobian elliptical functions of the first kind [72] to obtain [107]:

$$S_3\,(\varsigma) = -\frac{S_{20}}{f}\,\text{sd}\,(f\,\varsigma;m), \qquad (4.3.19)$$

where

$$f = \left(1 + 4\,p^2 + 4\,p\,S_{10}\right)^{\frac{1}{4}} \qquad (4.3.20)$$

and the Jacobian parameter m takes the form

$$\begin{aligned} m &= \frac{\alpha_1}{\alpha_1 + \alpha_2} \\ &= 0.5\left(1 - \frac{1+2\,p\,S_{10}}{f^2}\right). \end{aligned} \qquad (4.3.21)$$

Therefore,

$$\begin{aligned} S_2\,(\varsigma) &= -\frac{d\,S_3\,(\varsigma)}{d\,\varsigma} \\ &= S_{20}\,\text{cd}\,(f\,\varsigma;m)\,\text{nd}\,(f\,\varsigma;m), \end{aligned} \qquad (4.3.22)$$

and

$$\begin{aligned} S_1\,(\varsigma) &= S_{10} - p\,S_{30}^2 + p\,S_3^2\,(\varsigma) \\ &= S_{10} + p\left(\frac{S_{20}}{f}\right)^2\,\text{sd}\,(f\,\varsigma;m). \end{aligned} \qquad (4.3.23)$$

sd, nd and cd are the Jacobian elliptic functions of first kind [72]. Thus Eqs. (4.3.19), (4.3.22) and (4.3.23) represent the pump wave evolution [107]. For a linearly polarized pump wave,

$$S_{10} = \cos(2\,\theta),$$
$$S_{20} = \sin(2\,\theta),$$
$$S_{30} = 0, \qquad\qquad (4.3.24)$$

where θ is the angle of orientation of the pump wave with respect to the slow axis.

So far only the steady state solutions pertaining to the linearly polarized pump waves are considered. Now a perturbation procedure is followed where the steady state solutions are slightly perturbed first by considering only the spatial evolution (*ie. at* $\tau = 0$) of the perturbing amplitudes and then including the temporal evolution of the perturbing amplitudes as well which are in the form of Stokes and anti-Stokes side-band amplitudes [105]. Also, the approximation that higher harmonics do not significantly influence the system dynamics is considered. Now, at $\tau = 0$, the amplitudes of the two polarization components are perturbed slightly to obtain:

$$u(\varsigma) = (|U(\varsigma)| + u_0'(\varsigma))\,\exp(i\,\varphi_1(\varsigma)), \qquad (4.3.25)$$

and

$$v(\varsigma) = (|V(\varsigma)| + v_0'(\varsigma))\,\exp(i\,\phi_2(\varsigma)). \qquad (4.3.26)$$

On substituting Eqs.(4.3.25) and (4.3.26) into Eq.(4.2.6), the coupled equations

to the spatial dependance of the perturbed pump fields are of the form [107]:

$$
- i \frac{\partial u_0'(\varsigma)}{\partial \varsigma} = \left(p \left(1 - S_3(\varsigma) \right) - \frac{S_1(\varsigma)}{2 \left(1 - S_3(\varsigma) \right)} \right) u_0'(\varsigma) + p \left(1 - S_3(\varsigma) \right) u_0'^*(\varsigma)
$$

$$
+ \left(0.5 \frac{\left(S_1(\varsigma) - i S_2(\varsigma) \right)}{\sqrt{1 - S_3^2(\varsigma)}} + 2 p \sqrt{1 - S_3^2(\varsigma)} \right) v_0'(\varsigma) + 2 p \sqrt{1 - S_3^2(\varsigma)} \, v_0'^*(\varsigma),
$$

$$
- i \frac{\partial v_0'(\varsigma)}{\partial \varsigma} = \left(0.5 \frac{\left(S_1(\varsigma) + i S_2(\varsigma) \right)}{\sqrt{1 - S_3^2(\varsigma)}} + 2 p \sqrt{1 - S_3^2(\varsigma)} \right) u_0'(\varsigma)
$$

$$
+ 2 p \sqrt{1 - S_3^2(\varsigma)} \, u_0'^*(\varsigma) + \left(p \left(1 + S_3(\varsigma) \right) - \frac{S_1(\varsigma)}{2 \left(1 + S_3(\varsigma) \right)} \right) v_0'(\varsigma)
$$

$$
+ p \left(1 + S_3(\varsigma) \right) v_0'^*(\varsigma), \tag{4.3.27}
$$

where u_0' and v_0' denote the spatial evolution of the perturbing amplitudes at $\tau = 0$. In order to study the temporal evolution of the perturbing amplitudes as well, the full fledged spatio-temporal evolution of the perturbing amplitudes $u_0(\varsigma, \tau)$ and $v_0(\varsigma, \tau)$ are considered which are given by

$$
\begin{aligned}
u_0(\varsigma, \tau) &= u_{10}(\varsigma) \exp(i \, \Omega \, \tau) + u_{20}(\varsigma) \exp(-i \, \Omega \, \tau), \\
v_0(\varsigma, \tau) &= v_{10}(\varsigma) \exp(i \, \Omega \, \tau) + v_{20}(\varsigma) \exp(-i \, \Omega \, \tau).
\end{aligned} \tag{4.3.28}
$$

where (u_{10}, v_{10}) and (u_{20}, v_{20}) are the amplitudes of Stokes and anti-Stokes side bands respectively. Throughout, it is assumed that $|u_0| \ll |U|$ and $|v_0| \ll |V|$. The perturbed equation is given by:

$$
\begin{aligned}
u(\varsigma, \tau) &= \left(|U(\varsigma)| + u_0(\varsigma, \tau) \right) \exp(i \, \phi_1(\varsigma)) \\
v(\varsigma, \tau) &= \left(|V(\varsigma)| + v_0(\varsigma, \tau) \right) \exp(i \, \phi_2(\varsigma))
\end{aligned} \tag{4.3.29}
$$

Now on replacing u_0' and v_0' with $u_0(\varsigma, \tau)$ and $v_0(\varsigma, \tau)$ in Eq.(4.3.27) and substituting this along with Eqs. (4.3.28) and (4.3.29) into Eq.(4.2.6) and on linearizing

with respect to u_{10}, u_{20}^*, v_{10} and v_{20}^*, the following set of coupled linear differential equations in terms of the perturbing fields $u_{10}(\varsigma)$, $u_{20}^*(\varsigma)$, $v_{10}(\varsigma)$ and $v_{20}^*(\varsigma)$ are finally obtained which are of the form [107]:

$$-i\,\frac{d\,u_{10}(\varsigma)}{d\,\varsigma} = m_{11}(\varsigma)\,u_{10}(\varsigma) + m_{12}(\varsigma)\,u_{20}^*(\varsigma) + m_{13}(\varsigma)\,v_{10}(\varsigma) + m_{14}(\varsigma)\,v_{20}^*(\varsigma),$$

$$-i\,\frac{d\,u_{20}^*(\varsigma)}{d\,\varsigma} = m_{21}(\varsigma)\,u_{10}(\varsigma) + m_{22}(\varsigma)\,u_{20}^*(\varsigma) + m_{23}(\varsigma)\,v_{10}(\varsigma) + m_{24}(\varsigma)\,v_{20}^*(\varsigma),$$

$$-i\,\frac{d\,v_{10}(\varsigma)}{d\,\varsigma} = m_{31}(\varsigma)\,u_{10}(\varsigma) + m_{32}(\varsigma)\,u_{20}^*(\varsigma) + m_{33}(\varsigma)\,v_{10}(\varsigma) + m_{34}(\varsigma)\,v_{20}^*(\varsigma),$$

$$-i\,\frac{d\,v_{20}^*(\varsigma)}{d\,\varsigma} = m_{41}(\varsigma)\,u_{10}(\varsigma) + m_{42}(\varsigma)\,u_{20}^*(\varsigma) + m_{43}(\varsigma)\,v_{10}(\varsigma) + m_{44}(\varsigma)\,v_{20}^*(\varsigma),$$

$$(4.3.30)$$

where

$$m_{11}(\varsigma) = G_1\,\Omega^2 - G_3\,\Omega^4 + p\,(1 - S_3(\varsigma)) - \frac{S_1(\varsigma)}{2\,(1 - S_3(\varsigma))},$$

$$m_{12}(\varsigma) = p\,(1 - S_3(\varsigma)),$$

$$m_{13}(\varsigma) = \frac{0.5\,(S_1(\varsigma) - i\,S_2(\varsigma))}{\sqrt{1 - (S_3(\varsigma))^2}} + 2\,p\,\sqrt{1 - (S_3(\varsigma))^2},$$

$$m_{14}(\varsigma) = 2\,p\,\sqrt{1 - (S_3(\varsigma))^2},$$

$$m_{21}(\varsigma) = -p\,(1 - S_3(\varsigma)),$$

$$m_{22}(\varsigma) = -\left(G_1\,\Omega^2 - G_3\,\Omega^4 + p\,(1 - S_3(\varsigma)) - \frac{S_1(\varsigma)}{2\,(1 - S_3(\varsigma))}\right),$$

$$m_{23}(\varsigma) = -2\,p\,\sqrt{1 - (S_3(\varsigma))^2},$$

$$m_{24}(\varsigma) = -\left(0.5\,\frac{(S_1(\varsigma) + i\,S_2(\varsigma))}{\sqrt{1 - (S_3(\varsigma))^2}} + 2\,p\,\sqrt{1 - (S_3(\varsigma))^2}\right),$$

$$m_{31}(\varsigma) = \frac{0.5\,(S_1(\varsigma) + i\,S_2(\varsigma))}{\sqrt{1 - (S_3(\varsigma))^2}} + 2\,p\,\sqrt{1 - (S_3(\varsigma))^2},$$

$$m_{32}(\varsigma) = 2\,p\,\sqrt{1 - (S_3(\varsigma))^2},$$

$$m_{33}\left(\varsigma\right) = G_1\,\Omega^2 - G_3\,\Omega^4 + p\,\left(1 + S_3\left(\varsigma\right)\right) - \frac{S_1\left(\varsigma\right)}{2\left(1 + S_3\left(\varsigma\right)\right)},$$

$$m_{34}\left(\varsigma\right) = p\,\left(1 + S_3\left(\varsigma\right)\right),$$

$$m_{41}\left(\varsigma\right) = -2\,p\,\sqrt{1 - \left(S_3\left(\varsigma\right)\right)^2},$$

$$m_{42}\left(\varsigma\right) = -\left(0.5\,\frac{\left(S_1\left(\varsigma\right) - i\,S_2\left(\varsigma\right)\right)}{\sqrt{1 - \left(S_3\left(\varsigma\right)\right)^2}} + 2\,p\,\sqrt{1 - \left(S_3\left(\varsigma\right)\right)^2}\right),$$

$$m_{43}\left(\varsigma\right) = -p\,\left(1 + S_3\left(\varsigma\right)\right),$$

$$m_{44}\left(\varsigma\right) = -\left(G_1\,\Omega^2 - G_3\,\Omega^4 + p\,\left(1 + S_3\left(\varsigma\right)\right) - \frac{S_1\left(\varsigma\right)}{2\left(1 + S_3\left(\varsigma\right)\right)}\right)$$

All these can be represented in the matrix form as [107]:

$$\frac{d\,\mathbf{X}\left(\varsigma\right)}{d\,\varsigma} = \mathbf{M}\left(\varsigma\right)\mathbf{X}\left(\varsigma\right), \qquad (4.3.31)$$

where $\mathbf{X}\left(\varsigma\right) = \left(u_{10}, u_{20}^{*}, v_{10}, v_{20}^{*}\right)^{T}$ and the superscript T denotes transpose. $\mathbf{M}\left(\varsigma\right)$ is a complex periodic matrix with period given by $\varsigma_p = \dfrac{4\,K\left(m\right)}{f}$ where $K\left(m\right)$ is a complete elliptic integral of the first kind [72]. ς_p is defined as the normalized nonlinear beat length of the optical fiber.

Equation (4.3.31) is a linear homogenous (LH) system with periodic coefficients. The LH system is solved using Floquet theorem [109]. The periodic matrix $\mathbf{M}\left(\varsigma\right)$ has distinct eigenvalues for all values of ς and frequency detuning parameter Ω. Hence the corresponding eigenvectors would be linearly independent. Let $\mathbf{P}\left(\varsigma\right)$ denote a periodic matrix with the linearly independent eigen vectors written side by side. Then the solution to Eq.(4.3.31) is given by Floquet theorem as [109]:

$$\Phi\left(\varsigma\right) = \mathbf{P}\left(\varsigma\right)\exp\left(\mathbf{B}\,\varsigma\right), \qquad (4.3.32)$$

where $\mathbf{B}$ is a nonsingular matrix. $\Phi\left(\varsigma\right)$ is known as the fundamental matrix

with the property that

$$\Phi\left(\varsigma + \varsigma_p\right) = \Phi\left(\varsigma\right)\,\exp\left(\mathbf{B}\,\varsigma\right). \qquad (4.3.33)$$

The normalized form of the above equation is known as the state transition matrix $\mathbf{L}\left(\varsigma\right)$ which is given by

$$\mathbf{L}\left(\varsigma\right) = \Phi\left(\varsigma\right)\,\Phi^{-1}\left(\varsigma = 0\right). \qquad (4.3.34)$$

Therefore

$$\mathbf{L}\left(\varsigma = \varsigma_p\right) = \exp\left(\mathbf{B}\,\varsigma_p\right). \qquad (4.3.35)$$

In order to obtain $\mathbf{L}\left(\varsigma = \varsigma_p\right)$ numerically, $\mathbf{L}\left(\varsigma = 0\right)$ is chosen to be the unit matrix of order 4, such that each column vector of $\mathbf{L}\left(\varsigma = 0\right)$ depicts linearly independent initial conditions for Eq.(4.3.31). With this set of initial conditions, Eq.(4.3.31) is solved numerically using the Runge-Kutta-Gill method [108] to obtain $\mathbf{L}\left(\varsigma = \varsigma_p\right)$. As the next procedure, the eigen values Λ of $\mathbf{L}\left(\varsigma = \varsigma_p\right)$ known as Floquet multipliers are determined which are distinct. The instability condition is satisfied only if $|\Lambda| > 1$ [105]. The eigen values σ of the nonsingular matrix $\mathbf{B}$ are known as Floquet exponents. Floquet's theorem connects σ and Λ via the relation $\Lambda = \exp\left(\sigma\,\varsigma_p\right)$ [109] which is clear from Eq.(4.3.31). Thus the unstable sideband power gain G is given by the relation [105, 107]

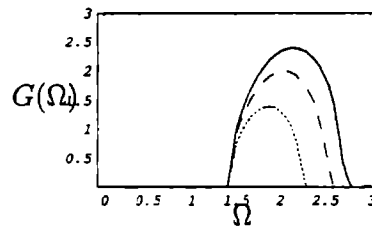$$G = \frac{2}{\varsigma_p}\,\ln|\Lambda| \qquad (4.3.36)$$

Using the above relation, one can draw parametric gain curves as functions of finite frequency detuning Ω as is clear from the linear homogeneous system given by Eq.(4.3.31). Figures (4.1(a)) and (4.1(b)) show the growth rate curves as functions of Ω when the linearly polarized pump wave is oriented at $\theta = 1°$ from the slow axis of the birefringent fiber.
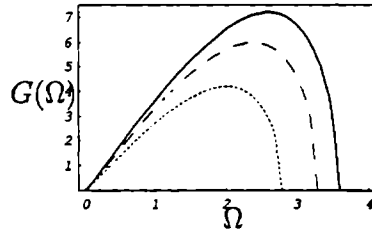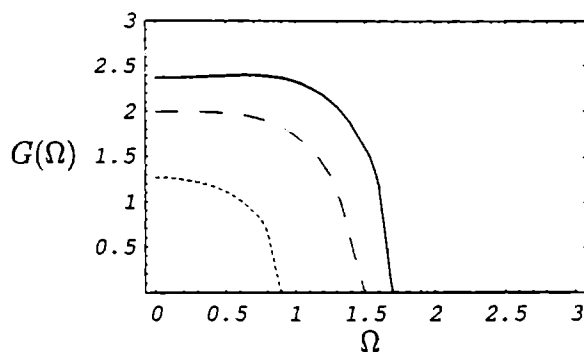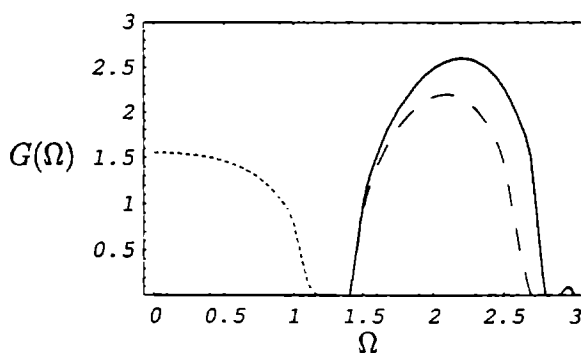
(a)
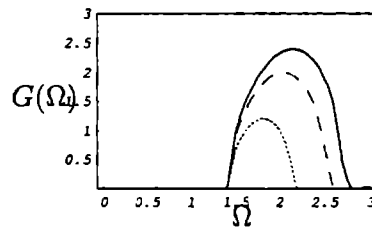
(b)

(c)

Fig. 4.1: The graphical relation between the parametric gain curve and the frequency detuning for $p = 0.7$ (dotted curve), 1.0 (dashed curve) and 1.2 (solid curve) and $G_3 = 0.005$. (a) The pump is oriented at an angle of 1° from the slow axis for the anomalous dispersion regime; (b) The pump is oriented at an angle of 1° from the slow axis for the normal dispersion regime; (c) The pump is oriented at an angle of 1° from the fast axis for the anomalous dispersion regime.

(a)

(b)

Fig. 4.2: The graphical relation between the parametric gain curve and the frequency detuning for various p values when the pump is oriented at an angle of 1° from the fast axis for the normal dispersion regime with $G_3 = 0.005$.
(a) $p = 0.7$ (dotted curve), 1.0 (dashed curve) and 1.2 (solid curve);
(b) $p = 0.6$ (dotted curve), 0.9 (dashed curve) and 1.3 (solid curve)

Figure (4.1(c)) is a repetition of Fig.(4.1(a)) for various values of p when the pump is oriented at an angle of 1° from the fast axis for the anomalous dispersion regime. It is observed that the parametric gain curve virtually remains the same whenever the pump is rotated from the slow axis by a few degrees for both the regimes. Also, when the linearly polarized pump wave is oriented close to the

fast axis, below $p = 0.5$ no MI is observed. As the value of p is steadily increased thereafter, the parametric gain curve is found to vary considerably for various values of p thereby confirming the fact that the slow and the fast axes of a polarization preserving fiber are not equivalent when one considers the influence of the fourth order dispersion effects also. Figures (4.2(a)) and (4.2(b)) depict this property of the parametric gain curve for various values of p when the linearly polarized pump wave is oriented at 1° from the fast axis for the normal dispersion regime. From the above plots it can be inferred that even for a polarization preserving fiber, large asymmetry exists between the slow and the fast axes for continuous wave evolutions in the case of both the anomalous and normal dispersion regimes.

4.4   Conclusions

Using Floquet theory, the unstable power gain is obtained as function of fine frequency sideband detuning when a linearly polarized pump wave is oriented at arbitrary angles with respect to the slow and fast axes for the anomalous and normal dispersion regimes on considering fourth order dispersion effects. It is observed that the parametric gain curve remains the same whenever the pump is rotated from the slow axis by a few degrees for both the regimes. Also, when the linearly polarized pump wave is oriented close to the fast axis, below $p = 0.5$ no MI is observed. As the value of p is steadily increased thereafter, the parametric gain curve is found to vary considerably for various values of p thereby confirming the fact that the slow and the fast axes of a polarization preserving fiber are not equivalent when one considers the influence of fourth order dispersion effects.

Chapter 5

Soliton propagation in a fiber with varying dispersion and having effective gain and effective phase modulation

5.1 Introduction

In the first four chapters, the group velocity dispersion coefficient is taken to be a constant under the assumption that the fiber is uniform in the sense that there are no variations in the lattice parameters of the fiber medium as well as those of the fiber geometry. But in real world, this may not be the case. So the study of pulse propagation through nonuniform media demands special attention as it pertains to real physical systems. The presence of nonuniformity can very much influence the dynamics of soliton pulse propagation resulting in the distortion of the pulse tail as well as causing damping to the soliton amplitude [112]. With the entry of nonuniformity in the fiber medium, the GVD coefficient can no longer be considered as constant, but as a function of the longitudinal distance [112]. It is a well known fact that when the group velocity dispersion (GVD) is varied even slightly, the behavior of the soliton pulse changes drastically from its regular

one where for example, when the GVD decreases (increases), the soliton pulse gets compressed (broadened) as it propagates along the length of the fiber [113]. By exploiting this property of the GVD of the fiber medium to good use, it will be possible to control optical solitons in soliton communication systems wherein high-quality, stable, polarization-insensitive soliton pulse compression and soliton train generation can be effectively realized [114].

An optical fiber possessing the property where its GVD monotonically and smoothly decreases from an initial value to a smaller value at the end of its length according to some specified dispersion profile is known as a dispersion decreasing fiber (DDF) [112]-[116]. Also by employing a DDF of a suitable profile, the distortion in the pulse tail can be removed as a result of the effective tailored gain which arises as a result of decreasing dispersion [113]. In this chapter, various dispersion decreasing profiles with both the fiber loss and phase modulation terms included, are discussed for both the scalar [116] and elliptically birefringent [119] cases. It is thereby shown that the the effect due to fiber loss can be nullified by employing optimum dispersion decreasing profiles which in turn produce an effective gain as a function of distance [116, 119]. In this regard the interplay between the effective gain and phase modulation which results in the compression of the pulse along the length of the fiber is shown [116, 119].

The remainder of the chapter is arranged as follows. In Sec.5.2 the model equations for both the scalar and elliptically birefringent case are presented. The modified scalar nonlinear Schrödinger equation is solved using the Bäcklund transformation technique in Sec.5.3 where the two soliton interaction scenario is analyzed in detail. Section 5.4 describes the single soliton solutions for the modified coupled nonlinear Schrödinger equation. Conclusions are presented in Sec.5.5.

5.2 Basic equations

In a dispersion decreasing fiber (DDF), as the waveguide contribution to the group velocity dispersion (GVD) parameter depends on the core size, its value decreases along the fiber length [112]-[116]. Hence, using a similar procedure as outlined in chapter one, pulse propagation in a dispersion decreasing single mode optical fiber is found to be characterized by a generalized normalized nonlinear Schrödinger equation (GNNSE) of the form [1, 113]:

$$i \, U_z + \frac{\beta(z)}{2} \, U_{\tau\tau} + |U|^2 \, U + i \, \Gamma \, U = 0, \qquad (5.2.1)$$

where the parameter $\beta(z) = \dfrac{|k''(z)|}{|k''(0)|}$ governs the dispersion variations along the fiber length. $k''(z)$ and $k''(0)$ are the GVD parameters at z and zero respectively. U is the slowly varying complex pulse envelope; τ is the normalized retarded time in the non-dimensional form and z is the normalized propagation distance also in the non-dimensional form. Extensive research centered around Eq.(5.2.1) has been carried out regarding soliton pulse compression [112]-[116]. On making the transformation [112]

$$\begin{aligned} U &= \sqrt{\beta(z)} \, u, \\ \zeta &= \int_0^z \beta(z') \, dz', \end{aligned} \qquad (5.2.2)$$

Eq.(5.2.1) reduces to the form of the scalar nonlinear Schrödinger equation given by [112]

$$i \, u_\zeta + \frac{1}{2} \, u_{\tau\tau} + |u|^2 \, u - i \, \frac{\alpha(\zeta)}{2} \, u = 0 \qquad (5.2.3)$$

where

$$\alpha(\zeta) = -\frac{1}{\beta(\zeta)} \, (\beta_\zeta(\zeta) + 2\Gamma). \qquad (5.2.4)$$

Equation(5.2.3) shows that the effect of decreasing dispersion is mathematically equivalent to adding a gain term to the nonlinear Schrödinger equation [112].

Use of inline electro-optic phase modulators is known as a rather simple way to control soliton transmission [117, 118]. An advantage of this control scheme is that no net gain has to be introduced into the transmission system to maintain the soliton power [117, 118]. Therefore, in this approach, it is not necessary to introduce an additional excess gain balancing the average energy flow into the system but resulting into growth of the continuous wave and noise [117, 118]. Solitons are stably guided at their temporal positions by the effective potential created due to phase modulation. Insertion of modulators with properly designed filters result in substantial suppression of the Gordon-Haus timing jitter [117, 118]. This is desirable for increasing the transmission capacity of a communication system placing carrier pulses close to each other. Mezentsev and Turitsyn have modelled a system which describes pulse propagation with inline phase-modulators, which is of the form [118]

$$i\, u_\zeta + \frac{1}{2}\, u_{\tau\tau} + |u|^2\, u - M\tau^2 u = 0, \qquad (5.2.5)$$

where the constant parameter M is positive or negative corresponding to the trapping or non trapping effective potential. In this chapter, soliton propagation in a dispersion decreasing fiber with the above mentioned inline-phase modulator is studied, represented by the equation [116]:

$$i\, U_z + \frac{\beta(z)}{2}\, U_{\tau\tau} + |U|^2\, U + i\,\Gamma\, U - M'(z)\, \tau^2\, U = 0, \qquad (5.2.6)$$

where the term $M'(z)\, \tau^2\, U$ accounts for electro optic phase modulation [117]. The coefficient of phase modulation $M'(z)$, in the quadratic approximation for lumped sinusoidal modulation, is the ratio of the product of the depth of modulation, square of the modulation frequency and the characteristic distance to the

modulator spacing [117]. Γ is the fiber loss coefficient [117]. Equation (5.2.6) suggests that the shape and the cross-section of the fiber mode are changed along the fiber length. When $M'(z) = 0$, Eq.(5.2.6) reduces to the form given in Refs.[117] where it has been studied in detail.

In a similar way, pulse propagation in an elliptically birefringent dispersion decreasing optical fiber is found to be characterized by a generalized normalized coupled nonlinear Schrödinger equation (GNCNSE) of the form [119]:

$$
\begin{aligned}
i\,U_z + \frac{\beta(z)}{2}\,U_{\tau\tau} + \left(|U|^2 + B\,|V|^2\right)U + i\,\Gamma\,U - M'(z)\,\tau^2\,U &= 0, \\
i\,V_z + \frac{\beta(z)}{2}\,V_{\tau\tau} + \left(B\,|U|^2 + |V|^2\right)V + i\,\Gamma\,V - M'(z)\,\tau^2\,V &= 0,
\end{aligned}
$$

$$(5.2.7)$$

where U and V are the orthogonally polarized slowly varying electric field envelopes. The parameter B is the cross-phase modulation coupling factor which depends on the ellipticity angle. The same variation of the second order dispersion along the two orthogonal polarization eigen modes is considered as both the modes have the same central frequency as a result of which there exists only slight difference between the forms of the second-order dispersion coefficients which can be neglected for the case of a fiber having strong birefringence [119].

5.3 Multi soliton solutions for the generalized normalized nonlinear Schrödinger equation

The following transformations are considered for Eq.(5.2.6) [116]:

$$
\begin{aligned}
U &= \sqrt{\beta(z)}\,u, \\
\zeta &= \int_0^z \beta(z')\,dz',
\end{aligned}
$$

$$(5.3.1)$$

whereby Eq.(5.2.6) gets transformed into the form [116]:

$$i\, u_\zeta + \frac{1}{2}\, u_{\tau\tau} + |u|^2\, u - i\, \frac{\alpha\,(\zeta)}{2}\, u - M\,(\zeta)\, \tau^2\, u = 0 \qquad (5.3.2)$$

where

$$\begin{aligned}
\alpha\,(\zeta) &= -\frac{1}{\beta\,(\zeta)}\, (\beta_\zeta\,(\zeta) + 2\,\Gamma)\,, \\
M\,(\zeta) &= \frac{M'\,(\zeta)}{\beta\,(\zeta)}.
\end{aligned} \qquad (5.3.3)$$

Thus the problem of pulse propagation through the DDF reduces to the problem of pulse propagation through a uniform fiber with an effective amplification [112]. Solutions are obtained for Eq.(5.3.2) and thereby the solutions for Eq.(5.2.6) are retrieved on employing Eq.(5.3.1). From Eq.(5.3.2) it is clear that by proper selection of the slowly decreasing second-order dispersion coefficient $\beta\,(\zeta)$ which is required for pulse amplification and for the negation of effective fiber loss, the form for the effective gain coefficient $\alpha\,(\zeta)$ and that for the effective phase modulation coefficient $M\,(\zeta)$ can be fixed [116]. $\alpha\,(\zeta)$ is instrumental in resulting optical pulse compression.

The case for which Eq.(5.3.2) is completely integrable is considered and hence admits Lax pair such that the effective gain term and the effective phase modulation term exactly balance each other [116]. Equation (5.3.2) is completely integrable only for the case [116]

$$M\,(\zeta) = \frac{1}{2}\, \left(\alpha_\zeta\,(\zeta) - \alpha^2\,(\zeta)\right). \qquad (5.3.4)$$

Equation (5.3.2) now takes the form [116]:

$$i\, u_\zeta + \frac{1}{2}\, u_{\tau\tau} + |u|^2\, u - i\, \frac{\alpha\,(\zeta)}{2}\, u - \frac{1}{2}\, \left(\alpha_\zeta\,(\zeta) - \alpha^2\,(\zeta)\right)\, \tau^2\, u = 0 \qquad (5.3.5)$$

The linear eigen value problem for Eq.(5.3.5) is of the form [116]

$$\psi_\tau = Q_1 \, \psi,$$

$$\psi_\zeta = Q_2 \, \psi,$$

$$\psi = (\psi_1, \psi_2)^T, \tag{5.3.6}$$

where [116]:

$$Q_1 = \begin{pmatrix} -i\,\lambda(\zeta) & u\,\exp\left(i\,\alpha(\zeta)\,\frac{\tau^2}{2}\right) \\ -u^*\,\exp\left(-i\,\alpha(\zeta)\,\frac{\tau^2}{2}\right) & i\,\lambda(\zeta) \end{pmatrix}, \tag{5.3.7}$$

and

$$Q_2 = i\,\lambda^2(\zeta)\begin{pmatrix} -1 & 0 \\ 0 & 1 \end{pmatrix}$$

$$+\lambda(\zeta)\begin{pmatrix} -i\,\alpha(\zeta)\,\tau & u\,\exp\left(i\,\alpha(\zeta)\,\frac{\tau^2}{2}\right) \\ -u^*\,\exp\left(-i\,\alpha(\zeta)\,\frac{\tau^2}{2}\right) & i\,\alpha(\zeta)\,\tau \end{pmatrix}$$

$$+\frac{i}{2}\begin{pmatrix} |u|^2 & \begin{pmatrix}(u_\tau - i\,\alpha(\zeta)\,\tau\,u)\\ \exp\left(i\,\alpha(\zeta)\,\frac{\tau^2}{2}\right)\end{pmatrix} \\ \begin{pmatrix}(u_\tau^* + i\,\alpha(\zeta)\,\tau\,u^*)\\ \exp\left(-i\,\alpha(\zeta)\,\frac{\tau^2}{2}\right)\end{pmatrix} & -|u|^2 \end{pmatrix} \tag{5.3.8}$$

such that $Q_{1\zeta} - Q_{2\tau} + [Q_1, Q_2] = 0$ gives back Eq.(5.3.5) only when the eigenvalue $\lambda(\zeta) = \epsilon\,\exp\left(\int_0^\zeta \alpha(\zeta')\,d\zeta'\right)$ which is nonisospectral and ϵ is a hidden spectral parameter [116]. Moreover, the nonisospectral eigen value $\lambda(\zeta)$ is an exponentially increasing function resulting in the exponential increase of the maximum intensity of the pulse. From the linear eigen value problem given by Eq.(5.3.6), soliton

solutions are generated for Eq.(5.3.5) using autoBäcklund transformation technique [65, 66] and thereby the recurrence relations connecting the nth (primed) and $(n-1)^{th}$ (unprimed) soliton wave functions are obtained which are of the form [116]:

$$\psi_1' = \left(-i\,\lambda\,(\zeta) + i\,\mu' - \frac{1}{2}\,\sqrt{4\,\nu'^2 - |u + u'|^2}\,\right)\,\psi_1 + \frac{1}{2}\,(u + u')\,\psi_2,$$

$$\psi_2' = -\frac{1}{2}\,(u^* + u'^*)\,\psi_1 + \left(i\,\lambda\,(\zeta) - i\,\mu' - \frac{1}{2}\,\sqrt{4\,\nu'^2 - |u + u'|^2}\,\right)\,\psi_2$$

$$(5.3.9)$$

where $\mu'\,(\zeta)$ and $\nu'\,(\zeta)$ are real denoting the soliton velocity and amplitude parameters respectively and $\lambda\,(\zeta) \equiv \mu'\,(\zeta) + i\,\nu'\,(\zeta)$. The recurrence relation connecting the nth (primed) and $(n-1)^{th}$ (unprimed) soliton solutions is of the form [116]:

$$u + u' = \frac{-4\,\Gamma\,\nu'}{1 + |\Gamma|^2} \tag{5.3.10}$$

where $\Gamma = \frac{\psi_1}{\psi_2}$. From the recurrence relation given by Eqs.(5.3.9) and (5.3.10), the fundamental soliton solution is obtained for Eq.(5.3.5) given by [116]:

$$u\,(\varsigma, \tau) = -2\,\nu_1\,(\varsigma)\,\mathrm{sech}\,(f_1\,(\varsigma, \tau))\,\exp\,(-i\,f_2\,(\varsigma, \tau)\,) \tag{5.3.11}$$

where

$$f_1\,(\varsigma, \tau) = 2\left(\nu_1\,(\varsigma)\,\tau + 2\int_0^\varsigma \mu_1\,(\varsigma')\,\nu_1\,(\varsigma')\,d\varsigma' + \nu_1\,(\varsigma)\,\Delta_1\right),$$

$$f_2\,(\varsigma, \tau) = 2\left(-\frac{\alpha\,(\zeta)\,\tau^2}{4} + \mu_1\,(\varsigma)\,\tau + \int_0^\varsigma \left(\mu_1^2\,(\varsigma') - \nu_1^2\,(\varsigma')\right)\,d\varsigma' + \delta_1\right)$$

$$(5.3.12)$$

Here $\mu_1\,(\varsigma)$ and $\nu_1\,(\varsigma)$ denote the respective soliton velocity and amplitude of the fundamental soliton with $\mu_1\,(\varsigma) = k_{11}\,\exp\left(\int_0^\varsigma \alpha\,(\varsigma')\,d\varsigma'\right)$; $\nu_1\,(\varsigma) = k_{21}\,\exp\left(\int_0^\varsigma \alpha\,(\varsigma')\,d\varsigma'\right)$.

k_{11} and k_{21} are arbitrary constants and δ_1 and Δ_1 are integration phase constants. Finally, the single soliton solution for pulse propagation in a dispersion decreasing fiber with a suitable profile can be retrieved from Eq.(5.3.1) which is of the form [116]:

$$U(z,\tau) = -2\sqrt{\beta(\varsigma)}\,\nu_1(\varsigma)\,\text{sech}\,(f_1(\varsigma,\tau))\,\exp\left(-i\,f_2(\varsigma,\tau)\right) \qquad (5.3.13)$$

where $\varsigma(z) = \int_0^z \beta(z')\,dz'$. The following dispersion decreasing profiles (DDP) are considered: i)hyperbolic, ii)linear, iii) exponential, iv)logarithmic and v) gaussian. Figure (5.1) gives the plots of the various dispersion profiles.
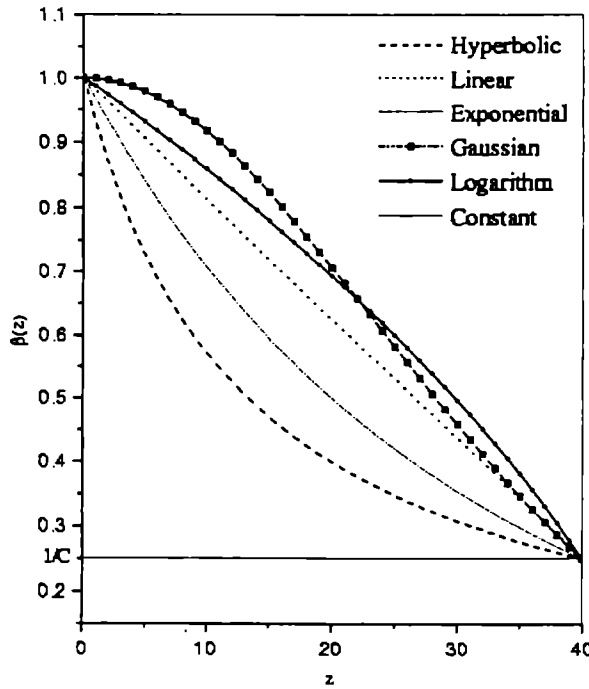

Fig. 5.1: The dispersion decreasing profiles given by Eqs.(5.3.14)-(5.3.18) are plotted

i) The hyperbolic DDP which is of the form:

$$\beta(\varsigma) = \frac{L}{(C-1)\,\varsigma + L}. \qquad (5.3.14)$$

123

On substituting Eq.(5.3.14) in Eq.(5.3.13), the compressed soliton solution after traversing the length L of the DDF having hyperbolic profile and having a loss rate $\Gamma = 0.0035$ is obtained. Figure (5.2(a)) depicts the surface plot for the fundamental soliton solution having the hyperbolic DDP. From Fig.(5.2(a)) it is clear that the soliton pulse gets compressed to the maximum with minimum compression ratio C for a given L and Γ. Thus a fiber having the hyperbolic DDP is found to achieve a fairly good compression even after compensating for the fiber loss and that too for a short fiber length L. This property can be verified by examining the fundamental soliton solution given by Eq.(5.3.13) by varying Γ for fixed C and L. Likewise, the other four profiles are examined: ii)linear profile, given by:

$$\beta(\varsigma) = \frac{(1-C)\,\varsigma}{C\,L} + 1,$$ (5.3.15)

iii) exponential profile, given by:

$$\beta(\varsigma) = \exp\left(-\frac{\varsigma}{L}\ln(C)\right),$$ (5.3.16)

iv) logarithmic profile, given by:

$$\beta(\varsigma) = \ln\left(e + \frac{\varsigma}{L}\left(\exp\left(\frac{1}{C}\right) - e\right)\right),$$ (5.3.17)

and v) gaussian profile, given by:

$$\beta(\varsigma) = \exp\left(-\left(\frac{\varsigma}{L}\right)^2 \ln(C)\right).$$ (5.3.18)

Figures (5.2(b))-(5.4(a)) show the surface plots of the respective profiles. All these surface plots corroborate that the hyperbolic profile is indeed the best suitable choice for DDP which is clear from Fig.(5.4(b)). Also, the following conclusions are made. The pulse amplitude increases exponentially due to the exponentially increasing nature of $\nu_1(\varsigma)$. Moreover, the pulse gets compressed proportionally

at each stage of propagation which is in a way similar to adiabatic process due to the presence of the term $f_1 (\varsigma, \tau)$ in Eq.(5.3.13). The form for $f_1 (\varsigma, \tau)$ is given in Eq.(5.3.12).
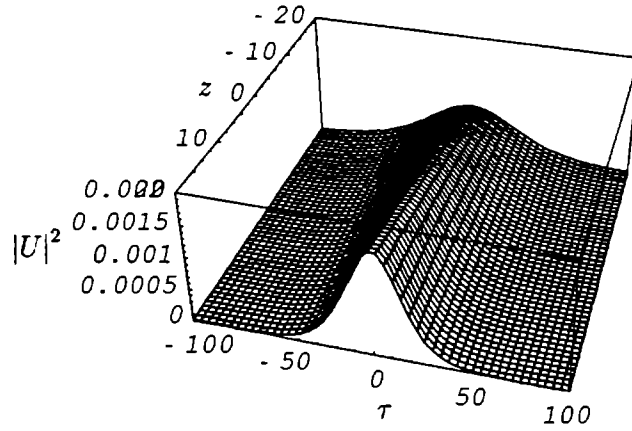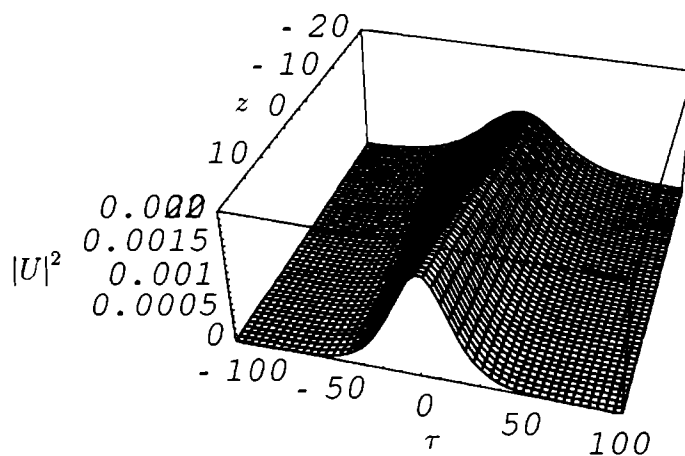
(a)
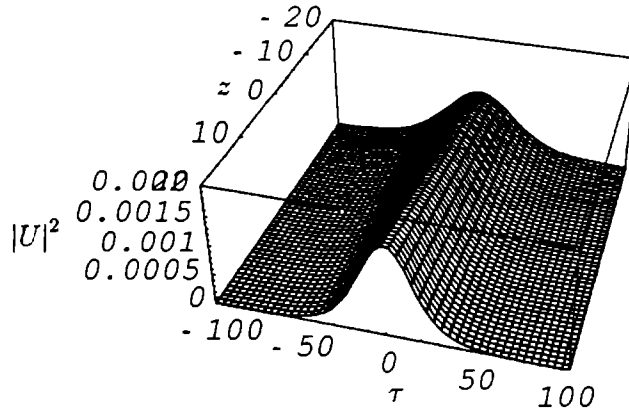
(b)

Fig. 5.2: Surface plots of the intensity of the soliton solution given by Eq.(5.3.13) for (a) hyperbolic DDP given by Eq.(5.3.14) and (b) linear DDP given by Eq.(5.3.15). Fiber loss rate $\Gamma = 0.0035$

(a)

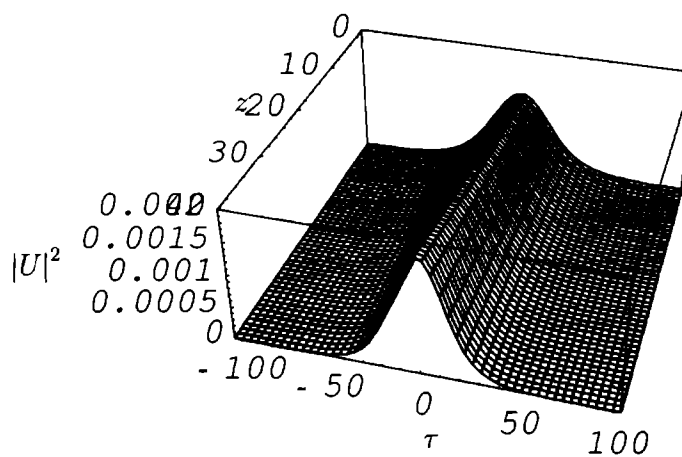

(b)

Fig. 5.3: Surface plots of the intensity of the soliton solution given by Eq.(5.3.13) for (a) exponential DDP given by Eq.(5.3.16) and (b) logarithmic DDP given by Eq.(5.3.17). Fiber loss rate $\Gamma = 0.0035$
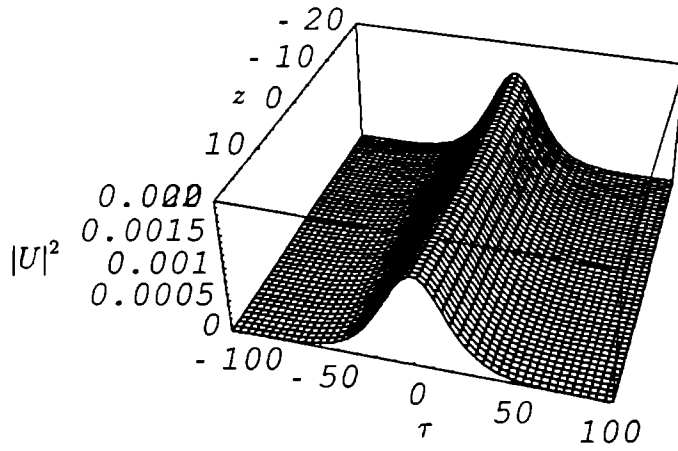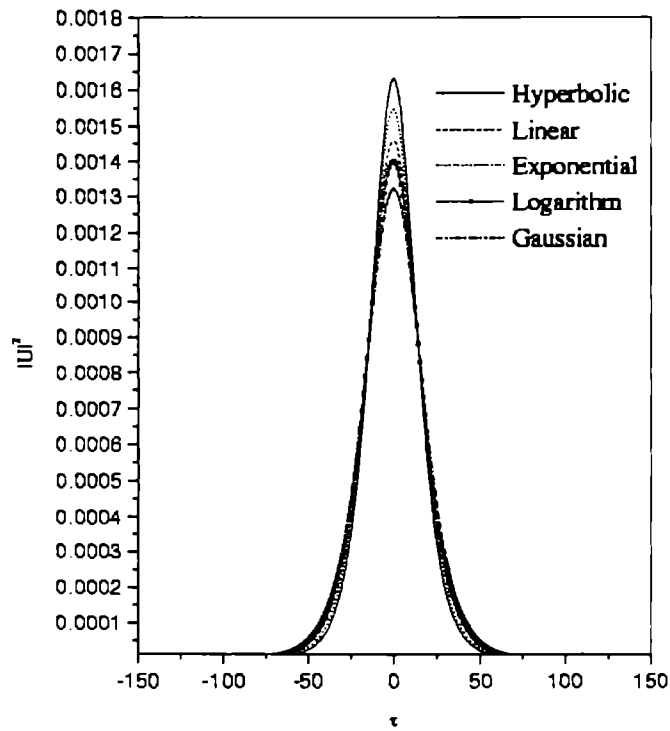
(a)

(b)

Fig. 5.4: (a)Surface plot of the intensity of the soliton solution given by Eq.(5.3.13) for gaussian DDP given by Eq.(5.3.18); (b) Comparison of the intensity plots for the various DDPs. Fiber loss rate $\Gamma = 0.0035$

Once again on using the recurrence relations given by Eqs.(5.3.9) and (5.3.10), the two soliton solution for the dispersion decreasing profile given by [116]:

$$U(z,\tau) = \sqrt{\beta(\zeta)}\,\frac{N(z,\tau)}{D(z,\tau)} \tag{5.3.19}$$

where [116]:

$$
\begin{aligned}
N(z,\tau) &= 2\,\nu_1(\varsigma)\,\operatorname{sech}(\xi_1)\,\exp(-i\,\chi_1'(\varsigma))\,(\Delta\mu(\varsigma))^2 \\
&\quad +4\,i\,\nu_1(\varsigma)\,\operatorname{sech}(\xi_1)\,\exp(-i\,\chi_1'(\varsigma))\,\nu_2(\varsigma)\,\Delta\mu(\varsigma)\,\tanh(\xi_2) \\
&\quad +2\,\nu_1(\varsigma)\,\operatorname{sech}(\xi_1)\,\exp(-i\,\chi_1'(\varsigma))\,(\nu_1^2(\varsigma)-\nu_2^2(\varsigma)) \\
&\quad +2\,\nu_2(\varsigma)\,\operatorname{sech}(\xi_2)\,\exp(-i\,\chi_2'(\varsigma))\,(\Delta\mu(\varsigma))^2 \\
&\quad -4\,i\,\nu_2(\varsigma)\,\operatorname{sech}(\xi_2)\,\exp(-i\,\chi_2'(\varsigma))\,\nu_1(\varsigma)\,\Delta\mu(\varsigma)\,\tanh(\xi_1) \\
&\quad -2\,\nu_2(\varsigma)\,\operatorname{sech}(\xi_2)\,\exp(-i\,\chi_2'(\varsigma))\,(\nu_1^2(\varsigma)-\nu_2^2(\varsigma))
\end{aligned}
\tag{5.3.20}
$$

and

$$
\begin{aligned}
D(z,\tau) &= (\Delta\mu(\varsigma))^2 + \nu_1^2(\varsigma) + \nu_2^2(\varsigma) \\
&\quad -2\,\nu_1(\varsigma)\,\nu_2(\varsigma)\,\tanh(\xi_1)\,\tanh(\xi_2) \\
&\quad -2\,\nu_1(\varsigma)\,\nu_2(\varsigma)\,\operatorname{sech}(\xi_1)\,\operatorname{sech}(\xi_1)\,\cos(\chi_2(\varsigma)-\chi_1(\varsigma))
\end{aligned}
\tag{5.3.21}
$$

where

$$
\begin{aligned}
\xi_i &= 2\left(\nu_i(\varsigma)\tau + 2\int_0^\varsigma \mu_i(\varsigma')\,\nu_i(\varsigma')\,d\varsigma' + k_{2i}\,\Delta_i\right), \\
\chi_i &= 2\left(\mu_i(\varsigma)\tau + 2\int_0^\varsigma (\mu_i^2(\varsigma')-\nu_i^2(\varsigma'))\,d\varsigma' + \delta_i\right), \\
\chi_i' &= \chi_i + \alpha(\varsigma)\frac{\tau^2}{2},
\end{aligned}
\tag{5.3.22}
$$

$$\mu_i\left(\varsigma\right) = k_{1i}\exp\left(\int_0^\varsigma \alpha\left(\varsigma'\right)\,d\varsigma'\right) \qquad \text{and}$$

$$\nu_i\left(\varsigma\right) = k_{2i}\exp\left(\int_0^\varsigma \alpha\left(\varsigma'\right)\,d\varsigma'\right), \qquad (5.3.23)$$

where $i = 1, 2$. Also $\Delta\mu\left(\varsigma\right) = \mu_2\left(\varsigma\right) - \mu_1\left(\varsigma\right)$. From the solution given by Eqs.(5.3.19)-(5.3.22), it can be observed that here also the two soliton pulses get compressed as they propagate along the length of the fiber. This behavior is clearly depicted in the surface plots given by Figs.(5.5) and (5.6(a)).
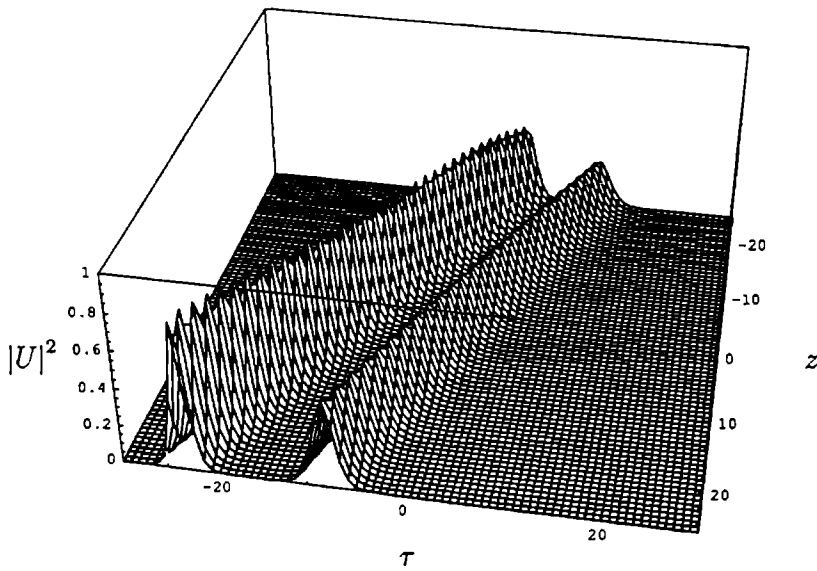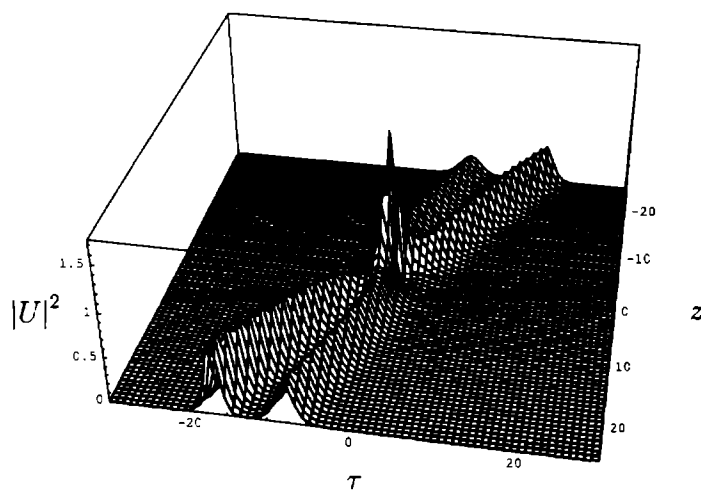

Fig. 5.5: Surface plot of the off-phase injection of the two soliton interaction given by Eq.(5.3.19) for the hyperbolic DDP. Fiber loss rate $\Gamma = 0.0035$

Figure(5.5) shows the off-phase injection of the two solitons with unequal amplitudes. In this case, the two solitons remain separated as they propagate along the length of the fiber.

(a)
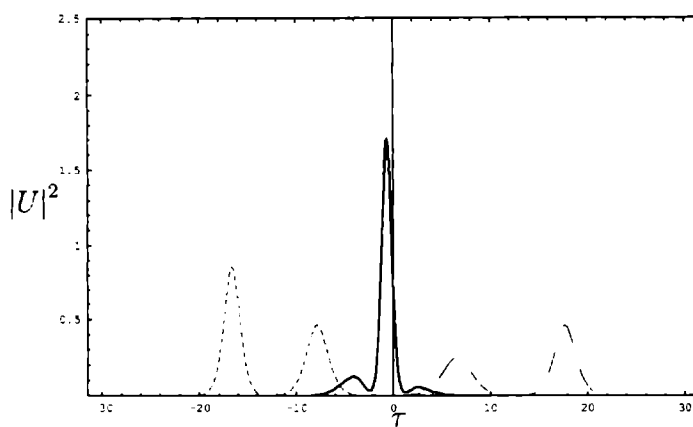
(b)

Fig. 5.6: (a) Surface plot of the in-phase injection of the two soliton interaction given by Eq.(5.3.19) for the hyperbolic DDP. Fiber loss rate $\Gamma = 0.0035$; (b) and (b) Comparison between the interaction scenarios before (dashed curve) and after (dotted curve) collision. Soliton interaction takes place at $z = 0$

Figure (5.6(a)) depicts the in-phase injection of the two solitons with unequal amplitudes. Here, the two solitons collide with each other at $z = 0$ where the two soliton pulses undergo maximum compression and have maximum intensity. After interaction, they traverse the length of the fiber with comparatively high

compression when compared with the scenario before collision. Figure (5.6(b)) brings out this nature of the two soliton pulses before and after collision where the dashed curve represents the scenario before collision and the dotted curve represents the scenario after collision. The solid curve represents the interaction scenario at $z = 0$.

5.4 Single soliton solutions for the generalized normalized coupled nonlinear Schrödinger equation

Proceeding in a similar way as in Sec.5.3, the fundamental soliton solution for the generalized normalized coupled nonlinear Schrödinger equation is determined as follows. The following transformations given by [119]

$$
\begin{aligned}
U &= \sqrt{\beta(z)}\, u, \\
V &= \sqrt{\beta(z)}\, v, \\
\zeta &= \int_0^z \beta(z')\, \mathrm{d}z',
\end{aligned}
\tag{5.4.1}
$$

transform Eq.(5.2.7) to the problem of pulse propagation through a uniform fiber with an effective amplification having the form [119]:

$$
\begin{aligned}
i\, u_\zeta + \frac{1}{2}\, u_{\tau\tau} + \left(|u|^2 + B\,|v|^2\right) u - i\,\frac{\alpha(\zeta)}{2}\, u - M(\zeta)\, \tau^2 u &= 0, \\
i\, v_\zeta + \frac{1}{2}\, v_{\tau\tau} + \left(B\,|u|^2 + |v|^2\right) v - i\,\frac{\alpha(\zeta)}{2}\, v - M(\zeta)\, \tau^2 v &= 0, \quad (5.4.2)
\end{aligned}
$$

where $\alpha(\zeta)$ and $M(\zeta)$ are given by Eq.(5.3.3). Equation (5.4.2) is completely integrable only for the case $B = 1$ and $M(\zeta) = \frac{1}{2}\left(\alpha_\zeta(\zeta) - \alpha^2(\zeta)\right)$. Equation

(5.4.2) now takes the form [119]:

$$i\,u_\zeta + \frac{1}{2}\,u_{\tau\tau} + \left(|u|^2 + |v|^2\right)u - i\,\frac{\alpha\left(\zeta\right)}{2}\,u - \frac{1}{2}\left(\alpha_\zeta\left(\zeta\right) - \alpha^2\left(\zeta\right)\right)\tau^2\,u \;=\; 0,$$

$$i\,v_\zeta + \frac{1}{2}\,v_{\tau\tau} + \left(|u|^2 + |v|^2\right)v - i\,\frac{\alpha\left(\zeta\right)}{2}\,v - \frac{1}{2}\left(\alpha_\zeta\left(\zeta\right) - \alpha^2\left(\zeta\right)\right)\tau^2\,v \;=\; 0,$$

$$(5.4.3)$$

which now models a physical situation where pulse propagation is through an ideal elliptical birefringent fiber where the self and cross-coupling terms are identical. For $\alpha\left(\zeta\right) = 0$, the Manakov model [78, 120] is obtained which characterizes optical switching achieved without any shadow. The linear eigen value problem for Eq.(5.4.3) is of the form [119]:

$$\psi_\tau \;=\; Q_1\,\psi,$$

$$\psi_\zeta \;=\; Q_2\,\psi,$$

$$\psi \;=\; \left(\psi_1, \psi_2, \psi_3\right)^T, \qquad (5.4.4)$$

where [119]:

$$Q_1 = \begin{pmatrix} -i\,\lambda\left(\zeta\right) & u\,\exp\left(i\,\alpha\left(\zeta\right)\frac{\tau^2}{2}\right) & v\,\exp\left(i\,\alpha\left(\zeta\right)\frac{\tau^2}{2}\right) \\ -u^*\,\exp\left(-i\,\alpha\left(\zeta\right)\frac{\tau^2}{2}\right) & i\,\lambda\left(\zeta\right) & 0 \\ -v^*\,\exp\left(-i\,\alpha\left(\zeta\right)\frac{\tau^2}{2}\right) & 0 & i\,\lambda\left(\zeta\right) \end{pmatrix},$$

$$(5.4.5)$$

and

$$Q_2 = i\,\lambda^2\left(\zeta\right)\begin{pmatrix} -1 & 0 & 0 \\ 0 & 1 & 0 \\ 0 & 0 & 1 \end{pmatrix}$$

$$+\lambda\left(\zeta\right)\begin{pmatrix} -i\,\alpha\left(\zeta\right)\tau & u\,\exp\left(i\,\alpha\left(\zeta\right)\frac{\tau^2}{2}\right) & v\,\exp\left(i\,\alpha\left(\zeta\right)\frac{\tau^2}{2}\right) \\ -u^*\,\exp\left(-i\,\alpha\left(\zeta\right)\frac{\tau^2}{2}\right) & i\,\alpha\left(\zeta\right)\tau & 0 \\ -v^*\,\exp\left(-i\,\alpha\left(\zeta\right)\frac{\tau^2}{2}\right) & 0 & i\,\alpha\left(\zeta\right)\tau \end{pmatrix}$$

$$+\frac{i}{2}\begin{pmatrix} |u|^2 + |v|^2 & \begin{pmatrix} (u_\tau - i\,\alpha(\zeta)\,\tau\,u) \\ \exp\left(i\,\alpha(\zeta)\,\frac{\tau^2}{2}\right) \end{pmatrix} & \begin{pmatrix} (v_\tau - i\,\alpha(\zeta)\,\tau\,v) \\ \exp\left(i\,\alpha(\zeta)\,\frac{\tau^2}{2}\right) \end{pmatrix} \\[4ex] \left\{ \begin{aligned} &(u_\tau^* + i\,\alpha(\zeta)\,\tau\,u^*) \\ &\exp\left(-i\,\alpha(\zeta)\,\frac{\tau^2}{2}\right) \\ &(v_\tau^* + i\,\alpha(\zeta)\,\tau\,v^*) \\ &\exp\left(-i\,\alpha(\zeta)\,\frac{\tau^2}{2}\right) \end{aligned} \right. & -|u|^2 & -v\,u^* \\[4ex] & -u\,v^* & -|v|^2 \end{pmatrix}$$

$$(5.4.6)$$

such that $Q_{1\zeta} - Q_{2\tau} + [Q_1, Q_2] = 0$ gives back Eq.(5.4.3) only when the eigenvalue λ has the form $\lambda(\zeta) = \mu \exp\left(\int_0^\zeta \alpha(\zeta')\,d\zeta'\right)$ which is nonisospectral and μ is a hidden spectral parameter [119]. As in Sec.5.3, the nonisospectral eigen value $\lambda(\zeta)$ is an exponentially increasing function resulting in the exponential increase of the maximum intensity of the pulse. From the linear eigen value problem given by Eq.(5.4.4), soliton solutions for Eq.(5.4.3) can be generated using Backlund transformation technique and obtain the recurrence relation connecting the nth (primed) and $(n-1)^{th}$ (unprimed) soliton solutions [119]:

$$u(\zeta,\tau) - u'(\zeta,\tau) = \frac{2\,i\,\Gamma_1\,\Gamma_2^*\,(\lambda(\zeta) - \lambda^*(\zeta))\,\exp\left(-i\,\alpha(\zeta)\,\frac{\tau^2}{2}\right)}{1 + |\Gamma_1|^2 + |\Gamma_2|^2},$$

$$v(\zeta,\tau) - v'(\zeta,\tau) = \frac{u(\zeta,\tau) - u'(\zeta,\tau)}{\Gamma_2^*}, \qquad (5.4.7)$$

where Γ_1 and Γ_2 are the two pseudo potentials given by $\Gamma_1 = \frac{\psi_1}{\psi_3}$ and $\Gamma_2 = \frac{\psi_2}{\psi_3}$. From the recurrence relation given by Eq.(5.4.7), the fundamental soliton solutions for Eq.(5.2.3) given by [119]:

$$u(\varsigma,\tau) = \frac{2}{|C_1|^2}\,C_1\,C_2^*\,\alpha_2(\varsigma)\,\text{sech}\,(f_1(\varsigma,\tau) + \delta_1)\,\exp(-i\,f_2(\varsigma,\tau)),$$

$$v(\varsigma,\tau) = \frac{2}{|C_1|^2}\,C_1\,\alpha_2(\varsigma)\,\text{sech}\,(f_1(\varsigma,\tau) + \delta_2)\,\exp(-i\,f_2(\varsigma,\tau)), \quad (5.4.8)$$

where $\lambda\left(\varsigma\right) = \alpha_1\left(\varsigma\right) + i\,\alpha_2\left(\varsigma\right)$, with $f_1\left(\varsigma,\tau\right)$ and $f_2\left(\varsigma,\tau\right)$ given by Eq.(5.3.12). Also, $\alpha_1\left(\varsigma\right) = k_1\,\exp\left(\int_0^\varsigma \alpha\left(\varsigma'\right)\,d\varsigma'\right)$; $\alpha_2\left(\varsigma\right) = k_2\,\exp\left(\int_0^\varsigma \alpha\left(\varsigma'\right)\,d\varsigma'\right)$, such that $\mu = k_1 + i\,k_2$; k_1, k_2 being soliton velocity and amplitude parameters respectively. Moreover, $|C_1^2| \equiv 1 + |C_2^2|$. C_1, C_2, δ_1 and δ_2 are integration phase constants.
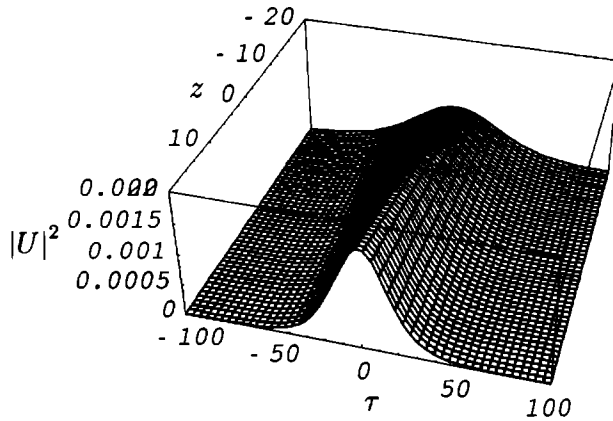

Fig. 5.7: Surface plot of the intensity of the soliton solution given by Eq.(5.4.9) for the hyperbolic DDP. Fiber loss rate $\Gamma = 0.0035$

Finally, the single soliton solution for pulse propagation in a decreasing dispersion fiber can be retrieved from Eq.(5.4.3) which is of the form [119]:

$$U\left(z,\tau\right) = \frac{2}{|C_1|^2}\,\sqrt{\beta\left(\varsigma\right)}\,C_1\,C_2^*\,\alpha_2\left(\varsigma\right)\operatorname{sech}\left(f_1\left(\varsigma,\tau\right) + \delta_1\right)\,\exp\left(-i\,f_2\left(\varsigma,\tau\right)\right),$$

$$V\left(z,\tau\right) = \frac{2}{|C_1|^2}\,\sqrt{\beta\left(\varsigma\right)}\,C_1\,\alpha_2\left(\varsigma\right)\operatorname{sech}\left(f_1\left(\varsigma,\tau\right) + \delta_2\right)\,\exp\left(-i\,f_2\left(\varsigma,\tau\right)\right),$$

$$(5.4.9)$$

where $\varsigma\left(z\right) = \int_0^z \beta\left(z'\right)\,dz'$. From the solution given by Eq.(5.4.9), the same conclusions in Sec.5.3 can be arrived at. Figure (5.7) portrays the surface plot of the intensity $|U|^2$ for the hyperbolic DDP. Similar plots can be obtained for the other DDPs both $|U|^2$ and $|V|^2$.

5.5 Conclusions

For the case of a GNNSE, the interaction scenario of the soliton pulses in a dispersion decreasing single mode fiber is arrived at. The pulse amplitudes increase exponentially and get compressed proportionally at each stage of propagation which is in a way similar to adiabatic process such that the soliton area is always conserved which is the property of soliton. Even after collision, the pulses propagate with increasing amplitudes paving way for effective pulse compression even after compensating for the fiber loss. Another important factor is that no fiber amplifiers have been considered. The pulse gets compressed solely as a result of the inherent gain of the dispersion decreasing profile of the fiber. This is mainly due to the interplay between the effective gain resulting in due to the dispersion decreasing profile and the effective phase modulation. Also the single soliton solution for the GNCNSE is determined from which the same conclusions can be arrived at.

Chapter 6

Soliton propagation in an erbium doped fiber amplifier

6.1 Introduction

Optical fibers attenuate like any other material. In the case of silica fibers, losses are relatively small, especially in the wavelength region near 1.55 μm. For this reason, losses can simply be ignored if the fiber length is 1km or less.In the case of long-haul fiber optic communication systems, transmission distances may exceed thousands of kilometers. Fiber amplifiers are commonly used to overcome transmission losses and restore optical signals in such systems. This chapter deals with the soliton pulse propagation in an erbium doped fiber amplifier which utilizes the self induced transparency (SIT) phenomenon [1, 2, 120, 122]. The SIT phenomenon pertains to the lossless pulse propagation in a resonant two-level media such that when the energy difference between the two levels of the media coincide with the optical wavelength, then coherent absorption takes place and the media becomes optically transparent to that particular wavelength. As the energy difference between erbium atoms is found to equal the soliton pulse wavelength, the fibers are generally doped with the erbium atoms in order to

induce SIT phenomenon [122].

The chapter is outlined as follows. In Sec.6.2 the mathematical formulation of the problem is presented. In Sec.6.3, single and two soliton solutions for the vacuum soliton case as well as that for the constant pumping source case are presented. In Sec.6.4, the conclusions are made.

6.2 Mathematical formulation of the problem

Rare earth ions in doped fibers can be modelled as a two level system by considering only the two energy levels that participate in light induced transitions. The dynamic response of a two level system is governed by the well known Maxwell-Bloch (MB) equations [120, 122]. These can be extended to the case of fiber amplifiers. So the fiber systems doped with erbium atoms is described by the coupled system of the nonlinear Schrödinger equation derived in chapter one along with the MB equations. Together they are known as the NLS-MB equations in which extensive research has been conducted [120]-[129]. When higher order effects such as higher order dispersion and the self steepening effects are included the coupled equation is known as the Hirota-Maxwell-Bloch equation (H-MB) [124, 126] given by

$$
\begin{aligned}
iu_\zeta + \frac{1}{2}u_{\tau\tau} + |u|^2 u + i\left(u_{\tau\tau\tau} + 6|u|^2 u_\tau\right) + \langle p\rangle &= 0, \\
p_\tau - 2i\left(\omega p + \eta u\right) &= 0, \\
\eta_\tau - i\left(pu^* - up^*\right) &= 0, \qquad (6.2.1)
\end{aligned}
$$

where $\langle\ldots\rangle$ is the averaging function over the entire frequency range. For exam-

ple,

$$\langle p(\zeta, \tau; \omega) \rangle = \int\limits_{-\infty}^{+\infty} p(\zeta, \tau; \omega) g(\omega) d\omega, \qquad (6.2.2)$$

such that

$$\int\limits_{-\infty}^{+\infty} g(\omega) d\omega = 1. \qquad (6.2.3)$$

$g(\omega)$ is the distribution function which represents the uncertainty in the energy level of the resonant atoms. u denotes the normalized slowly varying complex pulse envelope; τ is the normalized retarded time in the non-dimensional form and z is the normalized propagation distance also in the non-dimensional form. p is a measure of the polarization of the resonant medium and η denotes the extent of population inversion.

6.3 Soliton solutions

The linear eigen value problem for Eq.(6.2.1) is of the form :

$$\psi_\tau = Q_1 \psi,$$

$$\psi_\zeta = Q_2 \psi,$$

$$\psi = (\psi_1, \psi_2)^T \qquad (6.3.1)$$

where:

$$Q_1 = \begin{pmatrix} -i\lambda & u \\ -u^* & i\lambda \end{pmatrix}, \qquad (6.3.2)$$

and

$$Q_2 = \begin{pmatrix} A & B \\ C & -A \end{pmatrix}, \qquad (6.3.3)$$

where

$$A \;=\; -i\lambda^2 + \frac{i}{2}\,|u|^2 - 4i\lambda^3 \not= 2i\lambda\,|u|^2 + uu_\tau^* - u^*u_\tau - \left\langle \frac{i\eta}{2(\lambda+\omega)} \right\rangle,$$

$$B \;=\; \lambda u + \frac{i}{2}u_\tau + 4\lambda^2 u + 2i\lambda u_\tau - 2\,|u|^2\,u - u_{\tau\tau} + \left\langle \frac{p}{2(\lambda+\omega)} \right\rangle \quad \text{and}$$

$$C \;=\; -\lambda u^* + \frac{i}{2}u_\tau^* - 4\lambda^2 u^* + 2i\lambda u_\tau^* + 2\,|u|^2\,u^* + u_{\tau\tau}^* - \left\langle \frac{p^*}{2(\lambda+\omega)} \right\rangle, (6.3.4)$$

such that $Q_{1\zeta} - Q_{2\tau} + [Q_1, Q_2] = 0$ gives back Eq.(6.2.1). From the linear eigen value problem given by Eq.(6.3.1), soliton solutions are generated for Eq.(6.2.1) using autoBäcklund transformation technique and thereby the recurrence relations connecting the nth (primed) and $(n-1)^{th}$ (unprimed) soliton wave functions are obtained which are of the form :

$$\psi_1' \;=\; \left(-i\,\lambda + i\,\mu' - \frac{1}{2}\,\sqrt{4\,\nu'^2 - |u + u'|^2} \right)\psi_1 + \frac{1}{2}\,(u + u')\,\psi_2,$$

$$\psi_2' \;=\; -\frac{1}{2}\,(u^* + u'^*)\,\psi_1 + \left(i\,\lambda - i\,\mu' - \frac{1}{2}\,\sqrt{4\,\nu'^2 - |u + u'|^2} \right)\psi_2 (6.3.5)$$

where μ' and ν' are real denoting the soliton velocity and amplitude parameters respectively and $\lambda \equiv \mu' + i\,\nu'$. The recurrence relation connecting the nth (primed) and $(n-1)^{th}$ (unprimed) soliton solutions is of the form :

$$u + u' = \frac{-4\,\Gamma\,\nu'}{1 + |\Gamma|^2}, \tag{6.3.6}$$

where $\Gamma = \dfrac{\psi_1}{\psi_2}$. Moreover, $u' \equiv u(n)$ and $u \equiv u(n-1)$, $n = 1, 2, \ldots$ such that $u(1)$ refers to the single soliton solution and so on. Hence Eq.(6.3.6) can be rewritten as :

$$u(n-1) + u(n) = \frac{-4\,\Gamma(n-1)\,\nu(n)}{1 + |\Gamma(n-1)|^2} \tag{6.3.7}$$

Now two different cases are considered i) vacuum soliton case for which $u(0) = 0$ is taken as the seed solution and ii) $u(0) = \kappa$, which represents a constant pumping source. κ is complex.

i) vacuum soliton case

Here $u(0) = 0$. Hence from Eqs.(6.3.1) and (6.3.2), and with the condition for the pure state given by $p = 0$ [126] and $\eta = 1$, the relation between the wave functions is given by :

$$
\begin{aligned}
\psi_{1\tau}(0) &= -i\lambda\psi_1(0) \qquad \text{and} \\
\psi_{2\tau}(0) &= i\lambda\psi_2(0).
\end{aligned} \tag{6.3.8}
$$

Hence from Eq.(6.3.8),

$$
\begin{aligned}
\psi_1(0) &= c_1(\zeta)\exp(-i\lambda\tau), \\
\psi_2(0) &= c_2(\zeta)\exp(i\lambda\tau).
\end{aligned} \tag{6.3.9}
$$

where $c_i(\zeta)$ $(i = 1, 2)$ are integration constants. But again :

$$
\begin{aligned}
\psi_{1\zeta}(0) &= A\psi_1(0), \\
\psi_{2\zeta}(0) &= -A\psi_2(0).
\end{aligned} \tag{6.3.10}
$$

where A is given by Eq.(6.3.4). Here $B = C = 0$ as $u(0) = p = 0$. Hence on substituting Eq.(6.3.9) into Eq.(6.3.10), the corresponding wave functions are obtained as :

$$
\begin{aligned}
\psi_1(0) &= c_1(0)\exp(A\zeta - i\lambda\tau), \\
\psi_2(0) &= c_2(0)\exp(-(A\zeta - i\lambda\tau)),
\end{aligned} \tag{6.3.11}
$$

where $c_i(0)$ $(i = 1, 2)$ are integration constants. Hence the pseudo-spectral function $\Gamma(0)$ is given by :

$$
\begin{aligned}
\Gamma(0) &\equiv \frac{\psi_1(0)}{\psi_2(0)} \\
&= C(0)\exp(2(A\zeta - i\lambda\tau)),
\end{aligned} \tag{6.3.12}
$$

where $C(0) \equiv \dfrac{c_1(0)}{c_2(0)}$. On substituting these in Eq.(6.3.7), the single soliton solution is obtained as :

$$u(\zeta, \tau) \equiv u(1) = -2\nu(1)\,\mathrm{sech}\left(2\left((A_{11} + Av_1)\zeta + \nu(1)\tau + \nu(1)\Delta_1\right)\right)$$

$$\exp\left(-2i\left((A_{12} + Av_2)\zeta + \mu(1)\tau + \delta_1\right)\right), \qquad (6.3.13)$$

where δ_1 and Δ_1 are integration phase constants and

$$A_{11} = 2\mu(1)\nu(1) + 4\left(3\mu^2(1)\nu(1) - \nu^3(1)\right),$$

$$A_{12} = 4\left(\mu(1)\left(\mu^2(1) - 3\nu^2(1)\right)\right) + \left(\mu^2(1) - \nu^2(1)\right),$$

$$Av_1 = \left\langle \frac{\nu(1)}{2\left((\mu(1) + \omega)^2 + \nu^2(1)\right)} \right\rangle$$

$$Av_2 = \left\langle \frac{(\mu(1) + \omega)}{2\left((\mu(1) + \omega)^2 + \nu^2(1)\right)} \right\rangle. \qquad (6.3.14)$$

Figure (6.1) shows the surface plot of $|u(\zeta, \tau)|^2$ when $g(\omega)$ given by Eq.(6.2.3) takes the form of a Dirac-delta function $\delta(\omega - \omega_0)$ at the resonant frequency ω_0. Hence from Eq.(6.2.2), $\langle p(\zeta, \tau; \omega) \rangle = p(\zeta, \tau; \omega)$.
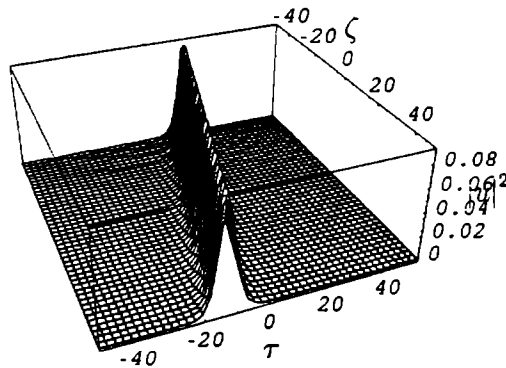

Fig. 6.1: Surface plot of the intensity of the soliton solution given by Eq.(6.3.13) when $g(\omega) = \delta(\omega - \omega_0)$, where the resonant frequency $\omega_0 = 0.5$

On substituting Eq.(6.3.7) into Eq.(6.2.2), the corresponding measure of the polarization of the resonant medium denoted by p and the extent of population inversion denoted by η can be readily obtained having the respective expressions

$$
\begin{aligned}
p(\zeta,\tau) = \nu(1)\,\text{sech}\,(a\zeta + b\tau + c)\Big(& 2f_1 - f_2^2(1 + 2f_2) - 2i\,(a - bf_2\,(1 + 3f_2)) \\
& \tanh(a\zeta + b\tau + c) + b^2\,(1 + 6f_2)\tanh^2(a\zeta + b\tau + c) - 2ib^3\tanh^3(a\zeta + b\tau + c) \\
& + \text{sech}^2(a\zeta + b\tau + c)\Big(- ((1 + 6f_2)(b^2 - 8\nu^2(1))) + 2ib\,(5b^2 - 24\nu^2(1)) \\
& \tanh(a\zeta + b\tau + c)\Big)\Big)\exp(f_1\zeta + f_2\tau + f_3)
\end{aligned}
\tag{6.3.15}
$$

and

$$
\begin{aligned}
\eta(\zeta,\tau) = \frac{1}{4}\Big[& 2b^2\,(24\nu^2(1) - 5b^2)\,\text{sech}^4(a\zeta + b\tau + c) + \text{sech}^2(a\zeta + b\tau + c) \\
& \Big(2ab - 3b^2 f_2\,(1 + 4f_2) + (1 + 6f_2)(8f_2\nu^2(1) + 16\omega_0\nu^2(1) - 2b^2\omega_0) \\
& + ib\,(1 + 8f_2 + 4\omega_0)(5b^2 - 24\nu^2(1))\tanh(a\zeta + b\tau + c) + 36b^2\,(b^2 - 4\nu^2(1)) \\
& \tanh^2(a\zeta + b\tau + c)\Big) + (f_2 + 2\omega_0 - ib\tanh(a\zeta + b\tau + c))\Big(2f_1 - f_2^2\,(1 + 2f_2) \\
& - 2i\,(a - bf_2\,(1 + 3f_2))\tanh(a\zeta + b\tau + c) + b^2\,(1 + 6f_2)\tanh^2(a\zeta + b\tau + c) \\
& - 2ib^3\tanh^3(a\zeta + b\tau + c)\Big)\Big],
\end{aligned}
\tag{6.3.16}
$$

where

$$
\begin{aligned}
a &= 2\,(A_{11} + A_{v1}), \\
b &= 2\nu(1), \\
c &= 2\nu(1)\Delta_1, \\
f_1 &= 2\,(A_{12} + A_{v2}), \\
f_2 &= 2\mu(1), \\
f_3 &= 2\delta_1.
\end{aligned}
$$

Once again on using the recurrence relations given by Eq.(6.3.5), the two soliton solution for Eq.(6.2.2) is obtained and is of the form :

$$u(2) \equiv u_2(\zeta, \tau) = \frac{N(\zeta, \tau)}{D(\zeta, \tau)}, \qquad (6.3.17)$$

where :

$$
\begin{aligned}
N(\zeta, \tau) =\ & 2\,\nu(1)\,\mathrm{sech}\,(\xi_1)\,\exp\,(-i\,\chi_1)\,(\Delta\mu)^2 \\
& +4\,i\,\nu(1)\,\mathrm{sech}\,(\xi_1)\,\exp\,(-i\,\chi_1)\,\nu(2)\,\Delta\mu\ \tanh\,(\xi_2) \\
& +2\,\nu(1)\,\mathrm{sech}\,(\xi_1)\,\exp\,(-i\,\chi_1)\,(\nu^2(1) - \nu^2(2)) \\
& +2\,\nu(2)\,\mathrm{sech}\,(\xi_2)\,\exp\,(-i\,\chi_2)\,(\Delta\mu)^2 \\
& -4\,i\,\nu(2)\,\mathrm{sech}\,(\xi_2)\,\exp\,(-i\,\chi_2)\,\nu(1)\,\Delta\mu\ \tanh\,(\xi_1) \\
& -2\,\nu(2)\,\mathrm{sech}\,(\xi_2)\,\exp\,(-i\,\chi_2)\,(\nu^2(1) - \nu^2(2))\,, \qquad \text{and}
\end{aligned}
$$

$$
\begin{aligned}
D(\zeta, \tau) =\ & (\Delta\mu)^2 + \nu^2(1) + \nu^2(2) - 2\,\nu(1)\,\nu(2)\,\tanh\,(\xi_1)\,\tanh\,(\xi_2) \\
& -2\,\nu(1)\,\nu(2)\,\mathrm{sech}\,(\xi_1)\,\mathrm{sech}\,(\xi_2)\,\cos\,(\chi_2 - \chi_1)\,, \qquad (6.3.18)
\end{aligned}
$$

where :

$$
\begin{aligned}
\xi_i =\ & 2\left(2\mu(i)\nu(i) - \frac{\nu(i)}{2\left((\mu(i) + \omega_0)^2 + \nu^2(i)\right)} + 4\left(3\mu^2(i)\nu(i) - \nu^3(i)\right)\right)\zeta \\
& +2\,(\nu(i)\tau + \nu(i)\Delta_i) \qquad \text{and} \\
\chi_i =\ & 2\left(\mu^2(i) - \nu^2(i) + \frac{\mu(i) + \omega_0}{2\left((\mu(i) + \omega_0)^2 + \nu^2(i)\right)} + 4\left(\mu^3(i)\nu(i) - 3\mu(i)\nu^2(i)\right)\right)\zeta \\
& +2\,(\mu(i)\tau + \delta_i) \qquad \text{with } i = 1, 2. \qquad (6.3.19)
\end{aligned}
$$

Also $\Delta\mu = \mu_2 - \mu_1$. Figure(6.2) depicts the in-phase injection of the two solitons with equal amplitudes. Here, the two solitons collide with each other at $\zeta = 0$.
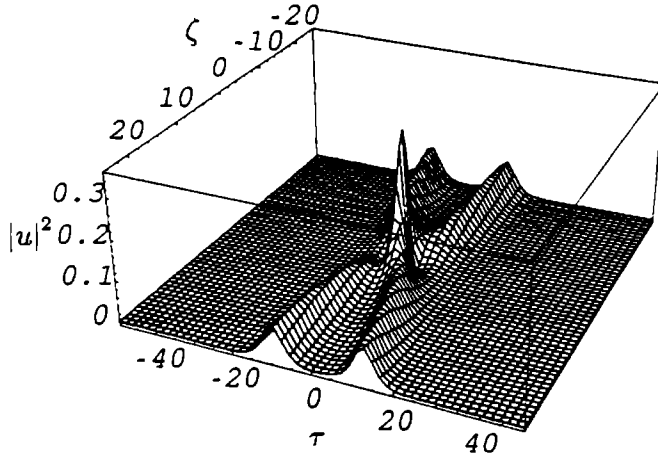
Fig. 6.2: In-phase injection of the two solitons with equal amplitudes given by Eqs.(6.3.17), (6.3.18) and (6.3.19) when $g(\omega) = \delta(\omega - \omega_0)$, where the resonant frequency $\omega_0 = 0.5$

ii)constant pumping source case

For the constant pumping source case, $u(0) = \kappa$, which is taken as the seed solution. Hence :

$$\begin{aligned}
\psi_{1\tau}(0) &= -i\lambda\psi_1(0) + \kappa\psi_2(0), \\
\psi_{2\tau}(0) &= \kappa\psi_1(0) + i\lambda\psi_2(0).
\end{aligned} \tag{6.3.20}$$

Hence from Eq.(6.3.20),

$$\begin{aligned}
\psi_1(0) &= c_1(\zeta)\exp\left(-i\sqrt{\lambda^2 + |\kappa|^2}\,\tau\right), \\
\psi_2(0) &= c_2(\zeta)\exp\left(i\sqrt{\lambda^2 + |\kappa|^2}\,\tau\right),
\end{aligned} \tag{6.3.21}$$

where $c_i(\zeta)$ $(i = 1, 2)$ are integration constants. But again :

$$\begin{aligned}
\psi_{1\zeta}(0) &= A\psi_1(0) + B\psi_2(0), \\
\psi_{2\zeta}(0) &= C\psi_1(0) - A\psi_2(0).
\end{aligned} \tag{6.3.22}$$

where A, B and C are given by Eq.(6.3.4). Thus from Eqs.(6.3.20) and (6.3.22), the corresponding wave functions are obtained as :

$$\psi_1(0) = c_1(0) \exp\left(\sqrt{A^2 + BC}\,\zeta - i\sqrt{\lambda^2 + |\kappa|^2}\,\tau\right),$$

$$\psi_2(0) = c_2(0) \exp\left(-\left(\sqrt{A^2 + BC}\,\zeta - i\sqrt{\lambda^2 + |\kappa|^2}\,\tau\right)\right),$$

$$(6.3.23)$$

where $c_i(0)$ $(i = 1, 2)$ are integration constants. Hence the pseudo-spectral function $\Gamma(0)$ is given by :

$$\Gamma(0) \equiv \frac{\psi_1(0)}{\psi_2(0)}$$

$$= C(0) \exp\left(2\left(\sqrt{A^2 + BC}\,\zeta - i\sqrt{\lambda^2 + |\kappa|^2}\,\tau\right)\right), \quad (6.3.24)$$

where $C(0) \equiv \dfrac{c_1(0)}{c_2(0)}$. On substituting these in Eq.(6.3.7), the single soliton solution is obtained as :

$$u(\zeta, \tau) \equiv u(1) = -\Big(\kappa + 2\nu(1)\,\mathrm{sech}\,(2\,(S_R\zeta + M_I\tau + \nu(1)\,\Delta_1))$$

$$\exp\left(2i\,(S_I\zeta - M_R\tau - \delta_1\,)\right)\Big), \qquad (6.3.25)$$

where δ_1 and Δ_1 are integration phase constants and

$$S_R = \sqrt{\frac{1}{2}\left(D_R + \sqrt{D_R^2 + D_I^2}\right)},$$

$$S_I = \frac{D_I}{2S_R},$$

$$M_R = \sqrt{\frac{1}{2}\left(L_R + \sqrt{L_R^2 + L_I^2}\right)},$$

$$M_I = \frac{L_I}{2M_R} \qquad (6.3.26)$$

where

$$L_R = \left(\mu^2(1) - \nu^2(1) + |\kappa|^2\right),$$

$$L_I = 2\mu(1)\nu(1),$$

$$D_R = A_R^2 - A_I^2 + B_R C_R - B_I C_I$$

$$D_I = 2A_R A_I + B_I C_R - B_R C_I,$$

$$A_R = 2\mu(1)\nu(1) - \left\langle \frac{\nu(1)}{2\left((\mu(1) + \omega)^2 + \nu^2(1)\right)} \right\rangle$$
$$+ 4\left(3\mu^2(1)\nu(1) - \nu^3(1)\right) - 2|\kappa|^2\nu(1),$$

$$A_I = -\left(\mu^2(1) - \nu^2(1)\right) + \frac{1}{2}|\kappa|^2 - \left\langle \frac{\mu(1) + \omega}{2\left((\mu(1) + \omega)^2 + \nu^2(1)\right)} \right\rangle$$
$$+ 4\left(3\mu(1)\nu^2(1) - \mu^3(1)\right) + 2|\kappa|^2\mu(1),$$

$$B_R = \mu(1)\kappa_+ - \nu(1)\kappa_- + 4\left(\kappa_+\left(\mu^2(1) - \nu^2(1)\right) - 2\mu(1)\nu(1)\kappa_-\right) - 2|\kappa|^2\kappa_+,$$

$$B_I = \mu(1)\kappa_- + \nu(1)\kappa_+ + 4\left(\kappa_-\left(\mu^2(1) - \nu^2(1)\right) - 2\mu(1)\nu(1)\kappa_+\right) - 2|\kappa|^2\kappa_-,$$

$$C_R = -\mu(1)\kappa_+ - \nu(1)\kappa_- - 4\left(\kappa_+\left(\mu^2(1) - \nu^2(1)\right) + 2\mu(1)\nu(1)\kappa_-\right) + 2|\kappa|^2\kappa_+,$$

$$C_I = -\mu(1)\kappa_- - \nu(1)\kappa_+ + 4\left(\kappa_-\left(\mu^2(1) - \nu^2(1)\right) - 2\mu(1)\nu(1)\kappa_+\right) - 2|\kappa|^2\kappa_-,$$

$$\kappa = \kappa_+ + i\kappa_-. \tag{6.3.27}$$

Figure (6.3) shows the surface plot for the intensity $|u(\zeta, \tau)|^2$ when $g(\omega) = \delta(\omega - \omega_0)$. From the figure, it is clear that $|u(\zeta, \tau)|^2$ has a constant value equal to $|\kappa|^2$ instead of zero when $\tau \to \pm\infty$. It can also be seen that when $\kappa \to 0$, Eq.(6.3.25) reduces to Eq.(6.3.13). Following a similar procedure as in case(i), the expressions for $p(\zeta, \tau)$ and $\eta(\zeta, \tau)$ pertaining to the soliton solution given by Eq.(6.3.25) can be readily obtained from the master equation (6.2.2).
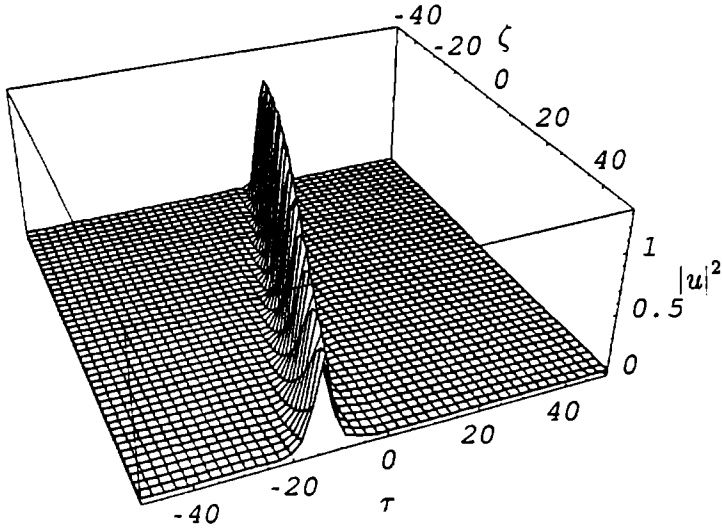
Fig. 6.3: Surface plot of the intensity of the soliton solution given by Eq.(6.3.25) when $g(\omega) = \delta(\omega - \omega_0)$, where the resonant frequency $\omega_0 = 0.9$

Once again on using the recurrence relations given by Eq.(6.3.5), the two soliton solution for Eq.(6.2.2) is obtained and is of the form :

$$u(2) \equiv u_2(\zeta, \tau) = \frac{\kappa D(\zeta, \tau) + N(\zeta, \tau)}{D(\zeta, \tau)}, \qquad (6.3.28)$$

where $N(\zeta, \tau)$ and $D(\zeta, \tau)$ have the same form as Eq.(6.3.18). In this case, ξ_i and χ_i $(i = 1, 2)$ have the following expressions:

$$\begin{aligned}
\xi_1 &= 2(S_R\zeta + M_I\tau + \nu(1)\Delta_1), \\
\xi_2 &= 2(S_{2R}\zeta + M_{2I}\tau + \nu(2)\Delta_2), \\
\chi_1 &= 2(-S_I\zeta + M_R\tau + \delta_1), \\
\chi_2 &= 2(-S_{2I}\zeta + M_{2R}\tau + \delta_2),
\end{aligned} \qquad (6.3.29)$$

where S_R, S_I, M_R and M_I are given by Eq.(6.3.26).

Now

$$S_{2R} = \sqrt{\frac{1}{2}\left(D_{2R} + \sqrt{D_{2R}^2 + D_{2I}^2}\right)},$$

$$S_{2I} = \frac{D_{2I}}{2S_{2R}},$$

$$M_{2R} = \sqrt{\frac{1}{2}\left(L_{2R} + \sqrt{L_{2R}^2 + L_{2I}^2}\right)},$$

$$M_{2I} = \frac{L_{2I}}{2M_{2R}} \tag{6.3.30}$$

where

$$L_{2R} = \left(\mu^2(2) - \nu^2(2) + |\kappa|^2\right),$$

$$L_{2I} = 2\mu(2)\nu(2),$$

$$D_{2R} = A_{2R}^2 - A_{2I}^2 + B_{2R}C_{2R} - B_{2I}C_{2I},$$

$$D_{2I} = 2A_{2R}A_{2I} + B_{2I}C_{2R} - B_{2R}C_{2I},$$

$$A_{2R} = 2\mu(2)\nu(2) - \left\langle \frac{\nu(2)}{2\left((\mu(2)+\omega)^2 + \nu^2(2)\right)}\right\rangle$$
$$+4\left(3\mu^2(2)\nu(2) - \nu^3(2)\right) - 2|\kappa|^2\nu(2),$$

$$A_{2I} = -\left(\mu^2(2) - \nu^2(2)\right) + \frac{1}{2}|\kappa|^2 - \left\langle \frac{\mu(2)+\omega}{2\left((\mu(2)+\omega)^2 + \nu^2(2)\right)}\right\rangle .$$
$$+4\left(3\mu(2)\nu^2(2) - \mu^3(2)\right) + 2|\kappa|^2\mu(2),$$

$$B_{2R} = \mu(2)\kappa_+ - \nu(2)\kappa_- + 4\left(\kappa_+\left(\mu^2(2) - \nu^2(2)\right) - 2\mu(2)\nu(2)\kappa_-\right) - 2|\kappa|^2\kappa_+,$$

$$B_{2I} = \mu(2)\kappa_- + \nu(2)\kappa_+ + 4\left(\kappa_-\left(\mu^2(2) - \nu^2(2)\right) - 2\mu(2)\nu(2)\kappa_+\right) - 2|\kappa|^2\kappa_-,$$

$$C_{2R} = -\mu(2)\kappa_+ - \nu(2)\kappa_- - 4\left(\kappa_+\left(\mu^2(2) - \nu^2(2)\right) + 2\mu(2)\nu(2)\kappa_-\right) + 2|\kappa|^2\kappa_+,$$

$$C_{2I} = -\mu(2)\kappa_- - \nu(2)\kappa_+ + 4\left(\kappa_-\left(\mu^2(2) - \nu^2(2)\right) - 2\mu(2)\nu(2)\kappa_+\right) - 2|\kappa|^2\kappa_-.$$

Figure(6.4) portrays the in-phase injection of the two solitons with equal amplitudes. From the figure, it is clear that $|u(\zeta,\tau)|^2$ has a constant value equal to $|\kappa|^2$ instead of zero when $\tau \to \pm\infty$. It can also be seen that when $\kappa \to 0$, Eq.(6.3.28) reduces to Eq.(6.3.17).
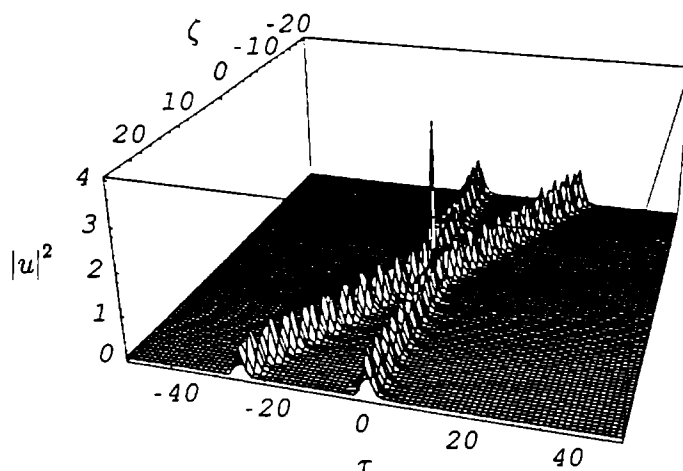
Fig. 6.4: In-phase injection of the two solitons with equal amplitudes given by Eqs.(6.3.28), (6.3.29)and (6.3.30) when $g(\omega) = \delta(\omega - \omega_0)$, where the resonant frequency $\omega_0 = 0.5$

6.4 Conclusions

This chapter concerns the coherent soliton pulse propagation in an erbium doped fiber system associated with the higher order dispersion, self-steepening and self-induced transparency effects. As usual, it is observed that there is exact balancing between higher order dispersion, self-steepening and self-induced transparency effects. Next the soliton solution when the erbium doped fiber system is driven by a constant pumping source is considered. In this case, the soliton solution will have a constant value equal to that of pumping source even at infinity, a phenomenon which differs from the case where the soliton solution asymptotically decreases to zero at infinity. This is depicted as the soliton in a continuous wave background. The interaction scenario is also studied in detail for both the cases.

Chapter 7

Conclusions

The major results and conclusions of the thesis work are summarised below:

i Extensive research has been carried out in the study of nonlinear pulse propagation in single mode optical fibers. Some of the nonlinear evolution equations describing pulse propagation in optical fibers yield exact soliton solutions while others yield either solitary wave solutions or periodic solutions in the form of cnoidal waves. Hence an in depth knowledge about the various types of solutions will lead much closer to the realistic world. In chapter two, employing the travelling wave method, various analytic expressions in the form of algebraic bright and dark solitary wave solutions and periodic solutions are obtained for for the higher order nonlinear Schrödinger equation by considering various forms for the given potential function. Moreover, as the total energy in this case is equal to zero, all the solutions for the corresponding potentials represent closed contours around stable centers and hence are stable.

ii Ultra-short optical pulses play a very crucial role in long haul optical communication systems as a result of which the demand for the generation of ultra-short optical pulses using various techniques is immense. One such technique

employs the generation of ultra-short pulses from continuous wave and quasi-continuous wave radiations using modulational instability phenomenon. Chapter three throws light on the conditions required for the generation of ultra-short pulses from continuous waves, using cross-phase modulational instability, as they traverse along a birefringent optical fiber. The conclusions in this are summarized as follows. The conditions for the occurrence of cross phase MI in the normal dispersion regime which occurs as a result of a group velocity mismatch between the linearly polarized eigen states when the linearly polarized pump is oriented at 45° with respect to the slow or fast axis are obtained. The instability conditions that govern the generation of ultrashort pulses are not affected irrespective of the presence or absence of S_2-the dimensionless third order dispersion coefficient. For variations in the pump polarization, maximum gain occurs for 45° polarization for all the cases considered in the chapter. The effect of SRS on MI is such that for comparative small values of the perturbation frequency, group velocity dispersion and cross-phase modulation terms dominate whereas for comparatively large values the perturbation frequency, the gain spectrum increases linearly with the result that the region of MI is widened due to SRS. Moreover the self-steepening effect reduce the maximum gain and bandwidth. As one slowly approaches towards the zero group velocity dispersion regime, the condition for the cross phase MI requires sufficiently large values of the total input power over a wide range of frequency detuning ω. At the zero group velocity dispersion regime, one obtains only the original MI. Furthermore, a modulational anstatz represented by Eq.(3.4.1) for the perturbation amplitudes is considered and have been able to retrieve all the results mentioned earlier in the chapter.

iii Even for a polarization preserving fiber, the slow and the fast axes may not be equivalent. Polarization modulational instability is a phenomenon phenomenon

which throws light into the above mentioned case. A knowledge about the PMI phenomenon will help to choose the range of parameter values that must be maintained in order to prevent chaotic switching if the fiber were to be used as an optical switch. Using Floquet theory in Chapter four, the unstable power gain is obtained as function of fine frequency sideband detuning when a linearly polarized pump wave is oriented at arbitrary angles with respect to the slow and fast axes for the anomalous and normal dispersion regimes on considering fourth order dispersion effects. It is observed that the parametric gain curve virtually remains the same whenever the pump is rotated from the slow axis by a few degrees for both the regimes. Also, when the linearly polarized pump wave is oriented close to the fast axis, below $p = 0.5$ no MI is observed. As the value of p is steadily increased thereafter, the parametric gain curve is found to vary considerably for various values of p thereby confirming the fact that the slow and the fast axes of a polarization preserving fiber are not equivalent when one considers the influence of the fourth order dispersion effects also.

iv In lossy optical fibers, the balance between group velocity dispersion and self-phase modulation is lost as a result of which pulses traversing along the length of the fibers get attenuated. In order to overcome this, dispersion decreasing fibers are employed in order to restore the balance between GVD and SPM. As their name suggest, the GVD of the fibers decrease in such a way that they compensate for the the reduced SPM experienced by the pulses as their energy is reduced by fiber loss. In chapter five, the interaction scenario of the soliton pulses in a dispersion decreasing single mode fiber is arrived at. The pulse amplitudes increase exponentially and get compressed proportionally at each stage of propagation which is in a way similar to adiabatic process such that the soliton area is always conserved which is the property of soliton. Even after collision,

conserved which is the property of soliton. Even after collision, the pulses propagate with increasing amplitudes paving way for effective pulse compression even after compensating for the fiber loss. Another important factor is that no fiber amplifiers have been considered. The pulse gets compressed solely as a result of the inherent gain of the dispersion decreasing profile of the fiber. This is mainly due to the interplay between the effective gain resulting in due to the dispersion decreasing profile and the effective phase modulation. Also the single soliton solution for the dispersion decreasing birefringent optical fiber is determined from which the same conclusions can be arrived at.

v Chapter six concerns with the coherent soliton pulse propagation in an erbium doped fiber system associated with the higher order dispersion, self-steepening and self-induced transparency effects. As usual, it is observed that there is exact balancing between higher order dispersion, self-steepening and self-induced transparency effects for only certain values of their corresponding coefficients. Next the soliton solution when the erbium doped fiber system is driven by a constant pumping source is considered. In this case, the soliton solution will have a constant value equal to that of pumping source even at infinity, a phenomenon which differs from the case where the soliton solution asymptotically decreases to zero at infinity. This phenomenon is depicted as the soliton in a continuous wave background The interaction scenario is also studied in detail for both the cases.

Appendix A

Mathematica source codes for determining the modulational instability conditions

A.1 Cross phase modulational instability studied in chapter three

```
Clear[ma,d,x,e1,e2,e3,e4,e5,s1,s2,s3,p,b,e11,e12,e13,e14,
e15,b1,b2,b3,cf,t0,dn,c,th,p1]
b=2/3;
th=45 Degree;
e11=0;
e12=0;
e14=0;
e15=0;
cf=100 10^(-6);
e13=N[ (e14+2 Cos[0 Degree]^2/(1+Sin[0 Degree]^2) e15)  ];
b2=69;
```

```
b3=.54 10^(-3);

b4=7 10^(-4);

t0=.5;

dn=3.25 10^(-4);

c=3 10^(-7);

d=N[t0 dn/(2 c b2)]

s1=.5;

s2=N[b3/(6 b2 t0)]

s3=N[b4/(24 b2 t0^2)]

e1=N[e11/(cf t0)]

e2=N[e12/(cf t0)]

e3=N[e13/t0]

e4=N[e14/t0]

e5=N[e15/t0]

ma[x_,p_]={{d x+6  e1 p x Cos[th]^2+2 e2 p x  Sin[th]^2+s2 x^3,

s1 x^2+2 I e5 p x  Sin[th]^2-s3 x^4,2 e2 p x Sin[2 th],

-I e5 p x Sin[2 th]},{s1 x^2+4 p Cos[th]^2+4  I e3 p x Cos[th]^2

+2 I e5 p x Sin[th]^2-s3 x^4,d x+2 e1 p x Cos[th]^2

+2 e2 p x Sin[th]^2+s2 x^3,2 b p Sin[2 th]

+2 I e4 p x Sin[2 th]+I e5 p x Sin[2 th],0},

{2 e2 p x Sin[2 th],- I e5 p x Sin[2 th],

-d x+6 e1 p x Sin[th]^2+2 e2 p x Cos[th]^2+s2 x^3,

s1 x^2+2 I e5 p x  Cos[th]^2-s3 x^4},{2 b p

Sin[2 th]+2 I e4 p x Sin[2 th]+I e5 p x Sin[2  th],

0,s1 x^2+4 p Sin[th]^2+4 I e3 x Sin[th]^2

+2 I e5 p x  Cos[th]^2-s3 x^4,-d x+2 e1 p x Sin[th]^2
```

```
+2 e2 p x Cos[th]^2+s2 x^3}};

Plot3D[N[Abs[Im[Eigenvalues[ma[x,p]][[4]]]]],

{x,-10,10},{p,0,50},Shading->False,PlotPoints->50,

AxesLabel -> {"x", "  y", "z    "},

TextStyle->{FontSlant->"Italic", FontSize->

15}]
```

A.2   Polarizational modulational instability studied in chapter four

```
Needs["ODE'"]

Clear[ma,p,an,th,s10,s20,s30,f,m,s1,s2,s3,sp,dd,g1,g3,

x,y,mp,h1,h2,n,mb,h,hh,hh1,y11,y21,y31,y41,y12,y22,y32,

y42,y13,y23,y33,y43,y14,y24,y34,y44,fmn,funm,

eig,gain,t1,t2,t3,t4,t5]

p=.75;

an=1;

th=N[an Pi/90];

s10=N[Cos[th]];

s20=N[Sin[th]];

s30=0;

f=N[((1+2 p s10)^2+(2 p s20)^2)^(.25)];

m=N[.5 (1-(1+2 p s10)/f^2)];

s3[x_]=N[-s20/f JacobiSD[f x,m]];

s1[x_]=N[s10+p (s3[x])^2];
```

```
s2[x_]=N[-s3'[x]];

sp=N[4 EllipticK[m]/f];

dd=0;

g1=.5;

g3=0.0005;

h1=0;

h2=4;

h=.4;

n=N[Round[(h2-h1)/h]];

xn=N[sp];

hh=N[sp/50];

n1=N[Round[xn/hh+1]];

hh1=0;

i=0;

While[i<=n,(

    y=N[hh1];

t1=N[Chop[ODE[{y11'==I ((g1 y^2-g3 y^4+p (1-s3[x])

-s1[x]/(2 (1-s3[x]))) y11+p (1-s3[x]) y21+(1/Sqrt[1-(s3[x])^2]

(.5-dd y) (s1[x]-I s2[x])+2 p Sqrt[1-(s3[x])^2]) y31

+2 p Sqrt[1-(s3[x])^2] y41),y21'==-I (p (1-s3[x]) y11

+(g1 y^2-g3 y^4+p (1-s3[x])-s1[x]/(2 (1-s3[x]))) y21

+2 p Sqrt[1-(s3[x])^2] y31+(1/Sqrt[1-(s3[x])^2] (.5+dd y)

  (s1[x]+I s2[x])+2 p Sqrt[1-(s3[x])^2]) y41),y31'==I

  ((1/Sqrt[1-(s3[x])^2] (.5-dd y) (s1[x]+I s2[x])

+2 p Sqrt[1-(s3[x])^2]) y11+2 p Sqrt[1-(s3[x])^2]

    y21+(g1 y^2-g3 y^4+p (1+s3[x])-s1[x]/(2 (1+s3[x]))) y31
```

+(p (1+s3[x])) y41),y41'==-I (2 p Sqrt[1-(s3[x])^2] y11

+(1/Sqrt[1-(s3[x])^2] (.5+dd y) (s1[x]-I s2[x])

+2 p Sqrt[1-(s3[x])^2]) y21+p (1+s3[x]) y31+(g1 y^2-

g3 y^4+p (1+s3[x])-s1[x]/(2 (1+s3[x]))) y41),y11[0]==1,

y21[0]==0,y31[0]==0,y41[0]==0},{y11,y21,y31,y41},{x,0,N[sp]},

Method->RungeKutta4,StepSize->N[hh]]],10][[n1,2]];

t2=N[Chop[ODE[{y12'==I ((g1 y^2-g3 y^4+p (1-s3[x])

-s1[x]/(2 (1-s3[x]))) y12+p (1-s3[x]) y22+(1/Sqrt[1-(s3[x])^2]

(.5-dd y) (s1[x]-I s2[x])+2 p Sqrt[1-(s3[x])^2]) y32

+2 p Sqrt[1-(s3[x])^2] y42),y22'==-I (p (1-s3[x]) y12

+(g1 y^2-g3 y^4+p (1-s3[x])-s1[x]/(2 (1-s3[x]))) y22

+2 p Sqrt[1-(s3[x])^2] y32+(1/Sqrt[1-(s3[x])^2] (.5+dd y)

(s1[x]+I s2[x])+2 p Sqrt[1-(s3[x])^2]) y42),y32'==I

 ((1/Sqrt[1-(s3[x])^2] (.5-dd y) (s1[x]+I s2[x])

+2 p Sqrt[1-(s3[x])^2]) y12+ 2 p Sqrt[1-(s3[x])^2] y22

+(g1 y^2-g3 y^4+p (1+s3[x])-s1[x]/(2 (1+s3[x]))) y32

+(p (1+s3[x])) y42),y42'==-I (2 p Sqrt[1-(s3[x])^2] y12

+(1/Sqrt[1-(s3[x])^2] (.5+dd y) (s1[x]-I s2[x])

+2 p Sqrt[1-(s3[x])^2]) y22+p (1+s3[x]) y32+(g1 y^2-g3 y^4

+p (1+s3[x])-s1[x]/(2 (1+s3[x]))) y42),y12[0]==0,y22[0]==1,

y32[0]==0,y42[0]==0},{y12,y22,y32,y42},{x,0,N[sp]},

Method->RungeKutta4,StepSize->N[hh]]],10][[n1,2]];

t3=N[Chop[ODE[{y13'==I ((g1 y^2-g3 y^4+p (1-s3[x])

-s1[x]/(2 (1-s3[x]))) y13+p (1-s3[x]) y23+(1/Sqrt[1-(s3[x])^2]

(.5-dd y) (s1[x]-I s2[x])+2 p Sqrt[1-(s3[x])^2]) y33

+2 p Sqrt[1-(s3[x])^2] y43),y23'==-I (p (1-s3[x]) y13

```
+(g1 y^2-g3 y^4+p (1-s3[x])-s1[x]/(2 (1-s3[x]))) y23

+2 p Sqrt[1-(s3[x])^2] y33+(1/Sqrt[1-(s3[x])^2] (.5+dd y)

(s1[x]+I s2[x])+2 p Sqrt[1-(s3[x])^2]) y43),y33'==I

((1/Sqrt[1-(s3[x])^2] (.5-dd y) (s1[x]+I s2[x])

+2 p Sqrt[1-(s3[x])^2]) y13+ 2 p Sqrt[1-(s3[x])^2] y23

+(g1 y^2-g3 y^4+p (1+s3[x])-s1[x]/(2 (1+s3[x]))) y33

+(p (1+s3[x])) y43),y43'==-I (2 p Sqrt[1-(s3[x])^2]  y13

+(1/Sqrt[1-(s3[x])^2] (.5+dd y) (s1[x]-I s2[x])

+2 p Sqrt[1-(s3[x])^2]) y23+p (1+s3[x]) y33+(g1 y^2-g3 y^4

+p (1+s3[x])-s1[x]/(2 (1+s3[x]))) y43),y13[0]==0,y23[0]==0,

y33[0]==1,y43[0]==0},{y13,y23,y33,y43},{x,0,N[sp]},

Method->RungeKutta4,StepSize->N[hh]]],10][[n1,2]];

t4=N[Chop[ODE[{y14'==I ((g1 y^2-g3 y^4+p (1-s3[x])

-s1[x]/(2 (1-s3[x]))) y14+p (1-s3[x]) y24+(1/Sqrt[1-(s3[x])^2]

(.5-dd y) (s1[x]-I s2[x])+2 p Sqrt[1-(s3[x])^2]) y34

+2 p Sqrt[1-(s3[x])^2] y44),y24'==-I (p (1-s3[x]) y14

+(g1 y^2-g3 y^4+p (1-s3[x])-s1[x]/(2 (1-s3[x]))) y24

+2 p Sqrt[1-(s3[x])^2] y34+(1/Sqrt[1-(s3[x])^2] (.5+dd y)

(s1[x]+I s2[x])+2 p Sqrt[1-(s3[x])^2]) y44),y34'==I

((1/Sqrt[1-(s3[x])^2] (.5-dd y) (s1[x]+I s2[x])

+2 p Sqrt[1-(s3[x])^2]) y14+ 2 p Sqrt[1-(s3[x])^2] y24

+(g1 y^2-g3 y^4+p (1+s3[x])-s1[x]/(2 (1+s3[x]))) y34

+(p (1+s3[x])) y44),y44'==-I (2 p Sqrt[1-(s3[x])^2] y14

+(1/Sqrt[1-(s3[x])^2] (.5+dd y) (s1[x]-I s2[x])

+2 p Sqrt[1-(s3[x])^2]) y24+p (1+s3[x]) y34

+(g1 y^2-g3 y^4+p (1+s3[x])-s1[x]/(2 (1+s3[x]))) y44),
```

```
y14[0]==0,y24[0]==0,y34[0]==0,y44[0]==1},{y14,y24,y34,y44},

{x,0,N[sp]},Method->RungeKutta4,StepSize->N[hh]]],10][[n1,2]];

fmn={N[Chop[t1]],N[Chop[t2]],N[Chop[t3]],N[Chop[t4]]};

funm=N[Chop[Transpose[fmn]]];

eig=N[Chop[Abs[Eigenvalues[funm][[1]]]]];

gain[y]=N[Chop[2/sp Log[eig]]];

hh1=N[hh1+h];

Print[Table[{i,y,N[Chop[gain[y]]]}]]

i++)];

t5=Table[{y,N[Chop[gain[y]]]},{y,h1,h2,h}];

Plot[Evaluate[Interpolation[t5]][y],{y,h1,h2}]
```

Appendix B

Stokes polarization parameters

B.1 The instantaneous optical field and the polarization ellipse

The electric field of a monochromatic plane wave can be described by two complex transverse components E_x and E_y such that

$$\mathbf{E}(z,t) = (\widehat{e}_x E_x + \widehat{e}_y E_y),$$
(B.1.1)

where the complex amplitudes can be written in the form:

$$
\begin{aligned}
E_x &= E_{0x} \exp(i\delta_x) \exp\left(i\left(kz - \omega t\right)\right), \\
E_y &= E_{0y} \exp(i\delta_y) \exp\left(i\left(kz - \omega t\right)\right),
\end{aligned}
$$
(B.1.2)

where E_{0x} and E_{0y} are real. Let

$$
\begin{aligned}
E_x &= E_x^R + iE_x^I, \\
E_y &= E_y^R + iE_y^I,
\end{aligned}
$$
(B.1.3)

where E_x^R, E_x^I, E_y^R and E_y^I are real. After separating Eq.(B.1.2) into real and imaginary parts and after some manipulations, the following set of equations can

160

be obtained:

$$\frac{E_x^R}{E_{0x}} \sin(\delta_y) - \frac{E_y^R}{E_{0y}} \sin(\delta_x) = \sin(\delta) \cos(kz - \omega t), \qquad \text{(B.1.4)}$$

$$\frac{E_x^R}{E_{0x}} \cos(\delta_y) - \frac{E_y^R}{E_{0y}} \cos(\delta_x) = \sin(\delta) \sin(kz - \omega t), \qquad \text{(B.1.5)}$$

$$\frac{E_x^I}{E_{0x}} \sin(\delta_y) - \frac{E_y^I}{E_{0y}} \sin(\delta_x) = \sin(\delta) \cos(kz - \omega t), \qquad \text{(B.1.6)}$$

and

$$\frac{E_x^I}{E_{0x}} \cos(\delta_y) - \frac{E_y^I}{E_{0y}} \cos(\delta_x) = -\sin(\delta) \sin(kz - \omega t), \qquad \text{(B.1.7)}$$

where the phase difference between the two amplitudes, $\delta = \delta_y - \delta_x$. On squaring Eqs.(B.1.4) and (B.1.5) separately and then adding, the "polarization ellipse" describing the state of polarization of the electric field can be arrived at and is given by [47,48]:

$$\left(\frac{E_x^R}{E_{0x}}\right)^2 - 2\frac{E_x^R E_y^R}{E_{0x} E_{0y}} \cos(\delta) + \left(\frac{E_y^R}{E_{0y}}\right)^2 = \sin^2(\delta). \qquad \text{(B.1.8)}$$

On squaring Eqs.(B.1.6) and (B.1.7) separately and then adding, an equation similar to Eq.(B.1.8) is obtained and is given by:

$$\left(\frac{E_x^I}{E_{0x}}\right)^2 - 2\frac{E_x^I E_y^I}{E_{0x} E_{0y}} \cos(\delta) + \left(\frac{E_y^I}{E_{0y}}\right)^2 = \sin^2(\delta). \qquad \text{(B.1.9)}$$

Equations (B.1.8) and (B.1.9) are recognized as the equations of an ellipse and show that at any instant of time, the locus of points described by the optical field as it propagates is an ellipse. This behavior is known as "optical polarization" and hence the name polarization ellipse for Eq.(B.1.8). The elliptical parameters E_{0x} E_{0y} and δ of the polarization ellipse are related to the orientation angle Ψ and ellipticity angle χ by the following equations [130]:

$$\begin{aligned}
\tan(2\Psi) &= \frac{2E_{0x} E_{0y}}{E_{0x}^2 - E_{0y}^2} \\
&= \tan(2\alpha) \cos(\delta), \\
\sin(2\chi) &= \sin(2\alpha) \sin(\delta), \qquad \text{(B.1.10)}
\end{aligned}$$

where $0 \leq \Psi < \pi$, $-\dfrac{\pi}{4} < \chi \leq \dfrac{\pi}{4}$ and $0 \leq \alpha < \dfrac{\pi}{2}$. Figure (B.1) shows the polarization ellipse.
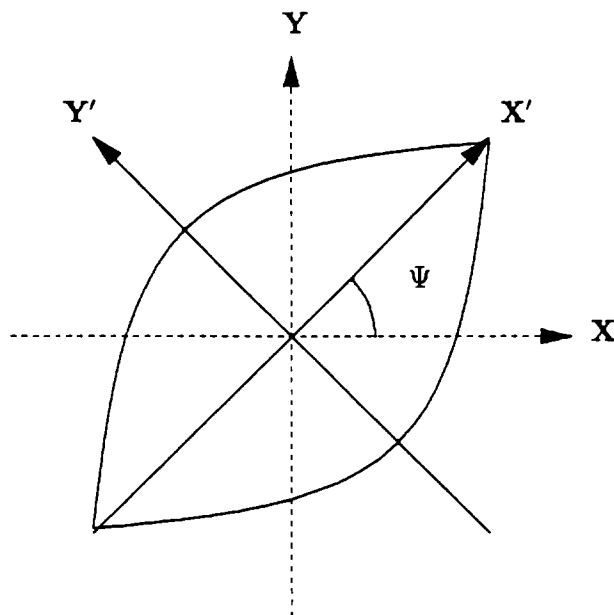

Fig. B.1: The rotated polarization ellipse. Ψ is the orientation angle

B.2 Derivation of Stokes polarization parameters

The Stokes polarization parameters can be derived from the Polarization ellipse given by Eq.(B.1.8). While the elliptical parameters E_{0x}, E_{0y} and δ are constants, E_x^R and E_y^R are functions of distance z and time t. For convenience, the derivation is carried out for the case $z = 0$ and finally generalized for arbitrary z. In order to represent the polarization ellipse in terms of the observables of the optical field, time average of the polarization ellipse must be considered. The time averaged

polarization ellipse for the case $z = 0$ has the form [130] :

$$\frac{\left\langle \left(E_x^R(z=0,t)\right)^2\right\rangle}{E_{0x}^2} - 2\frac{\left\langle E_x^R(z=0,t)E_y^R(z=0,t)\right\rangle}{E_{0x}E_{0y}}\cos(\delta) + \frac{\left\langle \left(E_y^R(z=0,t)\right)^2\right\rangle}{E_{0y}^2} = \sin^2(\delta),$$

$$\text{(B.2.1)}$$

where

$$\left\langle E_i^R(z=0,t)E_j^R(z=0,t)\right\rangle = \lim_{T\to\infty}\frac{1}{T}\int_0^T E_i^R(z=0,t)E_j^R(z=0,t)\mathrm{d}t \qquad (i,j=x,y)$$

$$\text{(B.2.2)}$$

Multiplying Eq.(B.2.1) by $4E_{0x}^2 E_{0y}^2$, it takes the form:

$$4E_{0y}^2\left\langle \left(E_x^R(z=0,t)\right)^2\right\rangle - 8E_{0x}E_{0y}\left\langle E_x^R(z=0,t)E_y^R(z=0,t)\right\rangle\cos(\delta)$$

$$+ 4E_{0x}^2\left\langle \left(E_y^R(z=0,t)\right)^2\right\rangle = \left(2E_{0x}E_{0y}\sin(\delta)\right)^2. \qquad \text{(B.2.3)}$$

On substituting the expressions for E_x and E_y given by Eq.(B.1.2) into Eq.(B.2.3), it gets reduced to the form:

$$\left(E_{0x}^2 + E_{0y}^2\right)^2 = \left(E_{0x}^2 - E_{0y}^2\right)^2 + \left(2E_{0x}E_{0y}\cos(\delta)\right)^2 + \left(2E_{0x}E_{0y}\sin(\delta)\right)^2. \quad \text{(B.2.4)}$$

Let

$$\begin{aligned}
S_0 &= \left(E_{0x}^2 + E_{0y}^2\right), \\
S_1 &= \left(E_{0x}^2 - E_{0y}^2\right), \\
S_2 &= 2E_{0x}E_{0y}\cos(\delta) \qquad \text{and} \\
S_3 &= 2E_{0x}E_{0y}\sin(\delta).
\end{aligned}$$

$$\text{(B.2.5)}$$

Equation (B.2.5) represents the Stokes polarization parameters. On substituting Eq.(B.2.5) into Eq.(B.2.4), the relation between the Stokes polarization parameters is given as

$$S_0^2 = S_1^2 + S_2^2 + S_3^2. \qquad \text{(B.2.6)}$$

In terms of the complex components E_x and E_y, the Stokes polarization parameters are written as

$$
\begin{aligned}
S_0 &= |E_x|^2 + |E_y|^2, \\
S_1 &= |E_x|^2 - |E_y|^2, \\
S_2 &= E_x E_y^* + E_x^* E_y \quad \text{and} \\
S_3 &= i\left(E_x E_y^* - E_x^* E_y\right).
\end{aligned}
\tag{B.2.7}
$$

In terms of the orientation angle Ψ and ellipticity angle χ, the Stokes polarization parameters are written as

$$
\begin{aligned}
S_1 &= S_0 \cos(2\chi)\cos(2\Psi), \\
S_2 &= S_0 \cos(2\chi)\sin(2\Psi) \quad \text{and} \\
S_3 &= S_0 \sin(2\chi).
\end{aligned}
\tag{B.2.8}
$$

Generally $S_0 \equiv 1$. Let

$$
\begin{aligned}
\theta &= \frac{\pi}{2} - 2\chi \\
\phi &= 2\Psi.
\end{aligned}
\tag{B.2.9}
$$

On substituting Eq.(B.2.9) into Eq.(B.2.8), the Stokes parameters can be written as

$$
\begin{aligned}
S_1 &= S_0 \sin(2\theta)\cos(\phi), \\
S_2 &= S_0 \sin(\theta)\sin(\phi) \quad \text{and} \\
S_3 &= S_0 \cos(\theta).
\end{aligned}
\tag{B.2.10}
$$

Equation (B.2.10) is the well known equation relating cartesian coordinates to spherical coordinates. Thus the Stokes parameters can be represented in a sphere

whose center is also the center of the cartesian coordinate system. This sphere is known as the Poincarè sphere. Figure (B.2) depicts the Poincarè representation of the polarized light on a sphere.
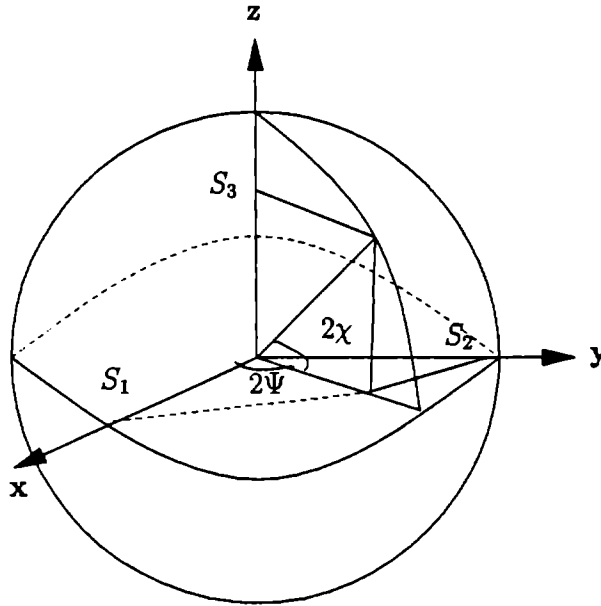

Fig. B.2: Poincaré representation of polarized light on a sphere

(S_1, S_2, S_3) can be viewed as the components of a Stokes vector **S**, having modulus $S_0 \equiv 1$. They define, on the Poincaré sphere, a certain point which identifies the polarization ellipse uniquely. From Eq.(B.2.8), it can be inferred that the state of polarization can be extracted from the location of the Stokes vector. The points on the Poincaré sphere corresponding to linearly polarized light are located along the equatorial line, with an azimuthal angle equal to twice the angle of orientation in the plane of polarization. The north and the south poles of the Poincaré sphere depict right circularly polarized and left circularly polarized light respectively. The upper hemisphere of the Poincaré sphere depicts

right elliptically polarized light while the lower hemisphere of the Poincaré sphere depicts left elliptically polarized light. Thus the Stokes parameters can be used as an effective tool to determine the given state of polarization. The Stokes representation can be effectively employed when considering soliton propagation in birefringent optical fibers.

Bibliography

[1] G. P. Agrawal, *Nonlinear Fiber Optics* (Academic Press, SanDiego, 2001).

[2] G. P. Agrawal, *Applications of Nonlinear Fiber Optics* (Academic Press, SanDiego, 2001).

[3] N. N. Akhmediev and A. Ankiewicz, *Solitons-Nonlinear Pulses and Beams* (Chapman and Hall, London, 1997).

[4] A. Hasegawa and Y. Kodama, *Solitons in Optical Communications*, (Clarendon Press, Oxford, 1995).

[5] M. J. Ablowitz, G. Biondini and L. A. Ostrovsky, *Chaos* **10**, 471 (2000).

[6] M. Nakazawa, H. Kubota, K. Suzuki, E. Yamada and A. Sahara, *Chaos* **10**, 486 (2000).

[7] A. Hasegawa, *Chaos* **10**, 475 (2000).

[8] A. Hasegawa, *Pramana J. Phys.* **57**, 1097 (2001).

[9] K. R. Tamura and M. Nakazawa, *Opt. Lett.* **26**, 762 (2001).

[10] T. Tomukai, T. Inui and M. Nakazawa, *IEEE J. Quantum Electron.* **36**, 409 (2000).

[11] T. Kanna and M. Lakshmanan, *Phys. Rev. Lett.***86**, 5043 (2001).

[12] M. Lakshmanan and T. Kanna, *Pramana J. Phys.* **57**, 885 (2001).

[13] P. C. Becker, N. A. Olsson and J. R. Simpson, *Erbium Doped Fiber Amp lifiers: Fundamentals and Technology*(Academic Press, SanDiego, 1999).

[14] B. C. Collings, S. T. Cundiff, N. N. Akhmediev, J. M. Soto-Crespo, K. Bergman and W. H. Knox, *J. Opt. Soc. Am. B***17**, 354 (2000).

[15] J. M. Soto-Crespo, N. N. Akhmediev, B. C. Collings, S. T. Cundiff, K. Bergman and W. H. Knox, *J. Opt. Soc. Am. B***17**, 366 (2000).

[16] A. D. Kim, J. N. Kuntz and D. J. Muraki, *IEEE J. Quantum Electron.* **36**, 366 (2000).

[17] Y. Gong, P. Shuma, T. Hianga, Chenga, Q. Wena and D. Tang, *Opt. Commun.***200**, 389 (2001).

[18] A. Ghatak and K. Thyagarajan, *Introduction to Fiber Optics*(Cambridge University Press, New Delhi, 1999).

[19] S. R. Nagel, J. B. MacChesney and K. L. Walker in *Optical Fiber Communications*(Ed. T. Li, Academic Press, Orlando, 1985).

[20] L. F. Mollenauer, R. H. Stolen and J. P. Gordon, *Phys. Rev. Lett.***45**, 1095 (1980).

[21] J. M. SotoCrespo, N. N. Akhmediev, V. V. Afanasjev and S. Wabnitz , *Phys. Rev. E***55**, 4783-4796 (1997).

[22] A. Picozzi, C. Montes and E. Picholle , *Phys. Rev. E***58**, 2548-2557 (1998).

[23] X. Liu, L. J. Qian and F. W. Wise , *Phys. Rev. Lett.***82**, 4631 (1999).

[24] C. Yeh and L. A. Bergman , *Phys. Rev. E***60**, 2306 (1999).

[25] P. K. A. Wai and C. R. Menyuk, *J. Lightwave Technol.***14**, 148 (1996).

[26] P. K. A. Wai, W. L. Kath, C. R. Menyuk and J. W. Zhang, *J. Opt. Soc. Am. B***14**, 2967 (1997).

[27] D. Mahgerefteh and C. R. Menyuk, *IEEE Photon. Technol. Lett.* **11**, 340 (1999).

[28] R. Khosravani, I. T. Lima, P. Ebrahimi, E. Ibragimov, A. E. Willner and C. R. Menyuk, *IEEE Photon. Technol. Lett.***13**, 127 (2001).

[29] J. Yang, W. L. Kath and C. R. Menyuk, *Opt. Lett.***26**, 1472 (2001).

[30] R. H. Stolen and C. Lin, *Phys. Rev. A***17**, 1448 (1978).

[31] H. Nakatsuka, D. Grischkowsky and A. C. Balant, *Phys. Rev. Lett.***47**, 910 (1981).

[32] A. Picozzi, C. Montes and E. Picholle , *Phys. Rev. E***58**, 2548 (1998).

[33] H. D. I. Abarbanel, M. B. Kennel, M. Buhl and C. T. Lewis , *Phys. Rev. A***60**, 2360 (1999).

[34] J. M. Fini and P. L. Hagelstein , *Phys. Rev. A***66**, 033818 (2002).

[35] R. H. Stolen, E. P. Ippen and A. R. Tynes , *Appl. Phys. Lett.***20**, 62 (1972).

[36] S. Tariq and J. C. Palais , *J. Lightwave Technol.***11**, 1914 (1993).

[37] J. Wang, X. Sun and M. Zhang , *IEEE Photon. Technol. Lett.***10**, 540 (1998).

[38] M. E. Marhic, F. S. Yang and L. G. Kazovsky , *J. Opt. Soc. Am. B*15, 957 (1998).

[39] S. Bigo, S. Gauchard, A. Bertaina and J. P. Hamaide , *IEEE Photon. Technol. Lett.*11, 671 (1999).

[40] E. P. Ippen and R. H. Stolen , *Appl. Phys. Lett.*21, 539 (1972).

[41] T. Sugie, *J. Lightwave Technol.*9, 1145 (1991).

[42] T. Sugie, *Opt. Quantum Electron.*27, 643 (1995).

[43] S. Song, C. T. Allen, K. R. Demarest and R. Hui , *J. Lightwave Technol.*17, 2285 (1999).

[44] H. Suzuki, S. Ohteru and N. Takachio , *IEEE Photon. Technol. Lett.*11, 1677 (1999).

[45] R. H. Stolen and C. Lin , *Phys. Rev. A*17, 1448 (1978).

[46] M. J. Potasek and G. P. Agrawal , *Phys. Rev. A*36, 3862 (1987).

[47] B. J. Eggleton, R. E. Slusher, C. M. de Sterke, P. A. Krug and J. E. Sipe , *Phys. Rev. Lett.*76, 1627 (1996).

[48] M. Fiorentino, J. E. Sharping, P. Kumar, D. Levandovsky and M. Vasilyev , *Phys. Rev. A*64, 031801 (2001).

[49] R. Grimshaw, B. A. Malomed and G. A. Gottwald , *Phys. Rev. E*65, 066606 (2002).

[50] G. P. Agrawal, P. L. Baldeck and R. R. Alfano , *Phys. Rev. A*40, 5063 (1989).

[51] C. Yeh and L. Bergman , *Phys. Rev. E***57**, 2398 (1998).

[52] C. Yeh, L. Bergman, J. Morookian and S. Monacos , *Phys. Rev. E***57**, 6135 (1998).

[53] O. Bang, L. Berg and J. J. Rasmussen , *Phys. Rev. E***59**, 4600 (1999).

[54] M. Nakazawa, K. Suzuki, H. Kubota and H. A. Haus , *Phys. Rev. A***39**, 5768 (1989).

[55] M. Yu, C. J. McKinstrie and G. P. Agrawal , *Phys. Rev. E***48**, 2178 (1993).

[56] I. Relke , *Phys. Rev. E***57**, 6105 (1998).

[57] H. He, A. Arraf, C. M. de Sterke, P. D. Drummond and B. A. Malomed , *Phys. Rev. E***59**, 6064 (1999).

[58] S. Pitois, G. Millot, P. Grelu and M. Haelterman , *Phys. Rev. E***60**, 994 (1999).

[59] R. Grimshaw, B. A. Malomed and G. A. Gottwald , *Phys. Rev. E***65**, 066606 (2002).

[60] A. Hasegawa and Y. Kodama , *Proc. IEEE***69**, 1145 (1981).

[61] A. C. Newell, *Nonlinear Optics* (Addison-Wesley Publishing Company, California, 1992).

[62] P. L. Chu and C. Desam , *Electron. Lett.***21**, 228 (1985).

[63] Y. Kodama and A. Hasegawa , *Opt. Lett.***7**, 339 (1982).

[64] F. M. Mitschke and L. F. Mollenauer , *Opt. Lett.***11**, 659 (1986).

[65] J. A. Rao and A. A. Rangwala in *Solitons-Introduction and Applications* (Ed. M. Lakshmanan, Springer-Verlag, Germany, 1988).

[66] A. A. Rangwala and J. A. Rao, *Phys.Lett.A.* **112**, 188 (1985).

[67] D. Pushkarov and S. Tanev, *Opt. Commun.* **124**, 354 (1996).

[68] R. W. Micallef, V. V. Afanasjev, Y. S. Kivshar and J. D. Love *Phys. Rev. E* **54**, 2936 (1996).

[69] Y. Kodama *Phys. Lett. A* **112**, 193 (1985).

[70] A. S. Gouveia-Neto, A. S. L. Gomes and J. R. Taylor *Opt. Lett.* **12**, 395 (1987).

[71] Xu Bingzhen and Wang Wenzheng, *Phys. Rev. E* **51**, 1493 (1995).

[72] P. F. Bryd and M. D. Friedman, *Handbook of Elliptic Integrals for Engineers and Scientists* (Springer-Verlag, Berlin, 1971).

[73] Alfinito, M. Leo, R. A. Leo, G. Soliani and L. Solombrino, *Phys. Rev. E* **52**, 3159 (1995).

[74] G. Millot, E. Seve, S. Wabnitz and S. Trillo , *Phys. Rev. Lett.* **80**, 504 (1998).

[75] N. F. Smyth and A. H. Pincombe , *Phys. Rev. E* **57**, 7231 (1998).

[76] N. F. Smyth and W. L. Kath , *Phys. Rev. E* **63**, 036614 (2001).

[77] C. R. Menyuk, *IEEE J. Quantum Electron.* **23**, 174 (1987).

[78] C. R. Menyuk, *IEEE J. Quantum Electron.* **25**, 2674 (1989).

[79] M. Romagnoli, S. Trillo and S. Wabnitz, *Optical and Quantum Electronics* **24**, S1237 (1992).

[80] S. Wabnitz, Y. Kodama and A. B. Aceves, *Opt Fiber Technol.* **1**, 187 (1995).

[81] R. Radhakrishnan and M. Lakshmanan, *Phys. Rev. E***54**, 1 (1996).

[82] R. Radhakrishnan, M. Lakshmanan and J. Hietarinta, *Phys. Rev. E***56**, 2213 (1997).

[83] J. Yang, *Phys. Rev. E***59**, 2393 (1999).

[84] R. Ganapathy, V. C. Kuriakose and K. Porsezian, *Opt. Commun.***194**, 299 (2001).

[85] L. A. Ostrovskii, *Sov. Phys. JETP* **24**, 797 (1966).

[86] V. I. Karpman, *JETP Lett.* **6**, 277 (1967).

[87] A. Hasegawa, *Phys. Rev. Lett.* **24**, 1165 (1970).

[88] A. Hasegawa and W. F. Brinkman, *IEEE J. Quantum Electron.* **16**, 694 (1980).

[89] E. J. Greer, D. M. Patrick and P. G. J. Wigley, *Electron. Lett.***25**, 1246 (1989).

[90] M. Yu, C. J. McKinistric and G. P. Agrawal, *J. Opt. Soc. Am. B***15**, 607 (1998).

[91] M. J. Steel, T. P. White and C. Martijn de Sterke, *Opt. Lett.***26**, 488 (2001).

[92] E. Seve, P. T. Dinda, G. Millot, M. Remoissenet, J. M. Bilbault and M. Haelterman, *Phys. Rev. A* **54**, 3519 (1996).

[93] J. R. Taylor, *Optical Solitons-Theory and Experiments*, (Cambridge University Press, Cambridge, 1992).

[94] J. M. Dudley, M. D. Thomson, F. Gutty, S. Pitois, P. Grelu and G. Millot, *Electron. Lett.* **35**, 2042 (1999).

[95] S. Pitois, M. Haelterman and G. Millot, *J. Opt. Soc. Am. B* **19**, 782 (2002).

[96] P. D. Drummond, T. A. B. Kennedy and J. D. Harvey, *Opt. Commun.* **78**, 137 (1990).

[97] R. Ganapathy and V. C. Kuriakose, *Pramana J. Phys.***58** 668 (2002).

[98] B. A. Malomed and R. A. Tasgal, *J. Nonlinear Opt. Phys. and Materials* **5**, 559 (1996).

[99] B. A. Malomed and R. A. Tasgal, *Pure Appl. Opt.* **5**, 947 (1996).

[100] S. B. Cavalcanti, J. C. Cressoni, H. R. da Cruz and A. S. Gouveia-Neto, *Phys. Rev. A* **43**, 6162 (1991).

[101] A. V. Buryak and N. N. Akhmediev, *Phys. Rev. E* **51**, 3572 (1995).

[102] N. N. Akhmediev, Alexander V. Buryak and J. M. Soto-Crespo, *Opt. Commun.* **112**, 278 (1994).

[103] Wen-cheng Xu, Shu-min Zhang, Wei-cheng Chen, Ai-ping Luo and Song-hao Liu, *Opt. Commun.* **199**, 355 (2001).

[104] M. Haelterman and A. P. Sheppard , *Phys. Rev. E* **49**, 3389 (1994).

[105] S. Trillo and S. Wabnitz, *Phys.Rev.E* **56**, 1048 (1997).

[106] P. V. Mamyshev, S. V. Cherinkov, E. M. Dianov and A. M. Prokhorov, *Opt.Lett.* **15**, 1365 (1990).

[107] R. Ganapathy and V. C. Kuriakose, *Pramana J. Phys.***57** 743 (2001).

[108] H. M. Antia, *Numerical Methods for Scientists and Engineers* (Tata McGraw-Hill, New Delhi, 1991).

[109] E. A. Coddington and N. Levison, *Theory of Ordinary Differential Equations*, (McGraw-Hill, New York, 1955).

[110] M. Eiselt, *J. Lightwave Technol.* **17**, 2261 (1999).

[111] C. R. Menyuk, *Opt.Lett.***12**, 614 (1987).

[112] P. V. Mamyshev, S. V. Cherinkov and M. Dianov, *IEEE J. Quantum Electron.* **7**, 2347 (1991).

[113] A. Mostofi, H. Hatami-Hanza and P. L. Chu, *IEEE J. Quantum Electron.* **33**, 620 (1997).

[114] K. T. Chan and W. H. Cao, *Opt. Commun.* **184**, 463 (2000).

[115] M. D. Pelusi and H. F. Liu, *IEEE J. Quantum Electron.* **33**, 1430 (1997).

[116] R. Ganapathy and V. C. Kuriakose, *Chaos, Solitons and Fractals***15**, 99 (2002).

[117] J. D. Moores, *Opt.Lett.* **21** 555 (1995).

[118] V. K. Mezentsev and S. K. Turitsyn , *Opt. Commun.* **146** 225 (1998).

[119] R. Ganapathy and V. C. Kuriakose, *J. Nonlinear Opt. Phys. and Materials***11**, 185 (2002).

[120] S. L. Mc Call and E. L. Hahn, *Phys. Rev. Lett.*18, 908 (1967).

[121] A. I. Maimistov and E. A. Manykin, *Sov. Phys. JETP*58, 685 (1983).

[122] M. Nakazava, E. Yamada and H. Kubota, *Phys. Rev. A*44,5973 (1991).

[123] S. Kakei and J. Satsuma, *J. Phys. Soc. Jpn.*63, 885 (1994).

[124] K. Porsezian and K. Nakkeeran, *J. Mod. Opt.*42,1953 (1995).

[125] K. Nakkeeran and K. Porsezian, *J. Phys. A:Math. General*28, 3817 (1995).

[126] K. Porsezian and K. Nakkeeran, *Phys. Rev. Lett.*74,2941 (1995).

[127] A. I. Maimistov and A. M. Basharov, *Nonlinear Optical Waves* (Kluwer Academic Publishers, Dordrecht, 1999).

[128] Q.-H. Park and R. W. Boyd , *Phys. Rev. Lett.*86, 2774 (2001).

[129] D. P. Caetano, S. B. Cavalcanti and J. M. Hickmann , *Phys. Rev. E*65, 036617 (2002).

[130] E. Collett, *Polarized Light-Fundamental and Applications* (Marker Dekker Inc., 1993).